RCA REVIEW

a technical journal

RADIO AND ELECTRONICS
RESEARCH · ENGINEERING

VOLUME XII DECEMBER 1951 NO. 4

PRINTED IN U.S.A.

RCA REVIEW, published quarterly in March, June, September and December by RCA Laboratories Division, Radio Corporation of America, Princeton, New Jersey. Entered as second class matter July 3, 1950 at the Post Office at Princeton, New Jersey, under the act of March 3, 1879. Subscription price in the United States, Canada and Postal Union; one year $2.00, two years $3.50, three years $4.50: in other countries; one year $2.40, two years $4.30, three years $5.70. Single copies in the United States, $.75; in other countries, $.85.

RCA REVIEW

a technical journal

RADIO AND ELECTRONICS
RESEARCH • ENGINEERING

Published quarterly by
RCA LABORATORIES DIVISION
RADIO CORPORATION OF AMERICA
in cooperation with

RCA VICTOR DIVISION
RADIOMARINE CORPORATION OF AMERICA
RCA INTERNATIONAL DIVISION
RCA COMMUNICATIONS, INC.
NATIONAL BROADCASTING COMPANY, INC.
RCA INSTITUTES, INC.

VOLUME XII DECEMBER, 1951 NUMBER 4

CONTENTS

PAGE

A Method of Improving the Electrical and Mechanical Stability of Point-Contact Transistors 651
B. N. SLADE

Relative Magnitudes of Undesired Responses in Ultra-High-Frequency Receivers 660
W. Y. PAN

A Study of Grounded-Grid, Ultra-High-Frequency Amplifiers 682
T. MURAKAMI

Fundamental Processes in Charge-Controlled Storage Tubes 702
B. KAZAN and M. KNOLL

Survey of Radio-Frequency Resistors with Kilowatt Ratings 754
D. R. CROSBY

RCA TECHNICAL PAPERS 764

AUTHORS 767

INDEX, Volume XII (1951) 769

RCA Review is regularly abstracted and indexed by *Industrial Arts Index Science Abstracts* (I.E.E.-Brit.), *Engineering Index, Electronic Engineering Master Index, Abstracts and References (Wireless Engineer*-Brit. and *Proc. I.R.E.)* and *Digest-Index Bulletin.*

RCA REVIEW

BOARD OF EDITORS

REPUBLICATION AND TRANSLATION

A METHOD OF IMPROVING THE ELECTRICAL AND MECHANICAL STABILITY OF POINT-CONTACT TRANSISTORS*

By

B. N. Slade

Tube Department, RCA Victor Division,
Harrison, N. J.

Summary—The use of thermosetting resins for embedding of point-contact transistors has resulted in a marked improvement in transistor mechanical and electrical stability. Developmental resin-embedded transistors have been subjected to severe impact and centrifuge tests with practically no change in electrical characteristics. Transistors utilizing this construction are highly resistant to the attack of water vapor and are able to withstand extended storage periods at elevated temperatures. Operation at low temperatures is satisfactory, but some changes in electrical characteristics occur at high ambient temperatures. The improvements described have extended the life of developmental transistors and indicate that their use may be feasible in applications having rigorous specifications with regard to mechanical ruggedness, high humidity, and extreme storage temperatures.

Introduction

THE extensive use of point-contact transistors as commercial devices greatly depends upon their reliability in operation. Up to the present, transistors have proven less reliable than electron tubes in many circuit applications both because of numerous early failures during operation and because of appreciable changes in operating characteristics and gain over short periods of time. Some of the sources of this instability may be traced to the germanium crystal material and to treatment of the crystal surface. Other transistor failures are directly related to the physical construction of the device. Four of the most important causes of instability are (1) high equivalent base resistance,[1] (2) the attack of moisture and other chemical agents of the atmosphere on the emitter and collector contact area, (3) mechanical shifting of the point contacts, and (4) excessive changes in ambient temperature. The purpose of this paper is to describe a method of improving the electrical and mechanical stability of point-contact transistors.

---

* Decimal Classification: R282.12.

[1] A committee of the IRE is presently considering the use of the term "equivalent block resistance" to replace the term "equivalent base resistance".

Equivalent Base Resistance

Because operational stability of the transistor requires a low value of equivalent base resistance, several methods of obtaining these low values have been proposed. One of these methods is the use of germanium crystals of low resistivity. Another method, careful surface processing of the germanium crystals, frequently will reduce surface leakage between the emitter and collector contacts, thus reducing the value of equivalent base resistance. It has been previously reported that the equivalent base resistance may be reduced considerably by spacing the emitter and collector contacts widely;[2] no sacrifice in gain results from the use of wide spacings although the frequency response of the device is decreased. It appears, therefore, that improvement of operational stability by decreasing the value of equivalent base resistance relates directly to the germanium crystal, the crystal surface, and the distance between the point contacts.

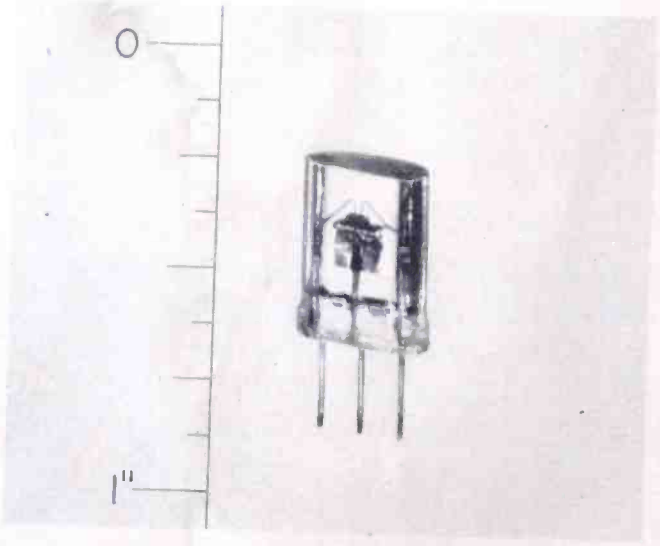

Fig. 1—Photograph of developmental embedded point-contact transistor.

The Embedded Transistor

Instability caused by moisture attack, mechanical shifting of the points, and excessive ambient temperatures are functions of the physical construction of the transistor. The need for a transistor which is stable electrically and mechanically has led to the development of a unit in which all of the parts are completely embedded in a thermosetting resin. A developmental embedded transistor is shown in Figure 1. The transistor leads, crystal, crystal support, and rectifying con-

[2] B. N. Slade, "A High-Performance Transistor with Wide Spacing Between Contacts," *RCA Review*, Vol. XI, No. 4, p. 517, December, 1950.

Table I—Impact Test (Acceleration = 1000 g).

	No. 1		No. 2		No. 3		No. 4	
	a	b	a	b	a	b	a	b
Emitter volts	0.25	0.3	0.1	0.12	0.26	0.31	0.32	0.33
Emitter ma.	0.67	0.72	0.34	0.34	0.62	0.68	0.89	0.92
Collector volts	20	20	20	20	15	15	20	20
Collector ma.	3.0	3.0	3.4	3.4	4.1	4.1	3.5	3.5
Power gain (db)	18.0	17.8	18.6	18.2	18.6	18.5	18.7	19.0

a. Before impact.
b. After impact.

tacts are all solidly embedded in the resin. Such a transistor is extremely rugged mechanically and is highly resistant to the attack of water vapor and other atmospheric chemical agents. The embedding process has extended the ambient temperature range over which transistors will satisfactorily operate, and has enabled transistors to withstand a wide range of storage temperatures.

Mechanical Stability

The mechanical stability of an embedded transistor is demonstrated by the high resistance of the device to shock and to centrifugal force. In Table I the amplifier characteristics of four developmental transistors are tabulated before and after receiving impacts causing acceleration 1000 times the acceleration due to gravity. Each transistor was subjected to five blows in each of four different directions. The directions of the impacts are indicated in Figure 2. The data in

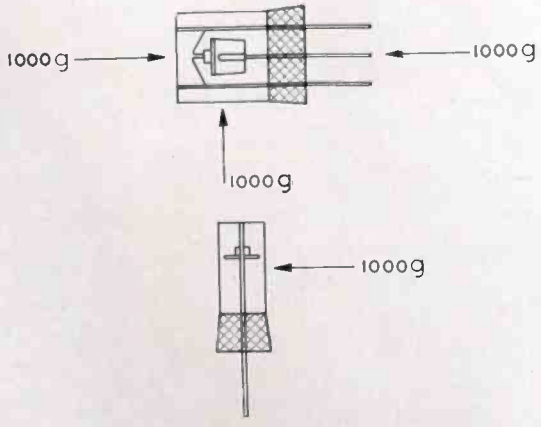

Fig. 2—Magnitude and directions of impacts applied to embedded transistors.

Table II—Centrifuge Test.

	No. 1		No. 2		No. 3		No. 4	
	a	b	a	b	a	b	a	b
Emitter volts	0.16	0.16	0.21	0.26	0.11	0.14	0.29	0.29
Emitter ma.	0.42	0.42	0.88	0.88	0.38	0.34	0.78	0.78
Collector volts	20	20	10	10	'20	20	22.5	22.5
Collector ma.	2.8	2.8	2.5	2.5	2.2	2.2	2.7	2.7
Power gain (db)	18.0	18.0	18.8	18.8	17.2	17.2	16.2	15.8

a. Before centrifuge test.
b. After centrifuge test.

Table I shows that the impact test had practically no effect on the transistor characteristics.

Additional indication of the mechanical stability of such transistors may be seen in Table II which shows the operating characteristics of four transistors which were tested in a centrifuge. The directions and magnitudes of the centrifugal forces applied to the transistors are indicated in Figure 3. The data in Table II indicates that practically no change in gain or operating characteristics occurred as a result of the test. Visual inspection of the transistors after the impact and centrifuge tests showed no evidence of any physical damage.

Effect of Moisture

The attack of moisture and other chemical agents of the atmosphere upon the point-contact area of the transistor contributes greatly to transistor instability. The presence of water vapor in the area of the emitter and collector contacts may cause large changes in the direct-current operating conditions and a considerable slump in gain, if not a complete failure of operation. The embedded transistor demonstrates a high degree of resistance to moisture provided, of course, the resin used has low moisture-absorption properties.

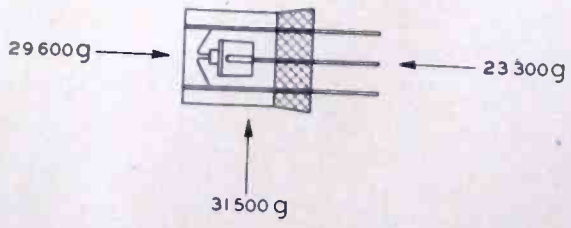

Fig. 3—Magnitude and directions of centrifugal accelerations applied to embedded transistors.

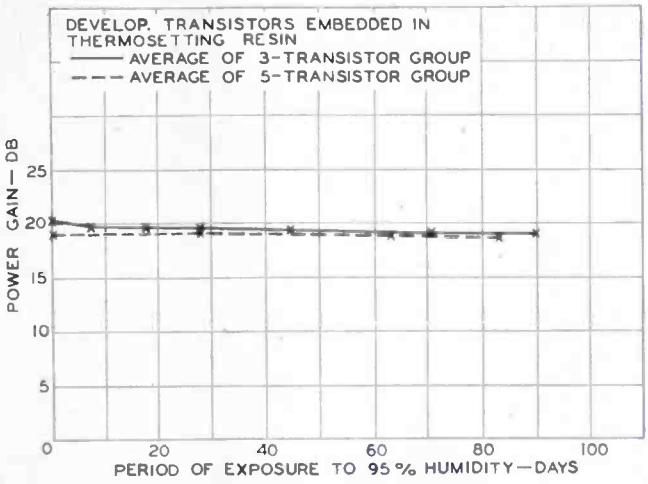

Fig. 4—Effect of high humidity on power gain.

The resistance of the embedded transistors to the attack of moisture is illustrated in Figure 4, in which curves of average power gain versus number of days at a relative humidity of 95 per cent are shown for two groups of transistors. The power gain of these transistors was relatively unaffected by the high humidity. Only one of the transistors in the two groups represented by the curves showed a variation in gain greater than $\pm$ 2.0 decibels during the test.

An additional indication of the resistance of the embedded transistors to the attack of moisture is given by Figure 5 which shows a curve of power gain versus days of immersion in water at room temperature. The power gain of one of these units remained approximately the same throughout the 100 days of the test; the power gain of the

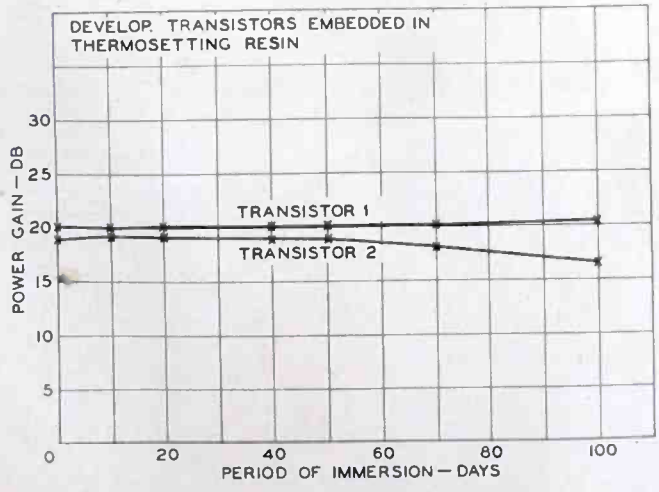

Fig. 5—Effect of water immersion on power gain.

second unit dropped approximately 2 decibels between the 50th and 100th day.

Effect of Temperature

Ambient-temperature changes may also contribute to transistor instability. Large variations in ambient temperature may cause considerable changes in transistor operating characteristics and gain. It is, of course, desirable that the operating temperature range of the transistor be extended as far as possible below and above normal room temperature, but that the resultant variation in transistor characteristics be kept small. A number of measurements of the effects of varying ambient temperature on embedded transistors are given here.

Table III shows that only small changes in gain and operating characteristics occur in operation at ambient temperatures ranging

Table III—Low-Temperature Test.

	No. 1			No. 2			No. 3			No. 4		
	a	b	c	a	b	c	a	b	c	a	b	c
Emitter volts	0.42	0.0	0.42	0.5	0.68	0.4	0.01	0.16	0	0.23	0.31	0.23
Emitter ma.	1.1	1.0	1.1	0.55	0.78	0.5	0.68	0.64	0.52	0.9	0,9	0.7
Collector volts	20	20	20	17.5	17.5	17.5	25	25	25	22.5	25.0	22.5
Collector ma.	4.6	4.6	4.6	3.6	3.6	3.6	3.3	3.3	3.3	2.6	2.6	2.6
Power gain (db)	17.9	18.9	18.8	26.5	24.0	26.5	19.8	19.8	19.8	18.5	18.1	17.8

a. Opération at 25°C before test.
b. Test operation at —70°C.
c. Operation at 25°C after test.

from —70°C to 25°C. Readings for four transistors were taken at 25°C, at —70°C, and then, a final reading at 25°C to determine if any permanent change had occurred in transistor characteristics. It can be seen from the table that the low temperatures caused some change in direct-current characteristics during operation although there was no appreciable change in power gain. The final reading at 25°C indicates that no permanent damage to the transistor resulted from operation at low temperatures. These readings suggest that transistor operation may be feasible at temperatures well below 0°C.

Several embedded transistors were operated at liquid-air ambient temperatures, approximately —180°C. The results of this test are of little practical significance, but they do indicate that embedded transistors will withstand extreme cold. None of the transistors tested

showed any appreciable change in power gain during operation for approximately 10 minutes at the liquid-air temperature. Some of the transistors, however, decreased a few decibels in gain after being returned to room temperature. This decrease may have been caused by slight mechanical changes in the resin due to the extremely large variations in temperature.

The characteristics of the point-contact transistor become more sensitive to changes in ambient temperature above 25°C. It has been reported previously that the current amplification factor, alpha, may increase slightly with increasing ambient temperature.[3] Despite this increase in current amplification at higher ambient temperatures, the over-all power gain of the transistor may remain the same or even decrease due to a decrease in the collector resistance. Not only does the change in collector resistance cause a change in the power gain at high ambient temperatures, but it also causes considerable changes in the direct-current operating characteristics of the transistor. The greatest changes in all of these characteristics generally occur at temperatures of 45°C to 50°C or greater. If the heat generated at the collector contact is rapidly removed from the crystal, the temperature gradient which exists between the contact area and the outer portion of the transistor may be reduced. Consequently, less variation in transistor characteristics would occur with ambient temperature changes. In the embedded transistor, the resin is a good conductor of heat and thus expedites the heat transfer from the crystal. The good heat-conduction properties of the resin used in the embedded transistor were determined qualitatively by measuring the change in power gain and collector resistance resulting when the ambient temperature was changed from 25°C to 60°C. For purposes of comparison, several transistors of the same construction but utilizing a wax impregnant rather than the resin were measured under the same conditions. The resulting data showed no appreciable change in power gain and a maximum of 20 per cent decrease in collector resistance over the 25°C to 60° C range in the case of the embedded transistors. The wax-impregnated units showed a decrease in collector resistance ranging from 20 per cent to 45 per cent; the power gain decreased by as much as 90 per cent. Several Type-A transistors were also measured in the same manner. The results obtained with these units are comparable to the results obtained with the embedded transistors. In the case of the Type-A transistors, the heat transfer from the crystal is obtained

[3] See, for example, J. Bardeen and W. H. Brattain, "Physical Principles Involved in Transistor Action," *Phys. Rev.*, Vol. 75, pp. 1208-1225, April 15, 1949.

by means of the large crystal support. The resin in the embedded transistor appears to accomplish the function of heat transfer from the crystal to about the same degree as the large-area crystal support. In point-contact transistors, however, the change in electrical characteristics at high ambient temperatures still remains a limiting operating factor.

Although point-contact transistors cannot be operated at high ambient temperatures, it is often necessary to store them at temperatures considerably higher than 25°C. A group of five embedded transistors was stored at 75°C for 50 days and tested at frequent intervals. Only minor changes in operating conditions and power gain occurred during the test. Several embedded transistors have been

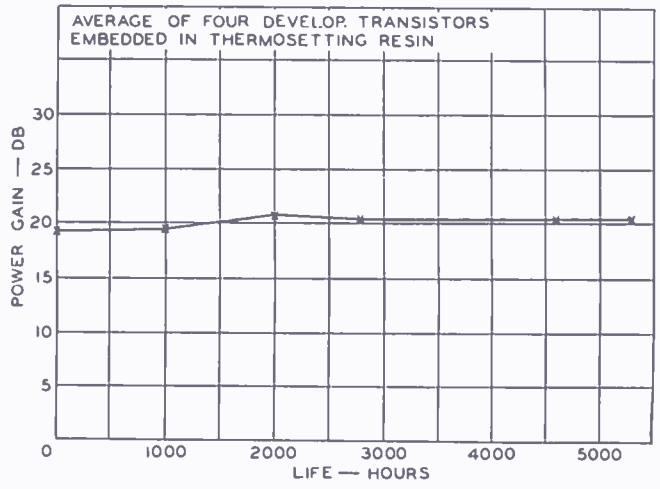

Fig. 6—Variation of power gain with life.

heated for five hours at 150°C with no effect upon the electrical characteristics. It may thus be feasible to use embedded transistors in circuits which will be completely embedded in resins requiring high setting temperatures.

Life Considerations

A life test conducted on several developmental transistors has shown a high degree of stability under normal operating conditions. In this test, voltages of fixed direct-current values were applied to the emitter and to the collector through a 10,000-ohm series resistor. Figure 6 shows a curve of average power gain versus hours of life testing for four transistors. At no time during this test did the measured power gain of any of the four transistors vary more than 2.5 decibels from

its original gain reading. The gain of all four units increased during the 5300 hours of test. Figure 7 shows curves of both average emitter and collector currents versus hours of life testing for the same units. None of the four transistors varied more than 6 per cent in emitter current or collector current during a period of 5300 hours.

Properties of Casting Resins

The properties of the thermosetting casting resins used for embedding point-contact transistors must be beneficial to transistor performance and life. The resin should have a very low mechanical

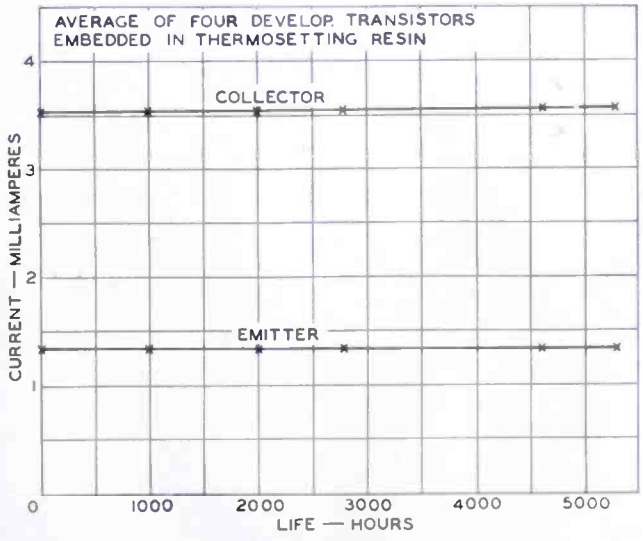

Fig. 7—Variation of emitter and collector currents with life.

shrinkage during the setting process in order to prevent appreciable changes in contact spacings and contact pressures. During the polymerization process the resin should not give off volatile material which might contaminate the point-contact area and the crystal surface. The resin should have very low moisture-absorption properties in order to assure long transistor life. It should possess a high degree of mechanical strength and should closely adhere to all parts of the transistor. Finally, the resin should be a good conductor of heat so that the transistor will have good stability with variations in ambient temperature.

The thermosetting resin "Araldite", manufactured by CIBA Ltd., possesses these characteristics to a high degree; it has been used quite successfully in this application.

RELATIVE MAGNITUDES OF UNDESIRED RESPONSES IN ULTRA-HIGH-FREQUENCY RECEIVERS*

By

Wen Yuan Pan

Home Instruments Department, RCA Victor Division, Camden, N. J.

Summary—Undesired responses in an ultra-high-frequency television tuner or converter are caused by one or more interfering signals, either dependent or independent of the local oscillator frequency. For television receivers employing crystal rectifiers as mixers, the second, third and possibly the fourth harmonics formed in the mixer may give rise to interference in the presence of a single interfering signal; but only the second harmonic is of importance if such interference is caused by two or more interfering signals.

The relative magnitudes of the undesired responses are measured by a special test setup including a test tuner which is basically similar to the ultra-high-frequency tuners and converters recently demonstrated by the industry, except that it has a broad-band characteristic preceding the mixer.

Knowing the origin and the relative magnitudes of the various undesired responses, the proper selectivity characteristics of the circuits preceding the mixer of an ultra-high-frequency receiver employing a given intermediate frequency can be determined so that the receiver responses to interfering signals are reduced to any desired value.

Introduction

RECENTLY ultra-high-frequency (UHF) tuners and converters of various designs have been tested and demonstrated in Bridgeport, Connecticut, by many television manufacturers. It was learned that practically all such tuners and converters employ either one or two radio-frequency (r-f) tuned circuits followed by a crystal-rectifier mixer, generally of the germanium type. An oscillator and a low-noise intermediate-frequency (i-f) amplifier are usually incorporated with each tuner or converter. At this experimental stage of the UHF art, the manufacturers are primarily interested, among other factors, in the stability of the UHF local oscillator and the quality of the picture with a certain field intensity of the UHF signal at the point of reception. The 529-535-megacycle and 849-855-megacycle transmitters at Bridgeport, Connecticut, regularly operated by the National Broadcasting Company, and several other UHF transmitters located in different parts of the country serve a good purpose insofar as the

* Decimal Classification: R361.208 × R310.

studies of propagation characteristics and receiver noise figures are concerned. However, the problem of undesired responses in a UHF receiver will undoubtedly confront receiver designers when more UHF stations are operating simultaneously, particularly if they are close by. An investigation, therefore, has been made to determine the formations and relative magnitudes of the undesired responses in a UHF test tuner[1] basically similar to the UHF tuners and converters being demonstrated recently by the industry.

Test Equipment

The block diagram of Figure 1 illustrates the test setup by which the investigation of the relative magnitudes of the undesired responses in a UHF receiver is made. The desired and the undesired signals are supplied by conventional signal generators. Each signal generator feeds to a pure resistive load through a high-pass (or low-pass) filter and a

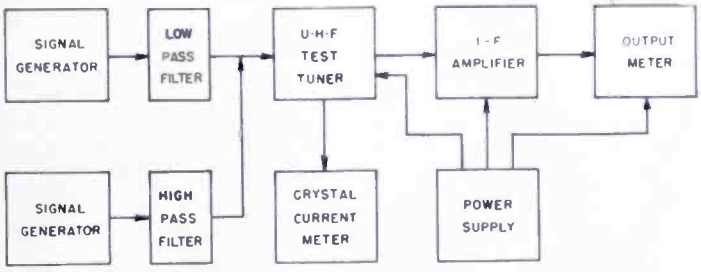

Fig. 1—Block diagram of the test setup for measuring the relative magnitudes of undesired responses in a UHF television receiver.

certain length of transmission line of proper characteristic impedance. The signal thus developed across this resistive load is coupled directly to the mixer stage which uses a crystal rectifier. It is to be noted that no selective circuit is employed preceding the mixer; consequently, full signal at any frequency from either signal generator is developed across the input terminals of the crystal mixer. The mixer is followed by an i-f amplifier consisting of a driven-grounded-grid stage and three additional pentode-connected stages to obtain sufficient gain and constant pass-band characteristics. Three alternative i-f amplifiers are provided for the measurements with center frequencies at 24 megacycles, 44 megacycles and 82 megacycles, respectively. Each amplifier has an effective band width of 3.5 megacycles.

The oscillator circuit of the test tuner of Figure 1 is shown in detail

[1] For design information see W. Y. Pan, "Some Design Considerations of Ultra-High-Frequency Converters," *RCA Review*, Vol. XI, pp. 377-398, September, 1950.

in Figure 2. The oscillator uses a 6AF4 tube, a type which has been used recently by most manufacturers of UHF tuners and converters. The oscillator frequency is varied by a specially constructed variable capacitor in conjunction with a transmission line of composite configuration. The oscillator tunes over a range from 340 megacycles to 950 megacycles, and the amount of oscillator injection to the crystal mixer is varied by an oscillator-injection equalizing device which consists of an 18-micromicrofarad capacitor in series with a parallel combination of a 27-ohm resistor and another specially constructed variable capacitor. The oscillator injection in terms of rectified crystal current can be varied in this test setup from 0.1 milliampere to 5.0 milliamperes.

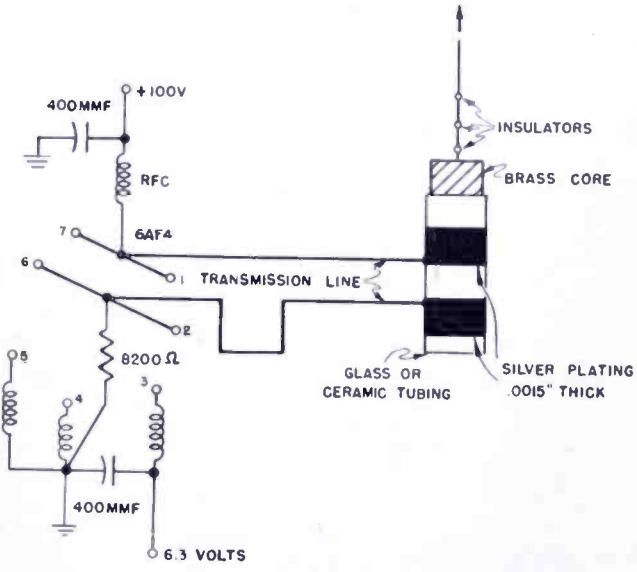

Fig. 2—Circuit diagram of the UHF oscillator used in the test setup.

Origin of Undesired Responses

Prior to the measurements of the undesired responses, it seems advisable to discuss briefly the origin of the undesired responses which may be expected in a UHF tuner. Knowing the origin of the undesired responses, it is possible to determine the frequencies at which a UHF tuner is liable to be affected if interfering signals exist at such frequencies.

It is a well-known fact that in the presence of two signals, $E_1 \cos \omega_1$ and $E_2 \cos \omega_2$, appearing across the input terminals of a rectifier or a nonlinear element, the output current of the rectifier contains a large number of frequency components. The frequency components are in the forms of $\cos n_1\omega_1$, $\cos n_2\omega_2$, $\cos (n_1\omega_1 \pm n_2\omega_2)$, $E_1^{m_1} E_2^{m_2} \cos \omega_1$,

$E_1^{m_1}E_2^{m_2}\cos\omega_2$, etc., where n and m are integral numbers.[2] Because of these frequency components in the output current of a rectifier, the receiver would respond to the desired as well as certain undesired signals if such undesired signals are present. The undesired signals do not necessarily originate from other UHF stations. Transmissions or radiations of various forms and for different services such as amplitude-modulated and frequency-modulated broadcasts, very-high-frequency (VHF) television signals, radar pulses, amateur and communication carriers, industrial, scientific, medical, and meteorological services, and navigational aids, etc., may all become interfering signals in UHF receivers. Radiations from nearby receivers or the harmonics of the i-f signals being coupled into the input terminals of the mixer may give rise to similar effects. With the recently proposed allocation of UHF television channels by the Federal Communications Commission, some of the interferences caused by other UHF television signals are minimized; but the harmonics of these signals as well as other types of transmissions and radiations can produce an interfering signal at almost any frequency. Furthermore, a relatively low-powered interfering signal can cause severe disturbance in a UHF receiver if the receiver is located very near the origin of the interfering signal.

Relative Magnitudes of Responses

The relative magnitude of an undesired or interfering signal is measured by comparing the ability of the receiver to respond to the interfering signal with its ability to respond to the desired signal.[3] If the relative response of the r-f circuit preceding the mixer is the same for all frequencies, as in the case of the test tuner of Figure 1 which has a fixed frequency i-f amplifier following the mixer, the relative magnitude of any particular undesired response is the ratio of the equivalent mixer efficiency in responding to the interfering signal to the equivalent mixer efficiency in responding to the desired signal.

Experimentally, the equivalent mixer efficiency can be measured by observing the noise figure of the i-f amplifier and the over-all noise figure of the test tuner, which depends, among other factors, upon the

---

[2] D. E. Foster, "A New Form of Interference—External Cross Modulation," *RCA Review*, Vol. I, p. 18, April, 1937.

[3] No external direct-current bias is applied to the crystal rectifier. It has been found that a certain amount of external direct-current bias may reduce the relative magnitude of a certain undesired response as much as 20 decibels as compared to the relative magnitude of the same undesired response with no external direct-current bias. However, the same amount of external direct-current bias may not be helpful at all for other undesired responses.

i-f, the oscillator injection, and the type of crystal rectifier being used as mixer. For most germanium crystal rectifiers such as the 1N72 and the CK-710, commonly used in the recent UHF tuners and converters, the equivalent mixer efficiency under optimum operating conditions is in the order of —8 decibels for frequencies up to about 750 megacycles and —10 decibels at 1000 megacycles. The variations of the over-all noise figure of the test tuner of Figure 2 are indicated in Figure 3. Three types of crystal rectifiers are used as mixers, with the desired signal frequency up to 890 megacycles. In all cases the crystal excitation power, or the oscillator injection, is so adjusted that the mixer is operated under the most favorable condition.

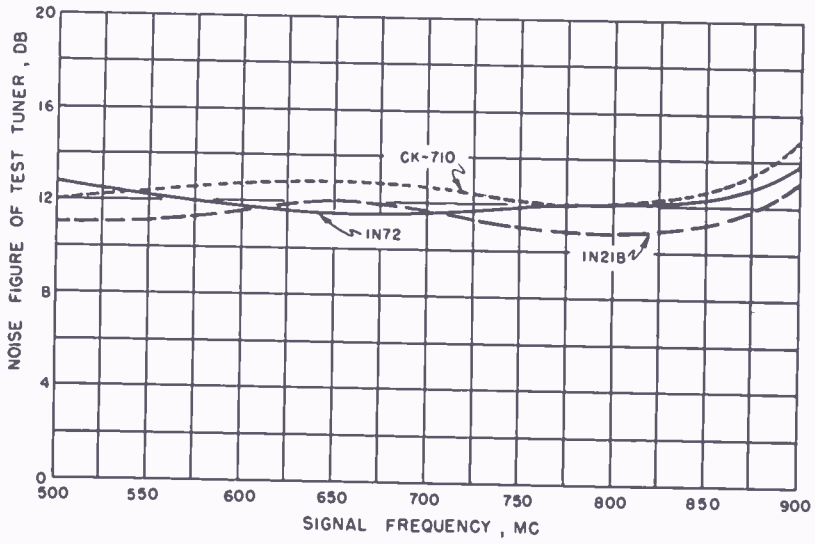

Fig. 3—Variation of over-all noise factor of the test tuner with frequency.

The noise figure of the 24-megacycle and the 44-megacycle i-f amplifiers is 4 decibels and that of the 82-megacycle amplifier is 5 decibels. The mixer loss, or the equivalent mixer efficiency, of the test tuner as a function of the oscillator injection in terms of rectified crystal current is shown in Figure 4. Either the 24-megacycle or the 44-megacycle i-f amplifier is used in conjunction with a typical silicon crystal rectifier 1N21B and two typical germanium crystal rectifiers 1N72 and CK-710. The lowest over-all noise figure or the highest equivalent mixer efficiency of the test tuner for all three types of crystal rectifiers is obtained with an oscillator injection such that the rectified crystal current is within the range from 0.6 milliampere to 2.0 milliamperes. This optimum range of crystal rectified current, however, may vary slightly with the intermediate frequency and the type of oscillator circuit being used.

Single-Frequency Interference, Independent of Local Oscillator

The undesired responses which fall into this category will exist when the frequency of the interfering signal, or any harmonic thereof, is equal to the intermediate frequency of the receiver, or

$$f_1 = f_i/h_m, \tag{1}$$

where f_1 = frequency of the interfering signal,

f_i = intermediate frequency of receiver,

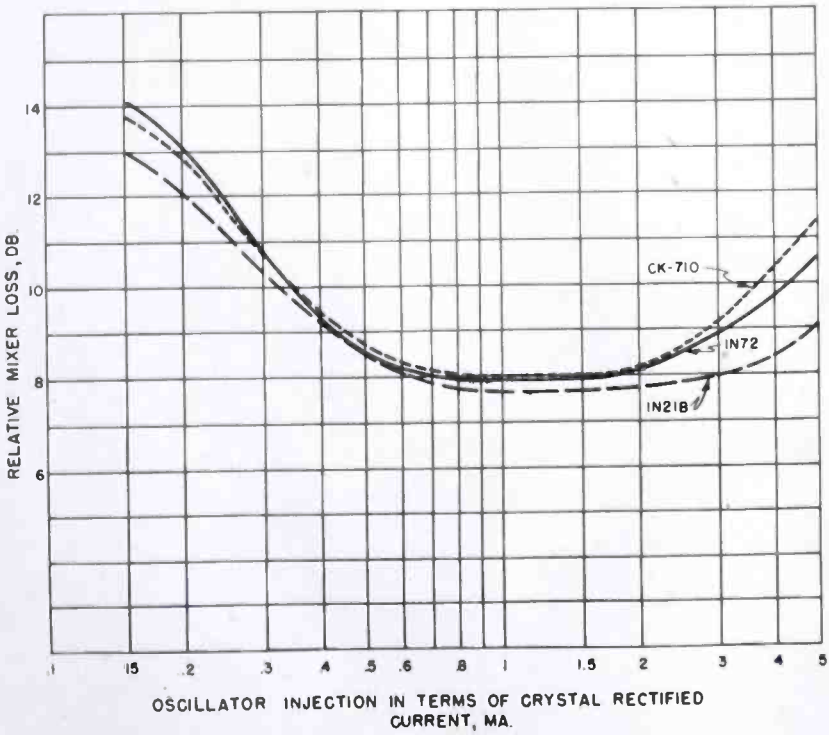

Fig. 4—Variation of relative mixer loss or equivalent mixer efficiency of the test tuner as a function of oscillator injection in terms of rectified current.

h_m = order of harmonic formed in the mixer during the process of mixing.

When h_m is unity, $f_1 = f_i$ which is known as the direct f_i response; when $h_m = 2$, $f_1 = \frac{1}{2}f_i$ which is called the $\frac{1}{2}f_i$ response, etc. Let

e_n = equivalent mixer efficiency in responding to the desired signal when the receiver is under normal operating conditions,

e_1 = equivalent mixer efficiency in responding to the direct f_i response, or when $h_m = 1$,

e_2 = equivalent mixer efficiency in responding to the $\frac{1}{2}f_i$ response, or when $h_m = 2$,

e_x = equivalent mixer efficiency in responding to the $\frac{1}{x}f_i$ response, or when $h_m = x$.

Then e_1/e_n is the relative magnitude of the direct f_i response and e_2/e_n is the relative magnitude of the $\frac{1}{2}f_i$ response, etc.

Table I—Equivalent Mixer Efficiency in Responding to a Single Interfering Signal, Independent of Local Oscillator Frequency, Formed by Mixer Harmonics

Strength of Interfering Signal in Millivolts	$\frac{e_1}{e_n}$ Decibels	$\frac{e_2}{e_n}$ Decibels	$\frac{e_3}{e_n}$ Decibels	$\frac{e_4}{e_n}$ Decibels	$\frac{e_5}{e_n}$ Decibels
50	6.0	—25.6	—40.0	—53.0	—68.0
20	6.0	—32.6	—58.0		
10	6.0	—38.1	—71.0		
5	6.0	—43.0			
2	6.0	—50.0			
1	6.0	—55.8			

With no selective circuits preceding the crystal mixer of a UHF receiver, the direct f_i response offers the highest equivalent mixer efficiency among all responses in the receiver including the desired signal. The equivalent mixer efficiency of this response is practically independent of the strength of the interfering signal. This undesired response is particularly important in UHF converters where one of the VHF channels is generally used as converter i-f. The relative magnitude of the $\frac{1}{2}f_i$ response, according to Table I, is approximately directly proportional to the strength of the interfering signal, and that of the $\frac{1}{3}f_i$ response is approximately proportional to the square of the strength of the interfering signal. A graphical presentation of the relative magnitudes of the various $(1/x)f_i$ responses is shown in Figure 5. For all practical purposes, the interference caused by the 4th or higher harmonic formed in the mixer may be disregarded.

A knowledge of the relative magnitude of the undesired response is particularly helpful to receiver designers. In the absence of disturbance other than noise, a good television picture on the receiver screen requires a signal power approximately 30 decibels higher than the noise power present in the receiver. Also, when a disturbance arises,

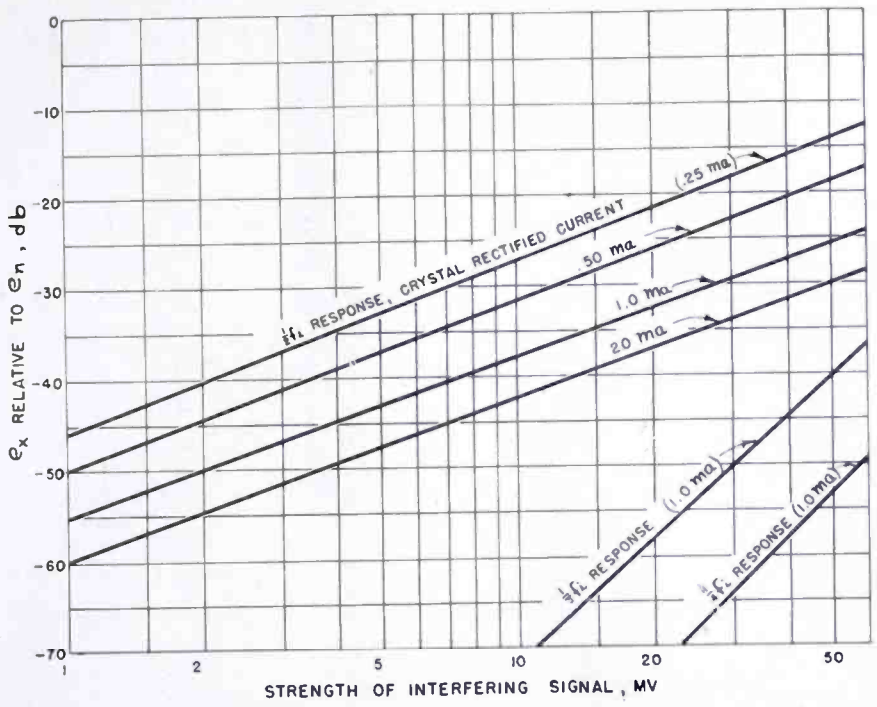

Fig. 5—Equivalent mixer efficiency e_x, in responding to single interfering signals independent of the local oscillator frequency, as a function of E_1, the strength of the interfering signal.

the strength of the interfering signal must be kept about 30 decibels below the strength of the desired signal to secure good picture quality, depending upon the nature of the interfering signal. Suppose that an interfering signal exists at the point of reception with a strength of 40 decibels higher than that of the desired signal. The selectivity of the receiver in responding to such an interfering signal must be at least 70 decibels below the selectivity of the receiver in responding to the desired signal. However, different undesired re-

Table II—Minimum Selectivity of a UHF Receiver Necessary to Combat Undesired Responses Caused by Single Interfering Signals, Independent of the Local Oscillator Frequency, Assuming 25-Millivolt Interfering Signal.

Frequency of Interfering Signal	$\frac{e_x}{e_n}$ (Decibels)	Required Receiver Selectivity (Decibels)
f_i	6.0	—76.0
$\frac{1}{2}f_i$	—31.1	—38.9
$\frac{1}{3}f_i$	—53.8	—16.2
$\frac{1}{4}f_i$	—68.0	—2.0

sponses offer widely different equivalent mixer efficiencies. An optimum selectivity characteristic of a UHF receiver must be designed on the basis of the relative magnitudes of the various undesired responses which the receiver may encounter.

Single-Frequency Interference Dependent on Local Oscillator

The frequency component of the form $\cos(\omega_1 - \omega_2)$ of the rectifier output current, in the presence of two signals $E_1\cos\omega_1$ and $E_2\cos\omega_2$ brings about a new series of interference when,

$$f_1 = f_o \pm f_i/h_m, \tag{2}$$

where f_o is the local oscillator frequency. Under these conditions, $E_1\cos\omega_1$ becomes the desired signal of a UHF receiver when $f_1 = f_o - f_i$; it becomes the image-frequency signal when $f_1 = f_o + f_i$. Insofar as the picture quality of a practical television receiver is concerned, the equivalent mixer efficiency for the reception of the desired and image-frequency signals is approximately equal and is independent of the strength of either signal.

The $f_o \pm \frac{1}{2}f_i$ Responses

The second harmonic formed in the mixer during the process of mixing an interfering signal and the signal of the local oscillator introduces interference at two new frequencies, $f_1 = f_o + \frac{1}{2}f_i$ and $f_1 = f_o - \frac{1}{2}f_i$. The interfering signal whose frequency is $\frac{1}{2}f_i$ above the frequency of the local oscillator of a UHF receiver is called the $f_o + \frac{1}{2}f_i$ response, while the interfering signal whose frequency is $\frac{1}{2}f_i$ below the frequency of the local oscillator of a UHF receiver is called the $f_o - \frac{1}{2}f_i$ response. As the order of harmonics formed in the mixer goes up, signals at still other frequencies will cause disturbances in superheterodyne reception. By the same analogy, these new interfering signals are called the $f_o + \frac{1}{3}f_i$ and $f_o - \frac{1}{3}f_i$, $f_o + \frac{1}{4}f_i$ and $f_o - \frac{1}{4}f_i$ responses, etc. It has been found that harmonics, higher than the 4th, formed in the mixer, may be disregarded for practical purposes because the equivalent mixer efficiency, when the mixer is operated on its 5th harmonic or higher order harmonics, is more than 70 decibels below the equivalent mixer efficiency under normal operation. It also has been found that the equivalent mixer efficiency in responding to the $f_o + \frac{1}{2}f_i$ interfering signal is approximately the same as that in responding to the $f_o - \frac{1}{2}f_i$ interfering signal.

Let e_{m2} = equivalent mixer efficiency in responding to the $f_o \pm \frac{1}{2}f_i$ interfering signals,

e_{m3} = equivalent mixer efficiency in responding to the $f_o \pm \frac{1}{3}f_i$ interfering signals, and

e_{my} = equivalent mixer efficiency in responding to the $f_o \pm (1/y)f_i$ interfering signals.

The ratio e_{m2}/e_n depends upon the strength of the interfering signal appearing across the input terminals of the mixer, the type of crystal rectifier being used as mixer and the amount of oscillator injection. With a given crystal rectifier and a given amount of oscillator injection, e_{m2}/e_n is approximately directly proportional to the strength of the interfering signal.

Table III—Effect of the Strength of Interfering Signal on the $f_o \pm \frac{1}{2}f_i$ Responses, Optimum Oscillator Injection Corresponding to a Rectified Current of 1.0 Milliampere.

Strength of Interfering Signal in Millivolts	$\frac{e_{m2}}{e_n}$ Decibels	
	1N72 Crystal	1N21B Crystal
60	—27.7	—22.5
30	—34.0	—28.5
15	—40.2	—34.4
6	—48.6	—42.4
3	—55.0	—48.5
1.5	—61.3	—54.4

It is interesting to note that the germanium crystal rectifier 1N72 is more desirable than the silicon crystal rectifier 1N21B for use as a UHF mixer insofar as the $f_o \pm \frac{1}{2}f_i$ responses are concerned. The difference in e_{m2}/e_n between a silicon and a germanium crystal rectifier is approximately 6 decibels regardless of the strength of the interfering signals. This means that for an interfering signal of frequency $f_o + \frac{1}{2}f_i$ or $f_o - \frac{1}{2}f_i$ and for a given field intensity of the desired signal, a UHF receiver using a germanium crystal mixer can operate with twice as strong an interfering signal as can a receiver using a silicon crystal mixer of the 1N21B type, if the other characteristics of the two receivers are identical.

The effect of oscillator injection in terms of rectified crystal current on the relative equivalent mixer efficiency e_{m2}/e_n with a constant interfering-signal strength is illustrated in Figure 6 for both silicon and germanium crystal rectifiers. At any given crystal-rectified current, the ratio e_{m2}/e_n for a 20-millivolt interfering signal is approximately 6 decibels higher than that for a 10-millivolt interfering signal and is

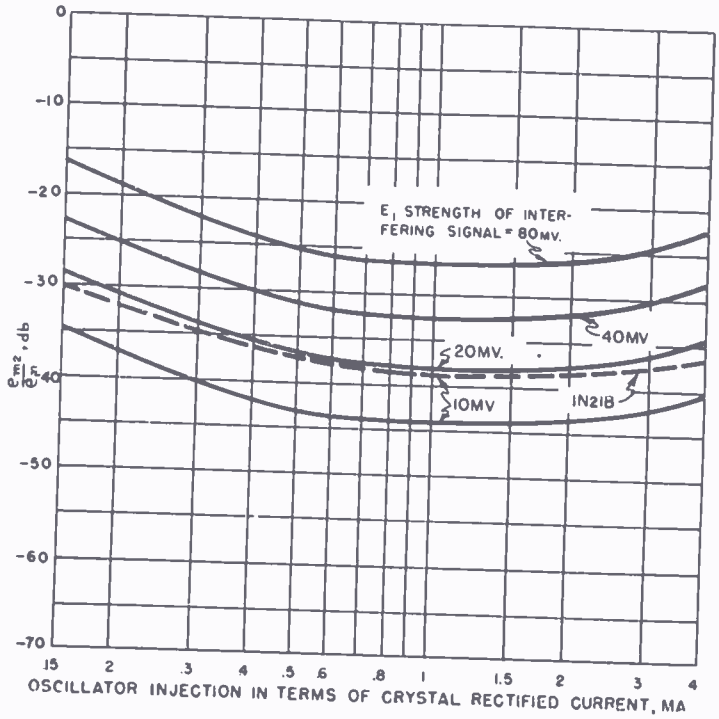

Fig. 6—Effect of oscillator injection in terms of rectified crystal current on the relative equivalent mixer efficiency e_{m2}/e_n.

approximately 6 decibels lower than that for a 40-millivolt interfering signal.

The $f_o \pm \frac{1}{3}f_i$ responses

The $f_o \pm \frac{1}{3}f_i$ responses are caused by the third harmonic formed in the mixer during the process of mixing an interfering signal and the signal of the local oscillator. They behave in the same general manner as the $f_o \pm \frac{1}{2}f_i$ responses. The relative magnitudes of such responses again depend upon the strength of the interfering signal, the type of crystal rectifier being used as mixer, and the amount of oscillator injection.

According to Table IV, the ratio e_{m3}/e_n increases approximately 12 to 13 decibels by doubling the strength of the interfering signal instead of 6 decibels as is the case for the ratio e_{m2}/e_n. Therefore, the equivalent mixer efficiency e_{m3} relative to e_n is approximately proportional to the square of the strength of the interfering signal.

The germanium crystal rectifiers are again preferred over the silicon crystal rectifiers of the 1N21B type insofar as the $f_o \pm \frac{1}{3}f_i$ responses are concerned. The effect of the oscillator injection in terms of rectified crystal current on the relative equivalent mixer efficiency e_{m3}/e_n for a 1N72 germanium crystal mixer is shown in Figure 7 with 80-millivolt, 40-millivolt, and 20-millivolt interfering signals. The

Table IV—Effect of the Strength of the Interfering Signal on the $f_o \pm \frac{1}{3}f_i$ Responses, with Optimum Oscillator Injection

Strength of Interfering Signal in Millivolts	$\frac{e_{m3}}{e_n}$ Decibels	
	1N72 Crystal	1N21B Crystal
60	—42.0	—29.1
30	—55.0	—41.1
15	—68.0	—54.0

dashed curve is for a 1N21B crystal mixer with a 40-millivolt interfering signal.

The $f_o \pm \frac{1}{4}f_i$ responses are relatively unimportant not only because the frequencies of these responses are farther away from the frequency of the desired signal, but also the magnitudes are substantially lower than the undesired responses formed by the mixer second or third harmonic. The general characteristics of the $f_o \pm \frac{1}{4}f_i$ responses are similar to those of the $f_o \pm \frac{1}{3}f_i$ responses except that their relative magnitudes are approximately proportional to the third power of the strength of the interfering signal.

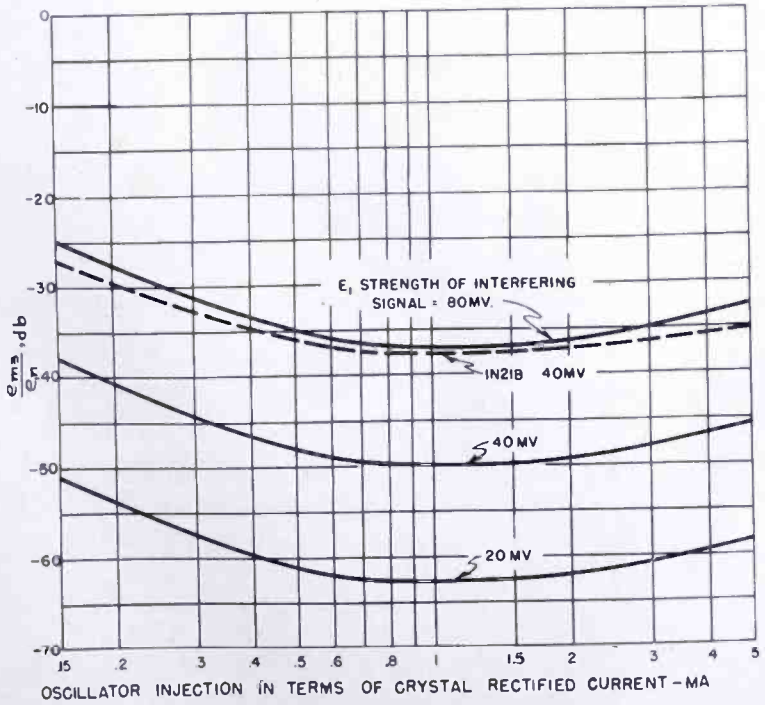

Fig. 7—Effect of oscillator injection in terms of rectified crystal current on the relative equivalent mixer efficiency e_{m3}/e_n.

The $2f_o \pm f_i/h_m$ Responses

The harmonics generated in the local oscillator must be distinguished from the harmonics of the oscillator frequency formed in the mixer during the process of mixing. The harmonics from the local oscillator are generated in the oscillator circuit before being injected to the mixer. Harmonics formed at the source are probably also present in any interfering signal, but such harmonics are not to be considered because any harmonic of an interfering signal may be treated as a new interfering signal. The harmonics from the local oscillator, however, can not be treated as new oscillator frequencies due to the fact that the crystal excitation or the oscillator injection to the mixer is primarily determined by the oscillator fundamental component.

For each operating frequency of the local oscillator, the mixer harmonics make possible the reception of the desired signal and the image-frequency signal, and the $f_o \pm f_i/h_m$ interfering signals. The entire series of undesired responses will be renewed in conjunction with the second or any harmonic from the local oscillator. The UHF test setup of Figure 1 is used to evaluate the relative magnitudes of the undesired responses caused by interfering signals in conjunction with the second harmonic from the local oscillator. Slightly different results may be obtained by using different oscillator tubes, oscillator-tuned circuits and oscillator operating conditions since the amplitudes of the second harmonic or any harmonic relative to that of the fundamental are undoubtedly subject to some variation with these changes.

Let e_{o2} = equivalent mixer efficiency in responding to an interfering signal at a frequency $f_1 = 2f_o \pm f_i$,

e_{o3} = equivalent mixer efficiency in responding to an interfering signal at a frequency $f_1 = 3f_o \pm f_i$, and

e_{oz} = equivalent mixer efficiency in responding to an interfering signal at a frequency $f_1 = zf_o \pm f_i$.

The ratio e_{o2}/e_n depends upon the type of crystal rectifier being used as mixer, the amplitude of the second harmonic generated in the oscillator relative to that of the fundamental, and also is a function of the amount of oscillator injection. Figure 8 shows this function over a wide range of oscillator injection in terms of crystal-rectified current from 0.1 milliampere to 4.0 milliamperes for both 1N21B and 1N72 crystal rectifiers. In the case of the 1N21B silicon crystal rectifier, the ratio e_{o2}/e_n is approximately —3.5 decibels within an operating

range from 0.5 to 1.5 milliamperes. Unless selective circuits are provided in the circuits preceding the crystal mixer, the responses caused by the interfering signals at frequencies $f_1 = 2f_o \pm f_i$ are only 3.5 decibels lower than the response of the desired signal of equal strength. On the other hand, the 1N72 germanium crystal rectifier behaves quite differently. The ratio e_{o2}/e_n of a germanium crystal rectifier is substantially lower than that of a silicon crystal rectifier of 1N21B type, particularly with a strong oscillator injection. Therefore, when a harmonic from the local oscillator is utilized for superheterodyne reception, it is necessary to add an auxiliary tuned circuit which tunes to the harmonic frequency, thus increasing the ratio e_{o2}/e_n toward unity.

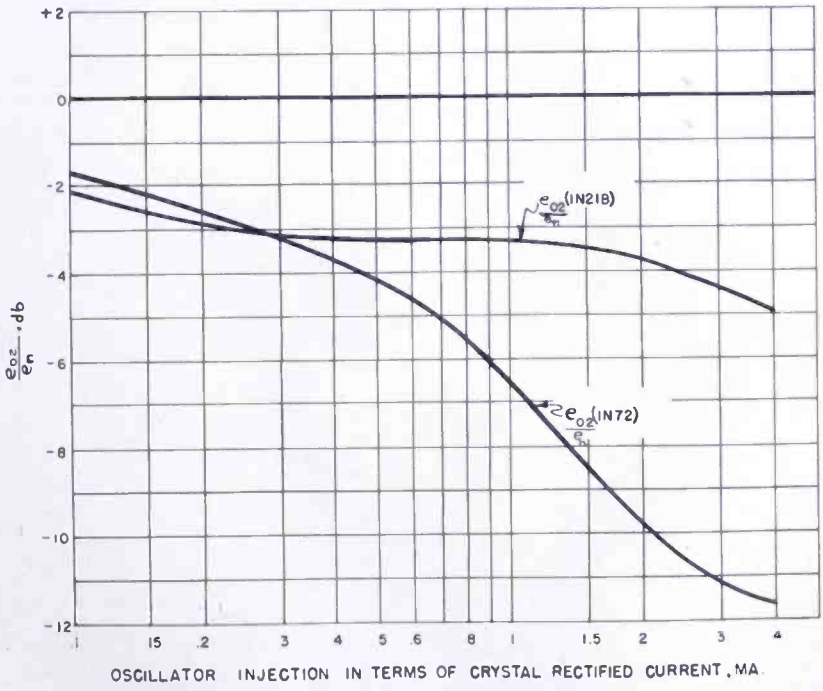

Fig. 8—Effect of oscillator injection on equivalent mixer efficiency e_{o2} in responding to interfering signal in conjunction with 2nd harmonic from local oscillator.

Let e_{o2m2} = equivalent mixer efficiency in responding to an interfering signal in conjunction with the second harmonic formed in the mixer and with the second harmonic from the local oscillator, or $f_1 = 2f_o \pm \frac{1}{2}f_i$.

e_{ozmy} = equivalent mixer efficiency in responding to an interfering signal in conjunction with the yth harmonic formed in the mixer and with the zth harmonic from the local oscillator, or $f_1 = zf_o \pm (1/y)f_i$.

Table V—Effect of Interfering-Signal Strength on the Equivalent Mixer Efficiency e_{o2m2}.

Strength of Interfering Signal in Millivolts	$\frac{e_{o2}}{e_n}$ Decibels	$\frac{e_{m2}}{e_n}$ Decibels	$\frac{e_{o2}}{e_n} \cdot \frac{e_{m2}}{e_n}$ Decibels	$\frac{e_{o2m2}}{e_n}$ Decibels
100	—6.5	—23	—29.5	—31
50	—6.5	—29	—35.5	—37.8
20	—6.5	—38	—44.5	—46.5
10	—6.5	—44.2	—50.7	—51.7
5	—6.5	—51.5	—58	—58
2	—6.5	—59	—65.5	—65.1

Then, with constant oscillator injection, the ratio e_{o2m2}/e_n is again a function of the strength of the interfering signal as shown by Figure 9. It is noted that the ratio is increased again about 6 decibels by doubling the strength E_1 of the interfering signal. The difference between the 1.0-milliampere curve and the .25-milliampere curve at any fixed interfering-signal strength is equal to the difference between the ratio e_{o2}/e_n at 1.0 milliampere and at .25 milliampere as shown by Figure 8. The dotted curve, which is to be compared with the corresponding solid curve, is calculated by multiplying e_{m2}/e_n of Figure 6 by e_{o2}/e_n of Figure 8.

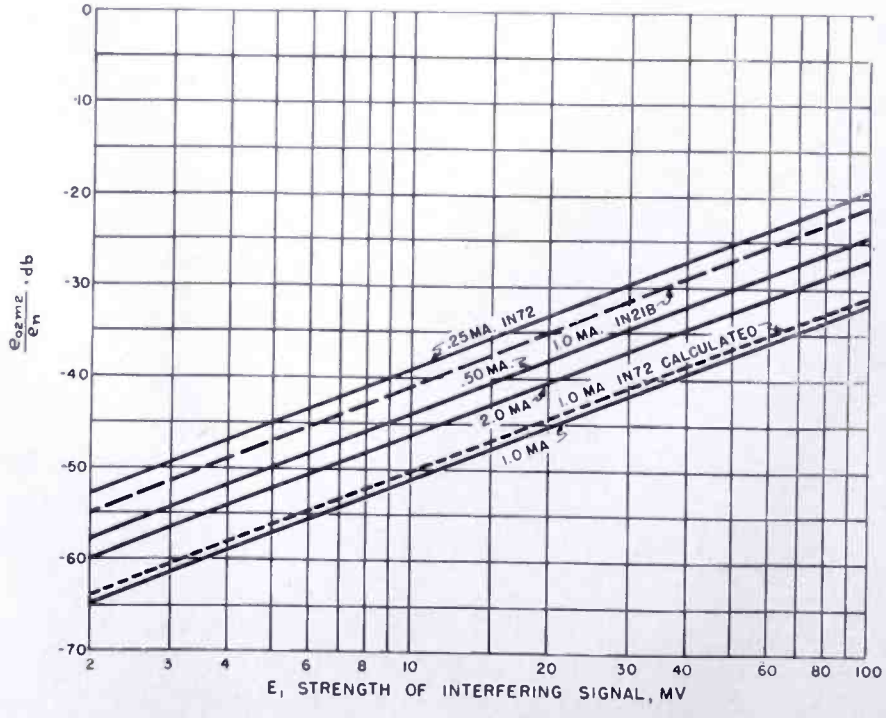

Fig. 9—Variation of $e_{o2}e_{m2}/e_n$ with the strength of the interfering signal.

The facts thus established lead to the conclusion that the equivalent mixer efficiency, e_{ozmy}, relative to e_n involves two independent factors, e_{oz}/e_n and e_{my}/e_n. Therefore,

$$\frac{e_{ozmy}}{e_n} = \frac{e_{oz}}{e_n} \cdot \frac{e_{my}}{e_n}. \tag{3}$$

With the aid of Equation (3), the relative magnitudes of all the undesired responses caused by interfering signals in conjunction with the harmonics formed in the mixer, and with harmonics from the local oscillator, may be determined by considering e_{oz}/e_n and e_{my}/e_n independently.

The undesired responses formed by the third or higher order harmonics from the local oscillator are analogous to those formed by its second harmonic. The frequencies of such undesired responses are generally farther away from the frequency of the desired signal, thus band-pass filters or a number of the conventional tuned circuits are usually effective in reducing such interference.

Two-Signal Interference, Independent of Local Oscillator

Any interference occurring in a UHF television receiver due to a frequency combination consisting of more than two interfering signals can be treated as if the interference is caused only by two interfering signals. In the case of three-signal interference, for instance, two of the three signals must be so related that a new frequency is formed which combines with the third signal to produce interference.

Cross Modulation

The frequency component in the form of $E_1^{m_1} E_2^{m_2} \cos \omega_1$ or $E_1^{m_1} E_2^{m_2} \cos \omega_2$ in the rectifier output current in the presence of two signals $E_1 \cos \omega_1$ and $E_2 \cos \omega_2$ represents the most important formation of cross modulation in UHF receivers. The modulation E_1 of the signal $E_1 \cos \omega_1$ is superimposed on the carrier $\cos \omega_2$ and vice versa.

To measure the relative magnitude of the cross-modulation response, one of the signal generators of the test setup shown in Figure 1 is tuned to the desired signal which is 30 per cent modulated at 400 cycles per second. The other signal generator is set at a different frequency also 30 per cent modulated but at 1000 cycles per second. The amplitude of the desired modulation, 400 cycles per second, is observed by an oscilloscope which is fed by a second detector connected to the output terminals of the i-f amplifier. The strength of the undesired signal is then increased so that the amplitude of the undesired modulation,

1000 cycles per second, is equal to that of the desired modulation. The ratio of the two signal generator outputs gives the relative "cross modulation ratio." In television receivers employing either a silicon or a germanium crystal rectifier as mixer, the cross modulation ratio usually exceeds 70 decibels.

The $n_1f_1 \pm n_2f_2 = f_i/h_m$ Responses

The most apparent case of the $n_1f_1 \pm n_2f_2 = f_i/h_m$ responses is of the form $f_1 = f_s \pm f_i$, where f_s is the frequency of the desired signal which is substituted for one of the two interfering signals. These responses are analogous to the $f_1 = f_o \pm f_i$ responses except for different relative magnitudes. To investigate the relative magnitudes of $f_s \pm f_i$ responses, the two signal generators of Figure 1 are isolated from each other by low-pass and high-pass filters of sharp cutoff characteristics. Each filter consists of six constant-K intermediate sections and one m-derived end section. The insertion loss in the pass band is about 3 decibels and the maximum attenuation beyond the cutoff frequencies is over 60 decibels. In each filter the rectified crystal current is prevented from flowing through the signal generator by a blocking capacitor.

It has been verified experimentally that with no selective circuits preceding the mixer of a UHF receiver, the magnitude of the image-frequency response is equal to that of the desired response for all practical purposes. It is equally true that the magnitude of the $f_s + f_i$ response is approximately the same as that of the $f_s - f_i$ response. Although there are two possible interfering signals for each harmonic being formed in the mixer, identical equivalent mixer efficiency in responding to each of such pairs of interfering signals will be observed.

Let e_{11} = equivalent mixer efficiency in responding to the $f_1 = f_2 \pm f_i$ interfering signals, approximately proportional to $\sqrt{E_1E_2}$,

e_{21} = equivalent mixer efficiency in responding to the $2f_1 = f_2 \pm f_i$ interfering signals,

e_{22} = equivalent mixer efficiency in responding to the $2f_1 = 2f_2 \pm f_i$ interfering signals,

$e_{11}e_{my}$ = equivalent mixer efficiency in responding to the $f_1 = f_2 \pm (1/y)f_i$ interfering signals.

Then the ratio e_{11}/e_n is the relative magnitude of the interfering signal $f_1 = f_2 \pm f_i$, and $e_{11}e_{m2}/e_n$ is the relative magnitude of the interfering signal $f_1 = f_2 \pm \frac{1}{2}f_i$, both of which are given in Figure 10 as a function of $\sqrt{E_1E_2}$. For a fixed strength of the interfering signal E_1,

the equivalent mixer efficiency e_{11} of the $f_2 \pm f_i$ response is higher with a stronger desired signal than it is with a weaker desired signal, if the desired signal is substituted for the second interfering signal E_2. If the strength of the desired signal is 3.0 millivolts, then the ratio e_{11}/e_n is —70 decibels in the presence of a 3.0-millivolt interfering signal at a frequency of either $f_s + f_i$ or $f_s - f_i$. The strength of the interfering signal must be increased to 30 millivolts for the same e_{11}/e_n ratio if the strength of the desired signal is 0.3 millivolt. All signals are measured across the input terminals of the mixer since no r-f selective circuits are used in the test setup.

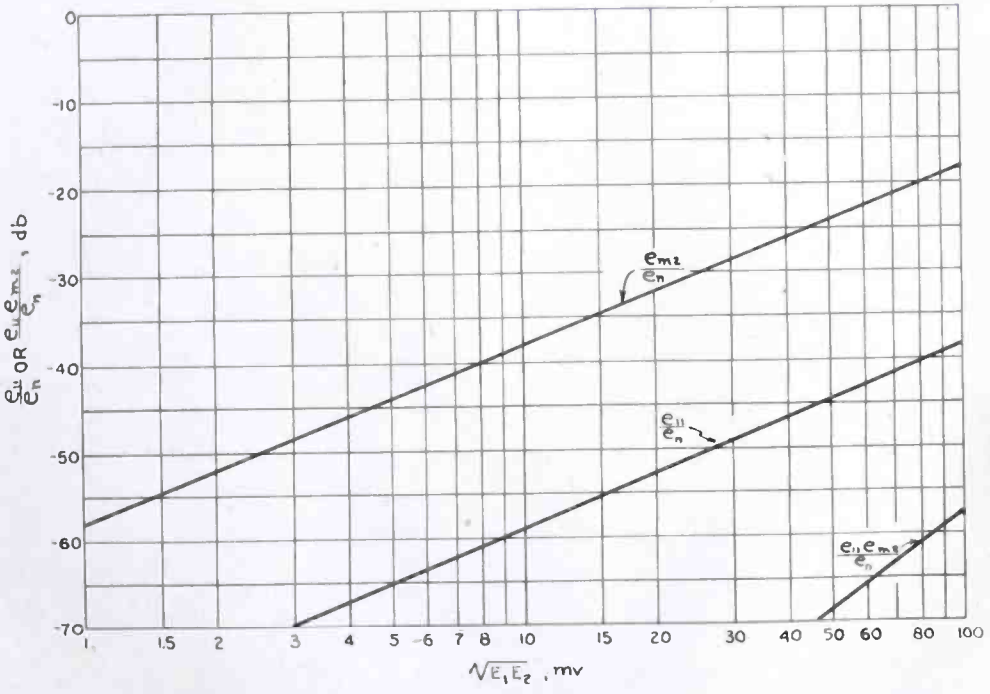

Fig. 10—Equivalent mixer efficiency e_{11} or e_s, in responding to two interfering signals independent of the local oscillator frequency, as a function of the quantity $\sqrt{E_1E_2}$.

The e_{m2}/e_n curve of Figure 6 is replotted in Figure 10 for comparison. It is noted that the sum of the e_{m2}/e_n and e_{11}/e_n curves coincides very closely with the $e_{11}e_{m2}/e_n$ curve. Therefore, the equivalent mixer efficiency $e_{11}e_{m2}$ depends upon two independent factors, e_{11} and e_{m2}, or

$$\frac{e_{11}e_{m2}}{e_n} \doteq \frac{e_{11}}{e_n} \cdot \frac{e_{m2}}{e_n}. \qquad (4)$$

The double frequency $2f_1$ of the $2f_1 = f_2 \pm f_i/h_m$ or $2f_2$ of the $f_1 = 2f_2 \pm f_i/h_m$ responses is formed in the mixer during the process of mixing. Under these conditions, the relationship established in Equation (4) is again valid. Therefore, it is necessary to consider only the simpler case of $2f_1 = f_2 \pm f_i$. The equivalent mixer efficiency e_{21} relative to e_n is approximately directly proportional to the strength of the interfering signal E_1 at frequency f_1 if the strength of the interfering signal E_2 at frequency f_2 is kept constant. It is independent of E_2 if E_1 is kept constant. Curves showing the equivalent mixer effi-

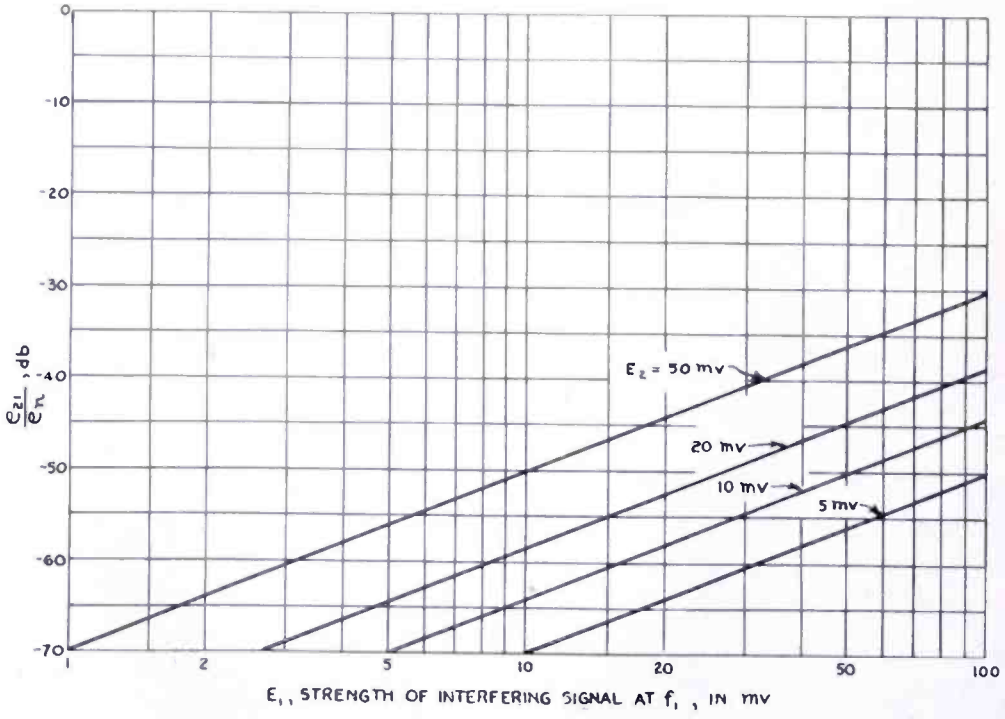

Fig. 11—Equivalent mixer efficiency e_{21} as a function of E_1 when E_2 is kept constant.

ciency e_{21} in responding to the interfering signal at f_1, with constant strength of the interfering signal at f_2, are illustrated in Figure 11. If both E_1 and E_2 are equal, the ratio e_{21}/e_n is —70 decibels when $E_1 = E_2 = 7.5$ millivolts which is to be compared with 3.0 millivolts for e_{11}/e_n. The relative magnitude of e_{21}/e_n is, accordingly, somewhat lower than that of e_{11}/e_n, but its importance can be appreciated by considering the fact that any transmission or radiation at frequencies somewhere between 200 and 500 megacycles may form $2f_1 \pm f_2 = f_i/h_m$ responses in a UHF television receiver in conjunction with the desired or other UHF television signals.

The equivalent mixer efficiency e_{22} relative to e_n is usually more

than —70 decibels for interfering signals up to 25 millivolts. Such undesired responses, therefore, become important only in the presence of extremely strong interfering signals.

Two-Signal Interference, Dependent on Local Oscillator

The undesired responses which fall into this general group are analogous to the $n_1f_1 \pm n_2f_2 = f_i/h_m$ responses, but they are more complicated by the fact that the signal from the local oscillator is also applied to the mixer in addition to the two interfering signals. Accordingly, the general form of such undesired responses may be represented as follows:

$$n_1f_1 \pm n_2f_2 = zf_o \pm f_i/h_m. \tag{5}$$

The simplest case of the responses indicated in Equation (5) is $f_1 \pm f_2 = f_o \pm f_i$. The frequencies f_1 and f_2 of the two interfering signals are combined to form a new frequency, either $f_1 + f_2$ or $f_1 - f_2$, which heterodynes with the local oscillator frequency to produce a signal at the intermediate frequency f_i.

The new frequency formed by f_1 and f_2 corresponds to the frequency of the desired signal or the image signal of the receiver. However, the relative magnitudes of the desired signal and the $f_1 + f_2 = f_o \pm f_i$ responses are substantially different owing to the fact that the equivalent mixer efficiency in responding to a signal at a frequency of $f_o + f_i$ or $f_o - f_i$ is much lower if the frequency is formed in the mixer by two signals of different frequencies than if it is a single signal at that frequency. Let

e'_{11} = equivalent mixer efficiency in responding to the $f_1 \pm f_2 = f_o \pm f_i$ responses,

e'_{21} = equivalent mixer efficiency in responding to the $2f_1 \pm f_2 = f_o \pm f_i$ responses,

$e'_{11}e_{my}$ = equivalent mixer efficiency in responding to the $f_1 \pm f_2 = f_o \pm f_i/h_m$ responses,

$e'_{11}e_{oz}$ = equivalent mixer efficiency in responding to the $f_1 \pm f_2 = zf_o \pm f_i$ responses, and

$e'_{11}e_{oz}e_{my}$ = equivalent mixer efficiency in responding to the $f_1 \pm f_2 = zf_o \pm f_i/h_m$ responses.

Then e'_{11}/e_n is the relative magnitude of the $f_1 \pm f_2 = f_o \pm f_i$ responses and is again approximately proportional to the quantity $\sqrt{E_1E_2}$.

The ratios e'_{11}/e_n and $e'_{11}e_{02}/e_n$ are plotted in Figure 12. It is again noted that

$$\frac{e'_{11}e_{02}}{e_n} \doteq \frac{e'_{11}}{e_n} \cdot \frac{e_{02}}{e_n}. \tag{6}$$

Therefore,

$$\frac{e'_{11}e_{oz}e_{my}}{e_n} \doteq \frac{e'_{11}}{e_n} \cdot \frac{e_{oz}}{e_n} \cdot \frac{e_{my}}{e_n}. \tag{7}$$

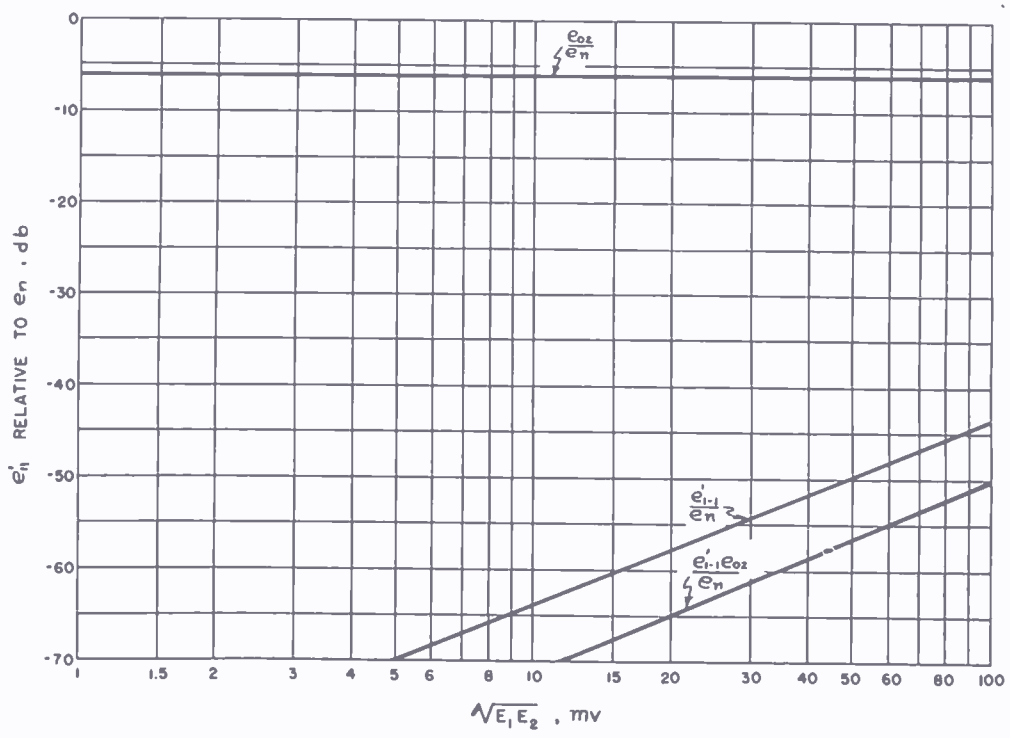

Fig. 12—Equivalent mixer efficiency e'_{11} as a function of E_2 when E_1 is kept constant.

The relative magnitude of e'_{21}/e_n is, as in the case of e_{21}/e_n, approximately directly proportional to the strength of the interfering signal E_1 at frequency f_1 if the strength of the interfering signal E_2 at frequency f_2 is kept constant. It is independent of E_2 if E_1 is kept constant. The ratio e'_{11}/e_n is approximately one half of the ratio e_{11}/e_n if the strengths of the respective interfering signals in these two cases are equal.

The undesired responses in the form $2f_1 \pm f_2 = zf_o \pm f_i/h_m$ are equally as important as those in the form $f_1 \pm f_2 = zf_o \pm f_i/h_m$. It is obvious that the UHF television channels higher in frequency than the channel being tuned in and the VHF television channels or FM broad-

cast signals may produce responses in the form $f_1 - f_2 = f_o \pm f_i/h_m$, while the UHF television channels lower in frequency than the channel being tuned in and the VHF television channels or FM broadcast signals may produce undesired responses in the form $f_1 + f_2 = f_o \pm f_i/h_m$. Similarly, undesired responses in the form $2f_1 \pm f_2 = zf_o \pm f_i/h_m$ may be formed by two VHF television channels or FM broadcast signals, or by one UHF television channel and one VHF television channel or FM broadcast signal. Of course, interfering signals from other sources may cause interference of both types.

Equivalent mixer efficiency e'_{22} in responding to $2f_1 \pm 2f_2 = f_o \pm f_i$ interfering signal, relative to e_n, is down more than 70 decibels for signal strength up to about 50 millivolts. Consequently undesired responses of this particular frequency combination and other combinations of higher order harmonics formed in the mixer are important only in the presence of extremely strong interfering signals.

ACKNOWLEDGMENT

The author wishes to acknowledge the valuable work contributed by C. W. Wittenburg, H. M. Wasson, and Lt. Commander W. W. Vallandigham, and the suggestions given by C. M. Sinnett and W. R. Koch during the course of the investigation.

A STUDY OF GROUNDED-GRID, ULTRA-HIGH-FREQUENCY AMPLIFIERS*

By

T. Murakami

Home Instrument Department, RCA Victor Division,
Camden, N. J.

Summary—A theoretical and experimental study has been made of the grounded-grid amplifier for use in the ultra-high-frequency range. Curves of voltage gain for various band widths have been computed and measured for amplifiers using several currently available tubes. The noise factor curves of amplifiers with matched or mismatched input or output circuits are given. The theoretical improvement in amplifier performance obtained by changing some of the tube constants of the pencil triode has been calculated. Experimental curves of signal attenuation from output to input are shown for an amplifier using a 5876 pencil triode or a 416A triode.

Introduction

ULTRA-HIGH-FREQUENCY amplifiers will probably be needed for antenna distribution systems, and as low noise preamplifiers for weak signal locations, even though high cost may prevent their general adoption in home receivers. Many types of amplifiers, such as traveling wave tubes, may be used but the grounded-grid triode type of amplifier appears to be the most satisfactory at present. A study of grounded-grid amplifiers for the ultra-high-frequency television band has been made. One of the main purposes of this investigation was to determine the best possible amplifier performance obtainable using several different ultra-high-frequency triodes. One of the functions of an amplifier stage is to increase the ability of the receivers to detect weak signals. Since a receiver using a crystal mixer and a low-noise intermediate-frequency amplifier may have a noise factor of between 10 and 13 decibels, a receiver with a radio-frequency amplifier would have to have a lower noise factor to be justified. The use of a grounded-grid amplifier with a low plate-to-cathode capacitance also reduces the amount of oscillator radiation through the antenna circuit.

Circuit Equations

The grounded-grid amplifier has been analyzed previously,[1-3] therefore, only the results of the analysis will be presented here.

---

* Decimal Classification: R363.1 × R310.

[1] E. W. Herold, "An Analysis of the Signal-to-Noise Ratio of Ultra-High-Frequency Receivers," *RCA Review*, Vol. VI, pp. 302-332, January, 1942.

Figure 1 shows a circuit diagram of the grounded-grid amplifier. In this analysis the effects of lead inductance in the grid circuit have been neglected since the tubes considered are of the disk-sealed variety with low lead inductance. Also the plate-to-cathode capacitance has been considered negligible.

The output impedance of the tube can be shown to be

$$Z_o = \frac{\mu + 1}{\frac{1}{R_1 N_1^2} + \frac{1}{R_t} + \frac{1}{R_\Omega}} + R_p. \tag{1}$$

The input impedance is given by

$$Z_i = \frac{E}{I_i} = \frac{(R_p + R_L)\, R_t}{[R_p + R_L + (\mu + 1)\, R_t]}. \tag{2}$$

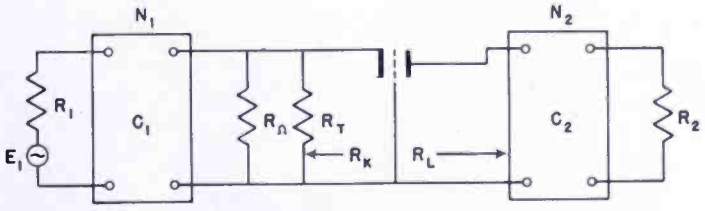

Fig. 1—Grounded-grid amplifier.

E_1 = open-circuit voltage of generator
R_1 = generator resistance
C_1 = input coupling network which includes grid-to-cathode capacitance
N_1 = effective voltage step-up ratio of C_1
R_Ω = effective resistance due to ohmic losses in the input network
R_t = resistance due to transit-time loading
R_k = effective resistance looking back from cathode to input
R_L = effective load resistance looking from the plate circuit $R_L = R_2/N_2^2$
C_2 = output coupling network which includes grid-to-plate capacitance
N_2 = effective voltage step-up ratio of C_2
R_2 = resistance termination of C_2

---

[2] Milton Dishal, "Theoretical Gain and Signal-to-Noise Ratio of the Grounded-Grid Amplifier at Ultra-High Frequencies," *Proc. I.R.E.*, Vol. 32, pp. 276-280, May, 1944.

[3] G. E. Valley and H. Wallman, *Vacuum Tube Amplifiers*, Vol. 18, Radiation Laboratories Series, pp. 621-635, McGraw-Hill Book Co., Inc., New York, N. Y., 1948.

The voltage gain of the amplifier is given by the ratio of the voltage V_2, across the final load resistor R_2, to the input voltage E_1.

$$G = \frac{V_2}{E_1} = \frac{(\mu + 1)\, N_1 N_2}{1 + \dfrac{R_1 N_1^2}{R_t} + \dfrac{R_1 N_1^2}{R_\Omega} + \dfrac{R_p N_2^2}{R_2} + \left[1 + \dfrac{R_t}{R_\Omega} + (\mu + 1)\dfrac{R_t}{R_p}\right]\dfrac{R_1 R_p N_1^2 N_2^2}{R_2 R_t}}. \quad (3)$$

Since E_1 is the open circuit generator voltage, the gain with reference to a terminated generator will be $2G$. In the ultra-high-frequency range, high-Q coaxial lines may be used as elements of the networks so that R_Ω may be made quite large compared to R_t and the transformed source impedance, $R_1 N_1^2$; R_Ω terms can therefore be neglected.[4] In this case the gain equation becomes

$$G \cong \frac{(\mu + 1)\, N_1 N_2}{1 + \dfrac{R_1 N_1^2}{R_t} + \dfrac{R_p N_2^2}{R_2} + \left[1 + (\mu + 1)\dfrac{R_t}{R_p}\right]\dfrac{R_p R_1 N_1^2 N_2^2}{R_2 R_t}}. \quad (4)$$

The maximum gain is given when both the input and output impedances are matched. This can be shown by setting $\dfrac{\partial G}{\partial N_1} = \dfrac{\partial G}{\partial N_2} = 0$, using Equation (4). When this is done the resulting values N_1^2 and N_2^2 are found.

$$N_1^2 = \frac{(R_p + R_2/N_2^2)\, R_t}{R_1 [R_p + R_2/N_2^2 + (\mu + 1)\, R_t]}, \quad (5)$$

$$N_2^2 = \frac{R_2}{R_p + \dfrac{R_t R_1 N_1^2 (\mu + 1)}{R_t + R_1 N_1^2}}. \quad (6)$$

[4] F. E. Terman, *Radio Engineers Handbook*, p. 192, McGraw-Hill Book Company, Inc., New York, N. Y., 1943.

If these equations are solved simultaneously for N_1^2 and N_2^2, then

$$N_1^2 = \frac{R_t}{R_1\left[1 + (\mu+1)\frac{R_t}{R_p}\right]^{\frac{1}{2}}}, \tag{7}$$

$$N_2^2 = \frac{R_2}{R_p\left[1 + (\mu+1)\frac{R_t}{R_p}\right]^{\frac{1}{2}}}. \tag{8}$$

If these values for N_1 and N_2 are substituted in Equation (4), the following expression for maximum gain is obtained:

$$G_{max} = \frac{(\mu+1)\sqrt{R_2/R_1}}{2\sqrt{R_p/R_t} + 2\sqrt{\mu+1+R_p/R_t}}. \tag{9}$$

In most ultra-high-frequency applications it will be desirable to match the input impedance of the amplifier to the source impedance. If the particular value of N_1 given by Equation (5) is substituted in Equation (4) and simplified, the gain for matched input impedance will be given by

$$G = \frac{(\mu+1)\sqrt{R_2/R_1}\sqrt{R_2/N_2^2}}{2\sqrt{(R_p + R_2/N_2^2)\left[(\mu+1) + (R_p + R_2/N_2^2)/R_t\right]}}. \tag{10}$$

If $R_1 = R_2$ and $R_2/N_2^2 = R_L$, then

$$G = \frac{\mu+1}{2\sqrt{\frac{R_p+R_L}{R_L}\left(\mu+1+\frac{R_p+R_L}{R_t}\right)}}. \tag{11}$$

Since gain in most cases is meaningless unless band width is specified, a method for determining gain for a given band width is shown. For a single-tuned output circuit, the load resistance, R_L, must be chosen such that when it is placed in parallel with the plate output impedance, the proper load is provided for the given band width. It is assumed here that the input circuit, due to the low effective shunt

resistance and the capacitances involved, is sufficiently broad so as to contribute little to the selectivity.

$$R'_L = \frac{R_0 R_L}{R_0 + R_L} = \frac{1}{2\pi C_{gp} \Delta f}, \tag{12}$$

where

$$R_0 = R_p + \frac{(\mu + 1)\, R_t R_1 N_1^2}{R_t + R_1 N_1^2}, \tag{13}$$

C_{gp} = tube grid to plate capacitance, and

Δf = band width of output circuit.

For the matched input condition, Equation (13) becomes

$$R_0 = R_p + \frac{(\mu + 1)\, R_t}{2 + \dfrac{(\mu + 1)\, R_t}{R_p + R_L}}. \tag{14}$$

With R'_L determined for a given band width, Equations (12) and (14) must be solved simultaneously for R_L. Another method of determining R_L is to plot a family of curves of R_0 versus R_L for various frequencies (R_t held constant for a particular frequency) using Equation (14). A family of these curves is shown in Figure 2 for the 5876 pencil tube. Figure 3 shows a similar family of curves for the 416A,[5,6] a high transconductance, planar type of triode. With R'_L known, it is not difficult to determine R_0 and R_L by the trial and error method for any frequency shown on the curves. Figures 2 and 3 also show curves of R'_L for various band widths.

The approximate input loading curves for several ultra-high-frequency triodes[7,8] are shown in Figure 4. The tube constants for several ultra-high-frequency triodes are shown in Table I. The gain of a

[5] J. A. Morton and R. M. Ryder, "Design Factors of the Bell Telephone Laboratories 1553 Triode," *Bell Sys. Tech. Jour.*, Vol. 29, pp. 496-530, October, 1950.

[6] A. E. Bowen and W. W. Mumford, "A New Microwave Triode: Its Performance as a Modulator and as an Amplifier," *Bell Sys. Tech. Jour.*, Vol. 29, pp. 531-552, October, 1950.

[7] S. D. Robertson, "Electronic Admittance of Parallel-Plane Electron Tubes at 4000 Megacycles," *Bell Sys. Tech. Jour.*, Vol. 28, pp. 619-646, October, 1949.

[8] G. M. Rose, D. W. Power, and W. A. Harris, "Pencil-Type UHF Triodes," *RCA Review*, Vol. 10, pp. 321-338, September, 1949.

grounded-grid 5876 pencil triode amplifier was computed using Equation (11) for various band widths and the results are plotted in Figure 5. All of the computed gain curves are with respect to a terminated generator, therefore equal to $2G$. In Figure 6, the gain curves are shown for the 416A tube. It is noted that the 416A amplifier has approximately 10 decibels more gain than the pencil tube in

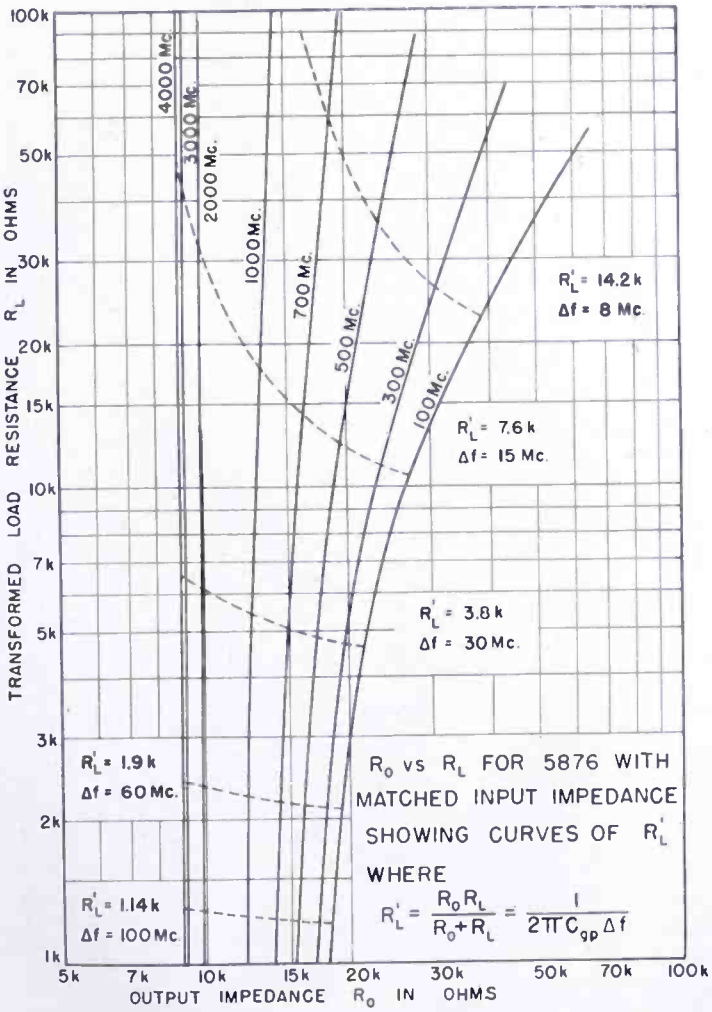

Fig. 2—R_0 versus R_L for 5876 with matched input impedance showing curves of R'_L where $R'_L = \dfrac{R_0 R_L}{R_0 + R_L} = \dfrac{1}{2\pi C_{gp} \Delta f}$.

the 500- to 900-megacycle frequency range. The maximum-gain curves for several ultra-high-frequency triodes shown in Figure 7 were computed using Equation (9) with $R_1 = R_2$. As indicated in Table I, tubes X and Y (hypothetical pencil-type tubes) have higher transconductance than the 5876. The g_m and μ were increased on tube X in order that the

gain and, as is shown later, the noise factor be improved over that of the 5876. In tube Y only the g_m is substantially changed and the improvement in gain is less than 2 decibels in the 500- to 900-megacycle frequency range. With tube X, an improvement of approximately 5 decibels over the gain of the 5876 in the same frequency range is obtained.

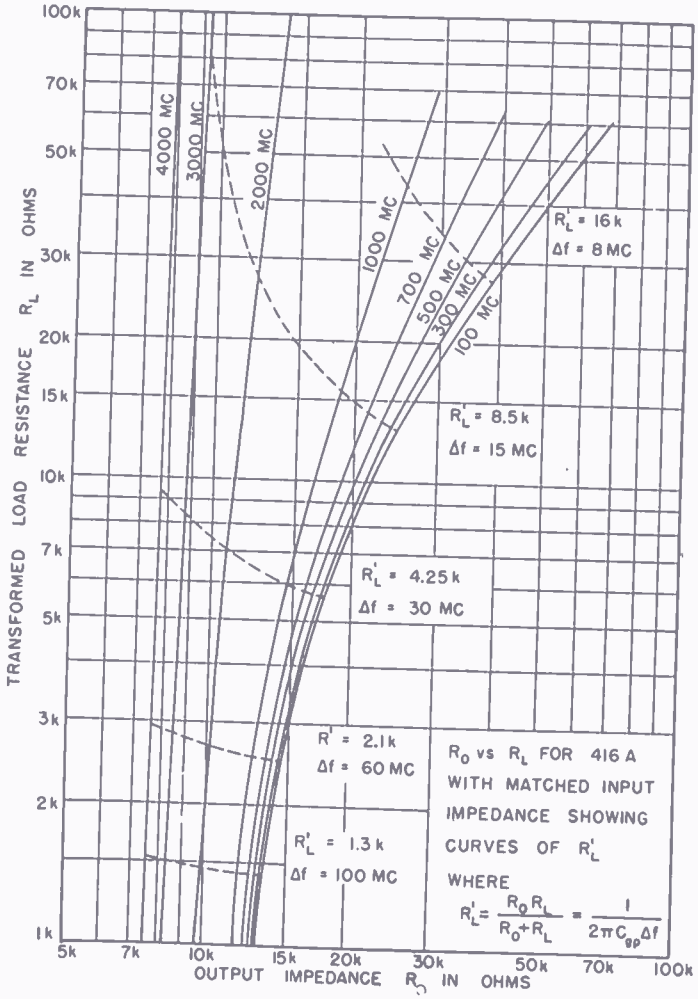

Fig. 3—R_o versus R_L for 416A with matched input impedance showing curves of R'_L where $R'L = \dfrac{R_o R_L}{R_o + R_L} = \dfrac{1}{2\pi C_{gp} \Delta f}$.

Under matched input and output conditions Equation (13) reduces to

$$R_0 = R_p \left[1 + (\mu + 1) \frac{R_t}{R_p} \right]^{\frac{1}{2}} \tag{15}$$

or

$$R_0 = R_2/N_2^2 = R_L. \tag{16}$$

R'_L then becomes equal to $R_0/2$ and the equation for band width for an amplifier using a single-tuned output circuit and adjusted for maximum

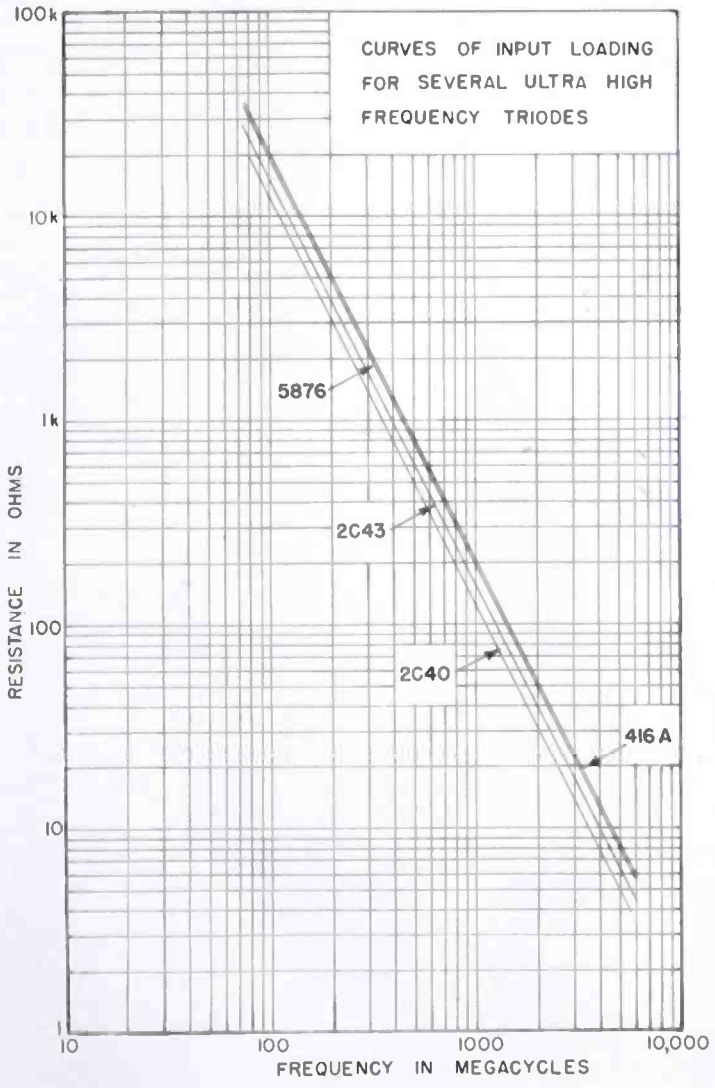

Fig. 4—Curves of input loading for several ultra-high-frequency triodes.

gain is given by

$$\Delta f = \frac{1}{\pi C_{gp} R_0}$$

$$= \frac{1}{\pi C_{gp} R_p \sqrt{1 + (\mu + 1) R_t / R_p}}, \qquad (17)$$

using Equations (12) and (15). The band-width curves corresponding to the maximum-gain curves in Figure 7 are shown in Figure 8.

Table I

Tube Type	Grid to Plate Cap. C_{gp} $\mu\mu f$	Grid to Cathode Cap. C_{gk} $\mu\mu f$	Cathode to Plate Cap. C_{pk} $\mu\mu f$	Amplification Factor μ	Plate Resistance R_p ohms	Plate Current I_p ma	Transconductance g_m μmhos	Equiv. Noise Resistance R_{eq} ohms
5876	1.4	2.5	0.035	56	8625	18	6,500	385
416A	1.25	7.5	0.01	300	6000	30	50,000	50
2C40	1.3	2.1	0.02	36	7500	16.5	4,800	521
2C43	1.7	2.8	0.02	48	6000	20	8,000	312
X	1.4			129	8600		15,000	167
Y	1.4			65	6500		10,000	250

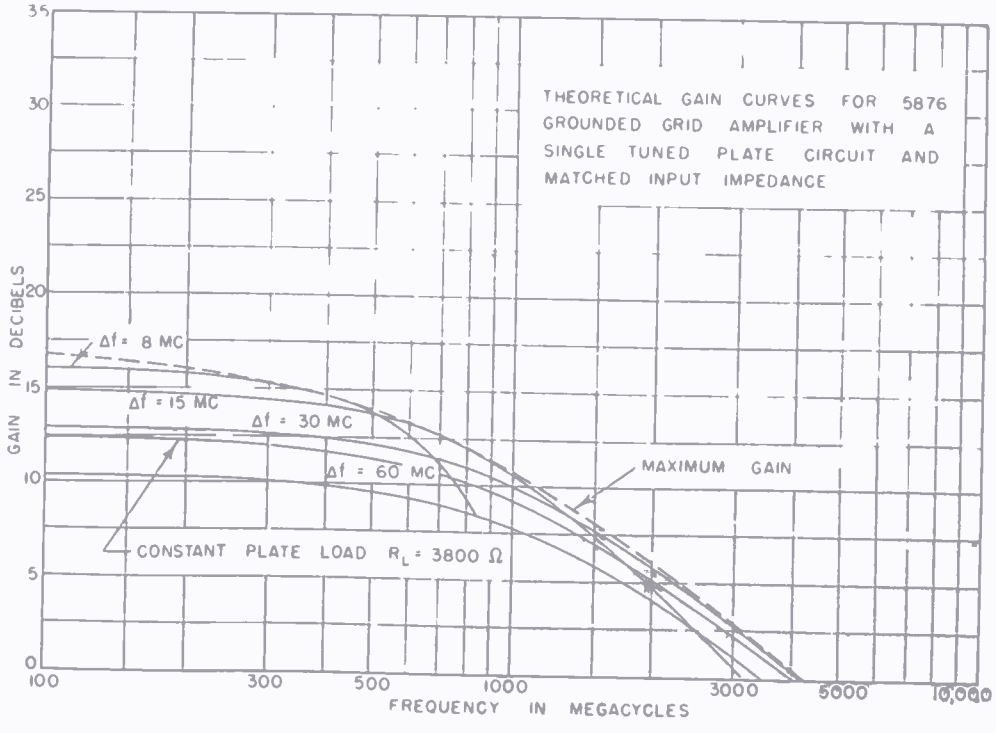

Fig. 5—Theoretical gain curves for 5876 grounded-grid amplifier with a single-tuned plate circuit and matched input impedance.

Experimental Results

The experimental gain and band-width curves were obtained using a 5876 pencil-triode grounded-grid amplifier and a 416A grid-separation amplifier. Photographs of these amplifiers are shown in Figures 9 and 10. A block diagram of the amplifier and measuring equipment is shown in Figure 11. The input matching stub and the 50-ohm termina-

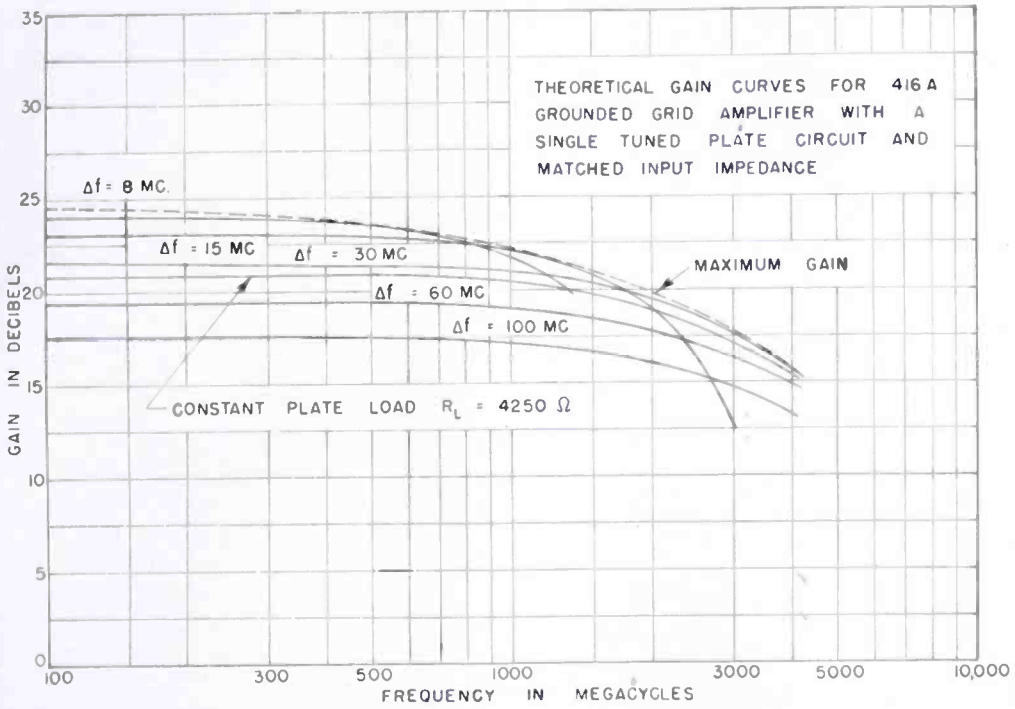

Fig. 6—Theoretical gain curves for 416A grounded-grid amplifier with a single-tuned plate circuit and matched input impedance.

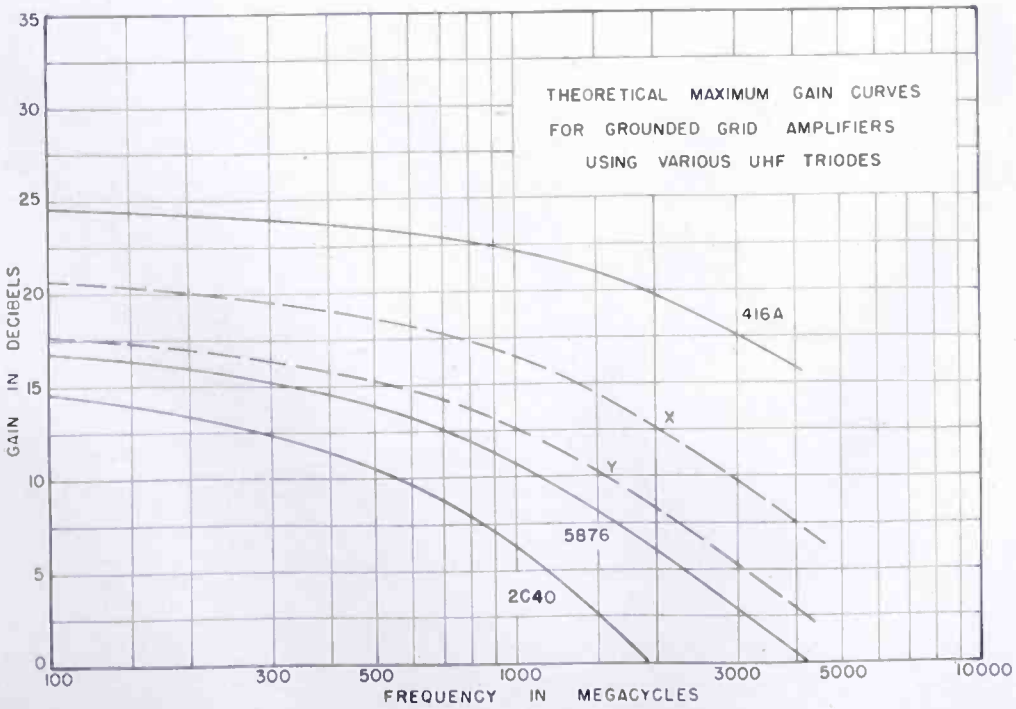

Fig. 7—Theoretical maximum-gain curves for grounded-grid amplifiers using various UHF triodes.

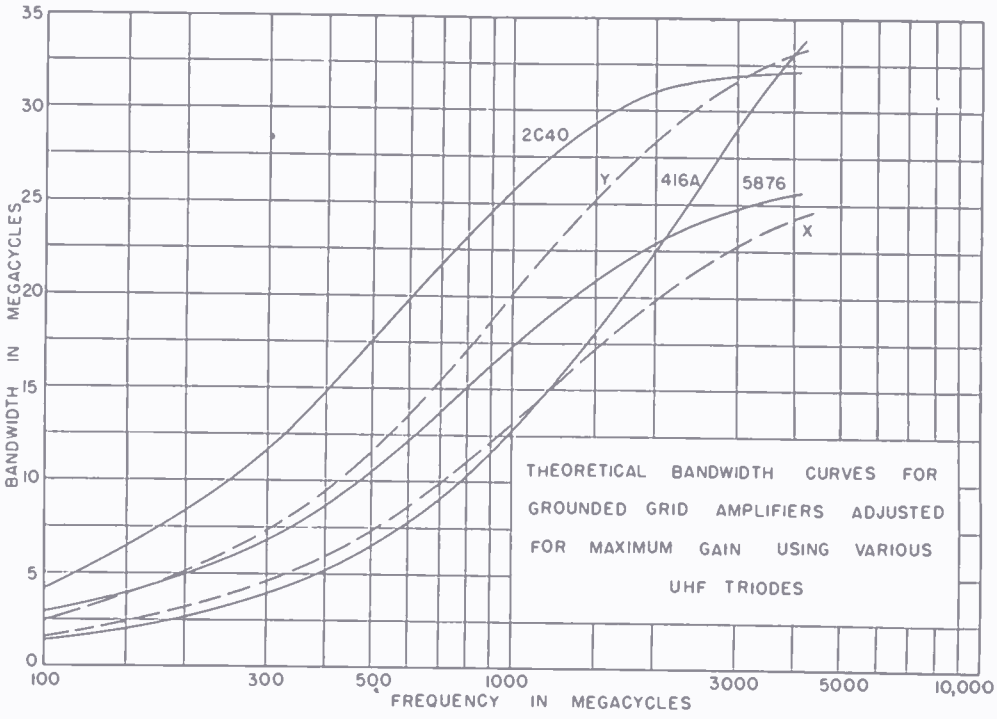

Fig. 8—Theoretical band-width curves for grounded-grid amplifiers adjusted for maximum gain using various UHF triodes.

tion and detector combination is shown in Figure 9. The experimental gain and band-width curves for the two amplifiers are shown in Figure 12. The experimental gain is about 2.5 decibels lower than the theoretical for the 416A amplifier and 1 decibel lower for the 5876 amplifier in the frequency range covered in the measurements.

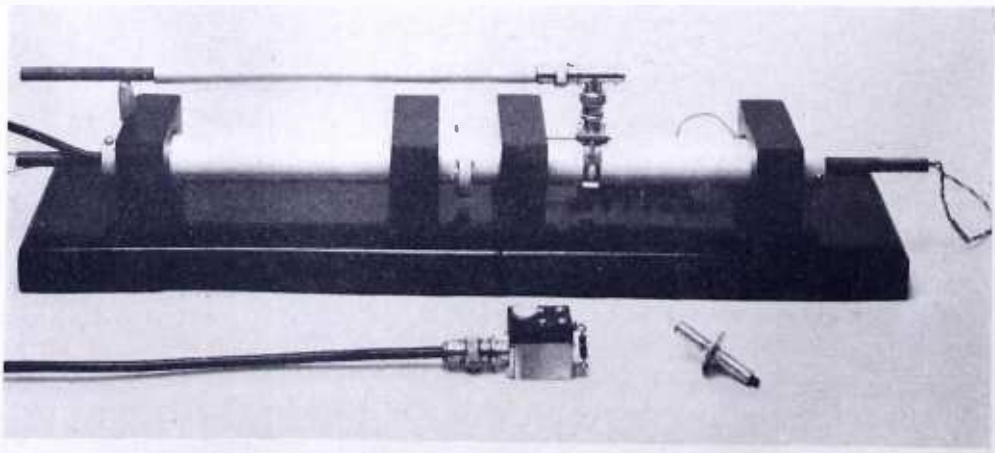

Fig. 9—5876 grounded-grid amplifier.

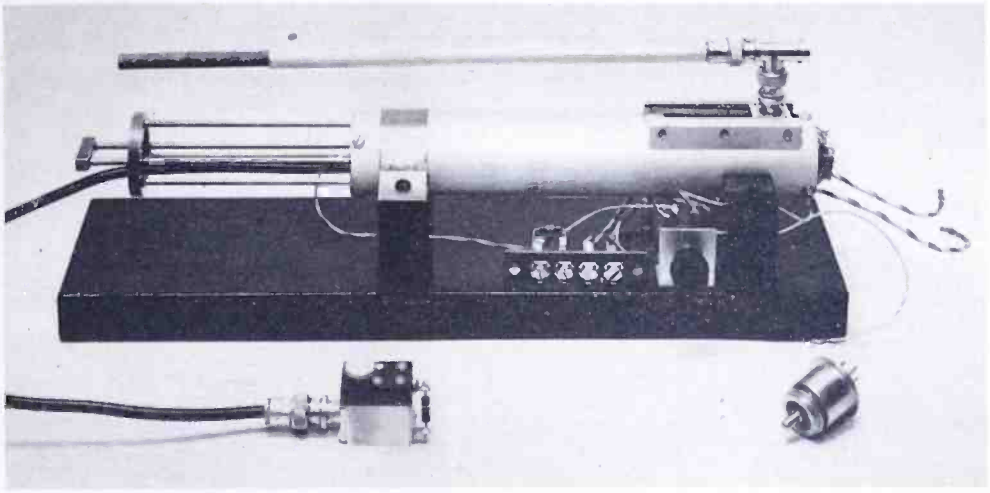

Fig. 10—416A grid-separation amplifier.

Noise Factor Considerations

By an analysis similar to that given by Dishal,[2] the signal-to-noise ratio can be shown to be

$$\frac{V^2_{\text{signal}}}{V^2_{\text{noise}}} = \frac{E_1^2}{4kT\Delta f R_1 \left[1 + \frac{R_1 N_1^2}{R_\Omega} + 5\frac{R_1 N_1^2}{R_t} + \frac{\mu^2}{(\mu+1)^2}\left(1 + \frac{R_1 N_1^2}{R_t} + \frac{R_1 N_1^2}{R_\Omega}\right)^2 \frac{R_{eq}}{R_1 N_1^2} \right]}. \tag{18}$$

This equation gives the signal-to-noise power ratio since both the signal and noise voltages are across the same resistance. The ratio of the total mean-square noise voltage produced across the output terminals of the amplifier to the mean-square noise voltage produced by the thermal-noise generator associated with the source resistance is called

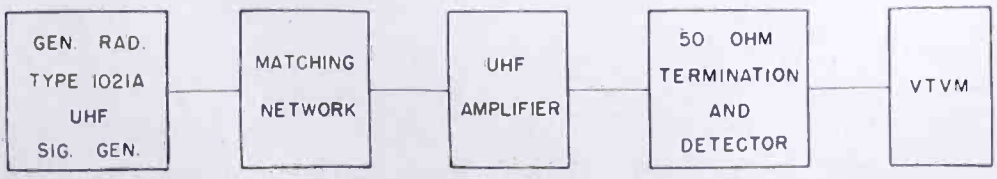

Fig. 11—Block diagram of measuring equipment.

the noise factor of the amplifier. The noise factor is given by the coefficient of $4kT\Delta fR_1$ in the denominator of Equation (18), since $4kT\Delta fR_1$ is the mean-square open circuit noise voltage produced by the resistance R_1.

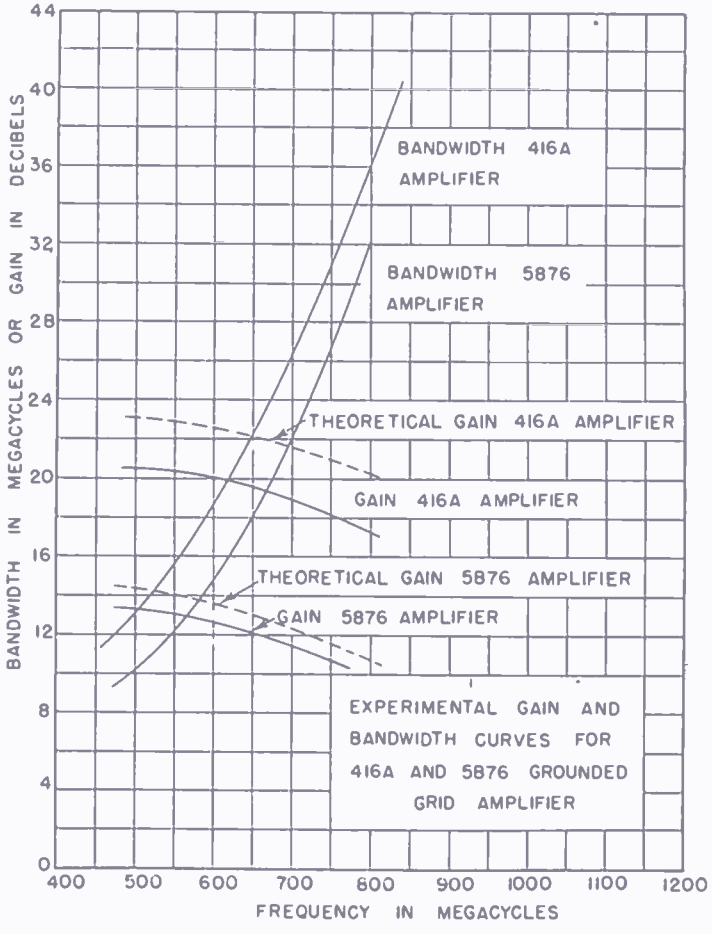

Fig. 12—Experimental gain and band-width curves for 416A and 5876 grounded-grid amplifiers.

$$F = 1 + \frac{R_1N_1^2}{R_\Omega} + 5\frac{R_1N_1^2}{R_t} + \frac{\mu^2}{(\mu+1)^2}\left(1 + \frac{R_1N_1^2}{R_t} + \frac{R_1N_1^2}{R_\Omega}\right)^2 \frac{R_{eq}}{R_1N_1^2}. \qquad (19)$$

If R_Ω is very high compared to the transformed source resistance $R_1N_1^2$ so that the terms containing it may be neglected, the noise-factor equation becomes

$$F = 1 + 5\frac{R_1 N_1^2}{R_t} + \frac{\mu^2}{(\mu+1)^2}\left(1 + \frac{R_1 N_1^2}{R_t}\right)^2 \frac{R_{eq}}{R_1 N_1^2}. \tag{20}$$

When the input and output impedances are both matched to give maximum gain, Equation (20) can be written as

$$F = 1 + 5\frac{\alpha}{R_t} + \frac{\mu^2}{(\mu+1)^2}\left(1 + \frac{\alpha}{R_t}\right)^2 \frac{R_{eq}}{\alpha}. \tag{21}$$

where $\alpha = R_t\left[1 + (\mu+1)\frac{R_t}{R_p}\right]^{-\frac{1}{2}}$

With the input impedance matched and the output impedance mismatched to give the required band width, the value of α in Equation (21) is changed to

$$\alpha = \frac{R_p + R_L}{\mu + 1 + \frac{R_p + R_L}{R_t}}. \tag{22}$$

The noise factor can be made a minimum if the input impedance is mismatched. The particular value of the step-up ratio N_1 which gives the minimum noise factor can be found by setting $\frac{\partial F}{\partial N_1} = 0$ using Equation (20). If this is done, the resulting transformed source impedance is given by

$$R_1 N_1^2 = \left[1 + 5\frac{(\mu+1)^2 R_t}{\mu^2 R_{eq}}\right]^{-\frac{1}{2}}. \tag{23}$$

The over-all noise factor of two networks a and b in cascade is given by Equation (24) provided the effective band width of each is the same.

$$F_{ab} = F_a + \frac{F_b - 1}{W_a}, \tag{24}$$

where F_{ab} = noise factor of the combination,

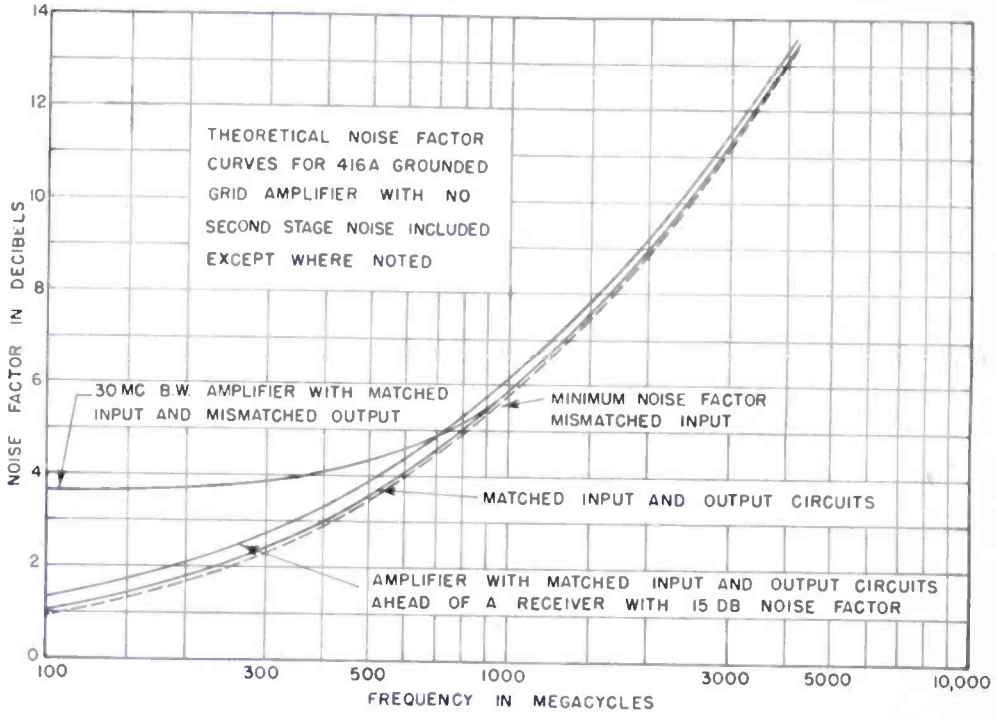

Fig. 13—Theoretical noise-factor curves for 416A grounded-grid amplifier with no second-stage noise included except where noted.

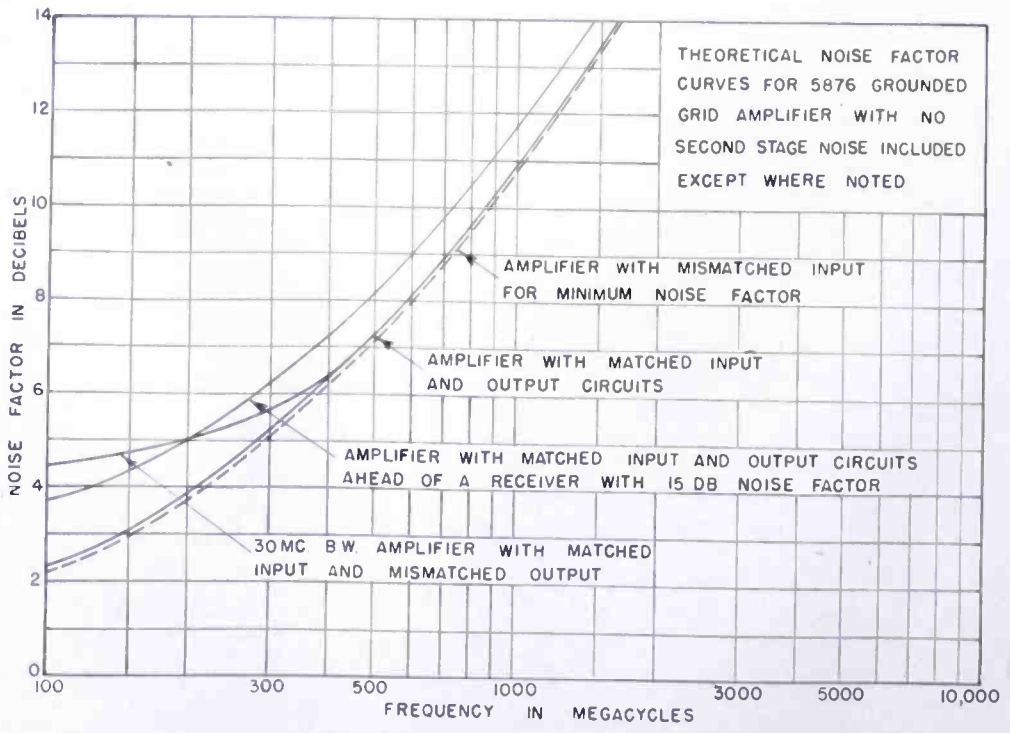

Fig. 14—Theoretical noise-factor curves for 5876 grounded-grid amplifier with no second-stage noise included except where noted.

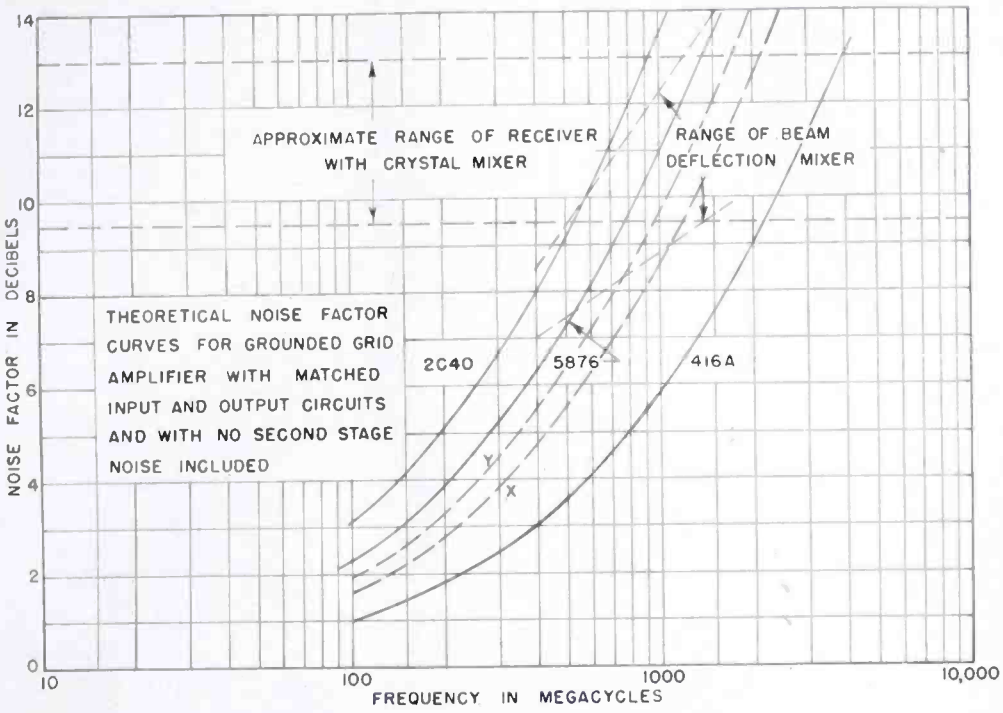

Fig. 15—Theoretical noise-factor curves for grounded-grid amplifier with matched input and output circuits and with no second-stage noise included.

F_a = noise factor of first network,

F_b = noise factor of second network, and

W_a = available power gain of the first network.

Several noise-factor curves were calculated for the 416A and 5876 triode grounded-grid amplifiers using Equations (20) to (24). Figure 13 shows curves for the 416A amplifier. It is noted that with a mismatched output circuit the noise factor is increased over that of the matched case, at the lower end of the frequency range shown. However, at 500 megacycles the deterioration is only one decibel for a 30-megacycle band width. Also the improvement in the noise factor obtained by mismatching the input circuit is negligible. Figure 14 shows similar noise-factor curves for the 5876 pencil-triode grounded-

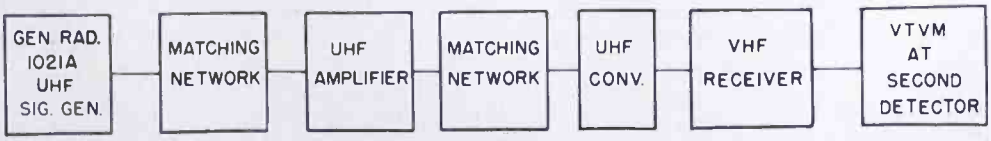

Fig. 16—Block diagram of noise-factor measuring equipment.

grid amplifier. When the pencil-tube amplifier is used ahead of a receiver with a 15-decibel noise factor, the noise factor of the combination is approximately 1 decibel greater than that of the pencil tube alone. When two stages of amplification are used, this difference will be made negligible in the 500- to 900-megacycle range. In the case of the 416A, there is approximately 0.3 decibel difference in the noise-factor curve of the tube alone and that of the combination.

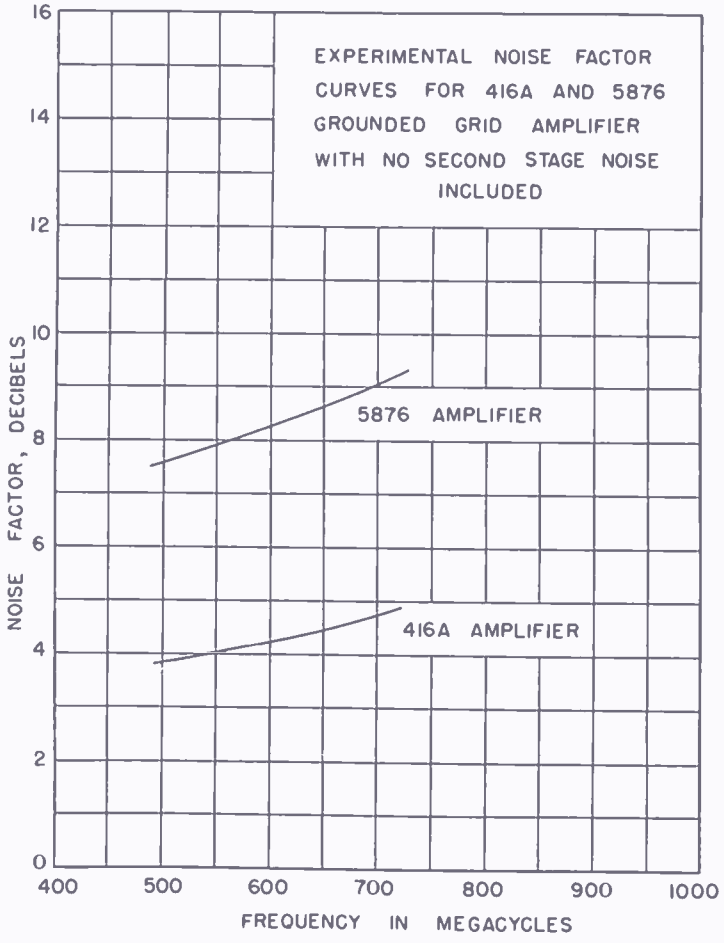

Fig. 17—Experimental noise-factor curves for 416A and 5876 grounded-grid amplifiers with no second-stage noise included.

Figure 15 shows the theoretical noise-factor curves for the grounded-grid amplifier using several different ultra-high-frequency tubes. The approximate noise factor of a receiver using a crystal mixer is also shown. The noise factor curves of tubes X and Y, which were previously discussed, are shown in Figure (15). If tube X were to be used in a grounded-grid amplifier ahead of a receiver with a 15-decibel noise factor, the over-all noise factor would be approximately 2.5 decibels better than the same receiver preceded by a

5876 amplifier. With tube Y this difference would be approximately 1 decibel due to the lower gain and higher noise factor of tube Y compared to tube X.

Experimental Results

Noise-factor measurements were made using the 416A and 5876 grounded-grid amplifiers. The signal-generator method was used to

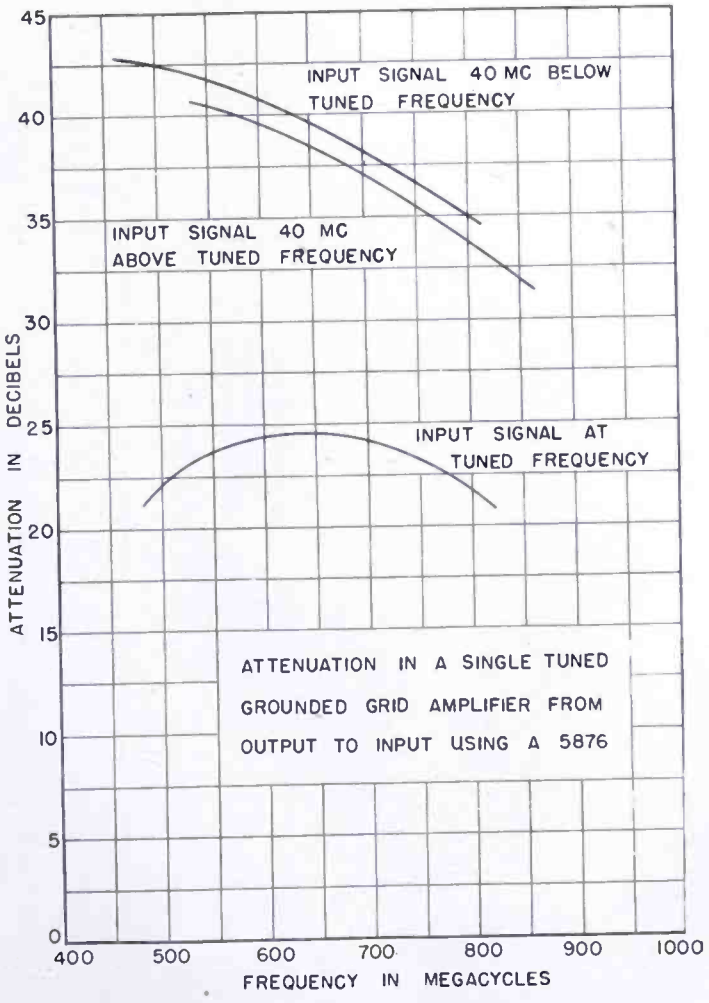

Fig. 18—Attenuation in a single-tuned, grounded-grid amplifier from output to input using a 5876.

obtain the noise factor of these amplifiers. A block diagram of the amplifier and associated measuring equipment is shown in Figure 16. The results which are shown in Figure 17 agree very well with the theoretical values for noise factor.

Signal Attenuation From Output To Input

The attenuation that a grounded-grid amplifier provides for signals from the output circuit to the input circuit was determined experimentally. Figure 18 shows the attenuation for signals at the tuned frequency of the 5876 pencil-tube amplifier and signals 40 megacycles above and below the tuned frequency. This corresponds to a receiver with a 40-megacycle intermediate frequency with the oscillator above or below the signal frequency. Similar curves are shown for the 416A tube in Figure 19. These curves were measured with the tubes in the amplifiers under operating conditions.

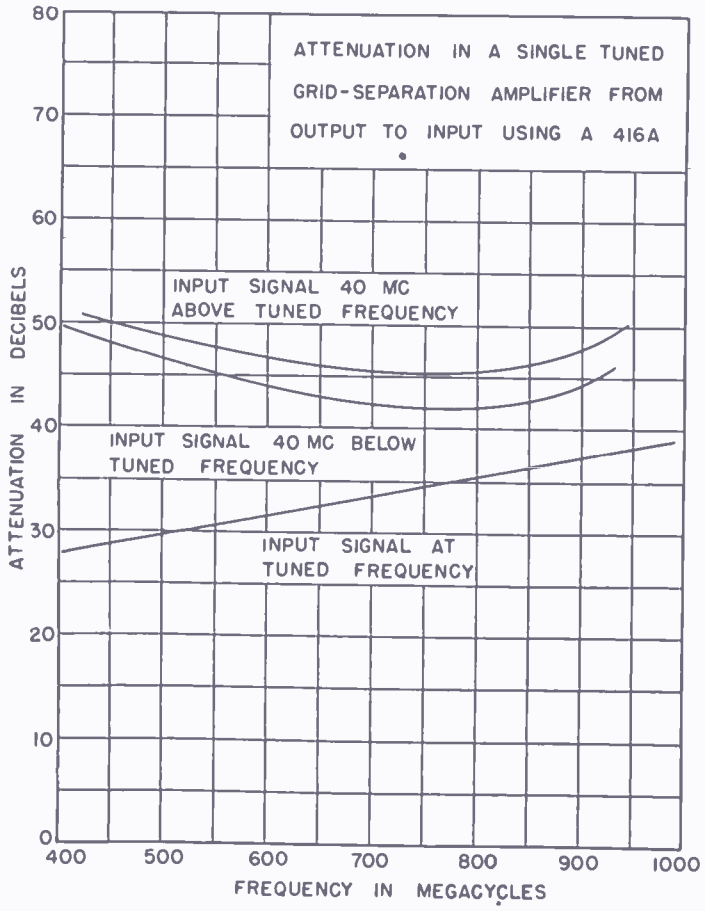

Fig. 19—Attenuation in a single-tuned, grid-separation amplifier from output to input using a 416A.

Conclusion

This study shows the performance that can be expected of ultra-high-frequency amplifiers using currently available tubes and the improvement that may be expected by changing some of the various

tube constants. Of the amplifiers considered, that using the 416A tube was the best although lighthouse tubes using the L-type cathodes may have superior noise figures.[9] A receiver using a 5876 pencil-triode amplifier will give a little better noise figure than a receiver using a crystal mixer at the lower end of the 500- to 900-megacycle range and have about the same noise figure in the upper part of this range. The maximum gain and best noise figure conditions may require the grounded-grid amplifier to have a narrower or wider band width than desired. The use of this type of amplifier will reduce the oscillator radiation through the antenna circuit by more than 30 decibels.

[9] G. Diemer and K. S. Knol, "Low Level Triode Amplifier for Microwaves," Phillips Research Report, Vol. 5, pp. 153-154, February, 1950.

FUNDAMENTAL PROCESSES IN CHARGE-CONTROLLED STORAGE TUBES*†

By

B. Kazan and M. Knoll

Research Department, RCA Laboratories Division,
Princeton, N. J.

Summary: *This paper discusses the basic methods of operation of charge-controlled storage tubes.*

Part 1 is concerned with the equilibrium potentials of insulated elements under electron bombardment and the action of light. It covers the following: (a) the equilibrium states of an electron-bombarded element, (b) the target potential shifting diagram, (c) the influence of the secondary emission velocity distribution on the curve of equilibrium potential, (d) the variation of instantaneous collector current as a function of target potential, (e) the equilibrium potentials resulting from photoemission, photoconductivity, and bombardment conductivity of the target, and (f) the equilibrium potentials due to redistribution.

In Part 2 definitions are given of the important dynamic storage tube functions.

In Part 3 the dynamic processes of writing, reading and erasing and also the capabilities of the different writing and reading methods for producing halftones are discussed.

Part 4 consists of a relatively complete bibliography on storage tubes and also includes references to the fundamental charging processes of insulating surfaces.

Introduction

ALTHOUGH charge-controlled storage tubes have been employed as television camera tubes since the early days of television, they have become increasingly important during the past decade as devices for signal conversion, direct viewing, and computing applications. Since the storage of information in such tubes depends neither on mechanical movement nor on physicochemical changes in a material, but on the establishing or removing of minute electrical charges on or within an insulating surface (or array of insulated elements), their speed of operation is very high. In practical tubes the amount of electrical charge stored per target element is in the order of 10^{-11} coulomb or less, thus permitting time-varying electrical information to be stored on (or removed from) successive elements at rates higher than 50 megacycles in some cases.

---

* Decimal Classification: R138.

† An essential portion of this paper was initially prepared for the Signal Corps under Engineering Report No. E-1069.

Because of the fact that a pattern of electric charges can be established on the storage surface corresponding to the light and dark areas of a visual picture, the storage tube has found its most extensive use in *television* applications, especially in the field of pickup tubes which convert visual to electrical signals. For these types of applications storage tubes such as the iconoscope and image orthicon have been developed.

In the transmission of picture information it is frequently necessary to change from one type of scanning to another (such as polar to rectangular) or to change the frequency of the transmitted electrical information. For these purposes the *signal converter* type of storage tube is very useful. It is also important in applications involving integration for increasing the signal-to-noise ratio, and the recording of single transients from which it is desired to produce a number of copies. Considerable development work has been done on several of these devices with many new applications expected.

Where the *direct viewing* of stored patterns or pictures is concerned, charge-controlled storage tubes, although not as fully developed as the other types, are expected to play an important part in applications where, for example, a short electrical transient signal is desired to be viewed for a long period with little decay, where the decay of a stored signal is desired to be controlled, or where higher light output is desired than can conveniently be obtained with ordinary scanning types of cathode-ray tubes.

During the past few years charge-controlled storage tubes have also become more and more important as essential components in *computing devices*. Because of the rapidity with which electrical information can be stored at an arbitrary target element (time durations as short as a few microseconds) storage tubes are finding one of their most important uses where complex operations require rapid storage of intermediary information and rapid access to this information. For computing applications, several successful types of tubes have already been designed, with additional development work continuing.

The operating mechanism of storage tubes is largely dependent on the control of secondary emission currents from the target for charging the individual areas. In the following text the equilibrium potentials acquired by insulated elements under steady electron bombardment are first discussed and on the basis of this discussion the various methods of establishing a charge pattern by dynamically controlling the secondary emission are then described. A more complete understanding of secondary emission itself may be obtained from the literature indicated in Section A of the bibliography. In particular, the works

of Bruining (2) and McKay (9) provide relatively complete surveys of the secondary emission of both insulators and metals.

In addition to secondary emission, the processes of photoemission and photoconductivity play an important rôle in the charging action of television camera tubes. These charging actions are also discussed in the text from the static and dynamic viewpoint.

PART 1—EQUILIBRIUM POTENTIALS ACQUIRED BY AN INSULATING SURFACE UNDER ELECTRON BOMBARDMENT AND THE ACTION OF LIGHT

A. Equilibrium States of an Electron-Bombarded "Floating" Surface

The establishing of a charge pattern in a storage tube is frequently accomplished by means of secondary emission. For an understanding of this process a knowledge of the potential acquired by an insulated element under steady bombardment is essential.

In Figure 1 an electrode arrangement typical of a storage tube is indicated. Under steady bombardment by primary electrons in a high vacuum, an insulated (metallic or nonmetallic) element of the target at an arbitrary initial potential, V_{ft}, will be charged to an equilibrium potential V_{eq}. For a given material the value of this equilibrium potential (measured with respect to the secondary current collector anode, G), depends, to a first approximation (within several volts) on the energy V_{pr} of the primary electrons striking the target, and the effective resistance R_i of the material between the target element and the backplate P.

Figure 2 indicates the well-known curve, characteristic of all materials (including metals) of secondary emission ratio δ_e as a function of primary electron energy V_{pr}, expressed in electron volts (Bibliography (2), (9)). (δ_e is defined as the ratio of the secondary current, i_s, to the primary current, i_{pr}.) The lower and higher values of V_{pr} corresponding to $\delta_e = 1$ are designated as first and second crossover potentials V_{cr1} and V_{cr2} respectively.[1] This curve always exhibits a maximum value[2] of δ_e between V_{cr1} and V_{cr2}. At primary energies below the maximum, δ_e increases with increasing V_{pr} because of the increasing primary energy available. At primary energies above the maximum, δ_e decreases as a function of V_{pr} because the secondary electrons are generated in progressively deeper layers of the material

[1] V_{cr1} is usually of the order of 100 volts or less and V_{cr2} of the order of 1,000 volts or greater.

[2] For some pure metals, and carbon in the form of soot, the maximum value of δ_e is less than unity. In such cases no crossover potentials exist.

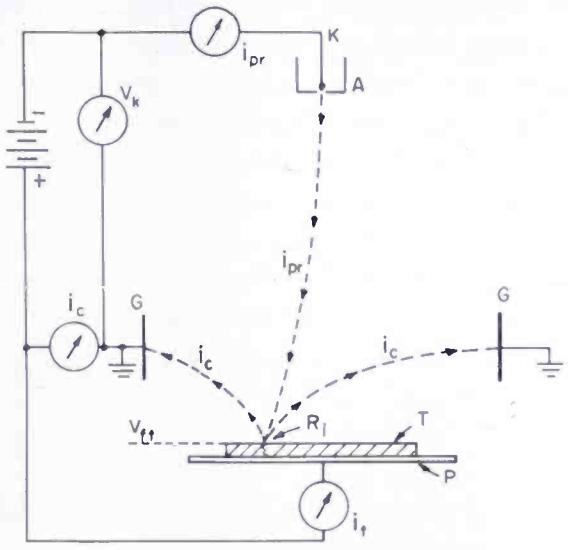

Fig. 1—Typical electrode arrangement for an electron-bombarded storage target.

A = accelerating anode,
G = collector cylinder,
i_c = collected current,
i_{pr} = primary current,
i_t = current reaching backplate from target (d-c target current),
K = cathode,
P = metal backplate,
R_l = resistance between surface of target element and backplate due to leakage, conductivity induced by bombardment or light, or both,
T = target (insulator sheet or coating),
V_{tt} = instantaneous potential of target surface with respect to collector,
V_k = potential of cathode with respect to collector.

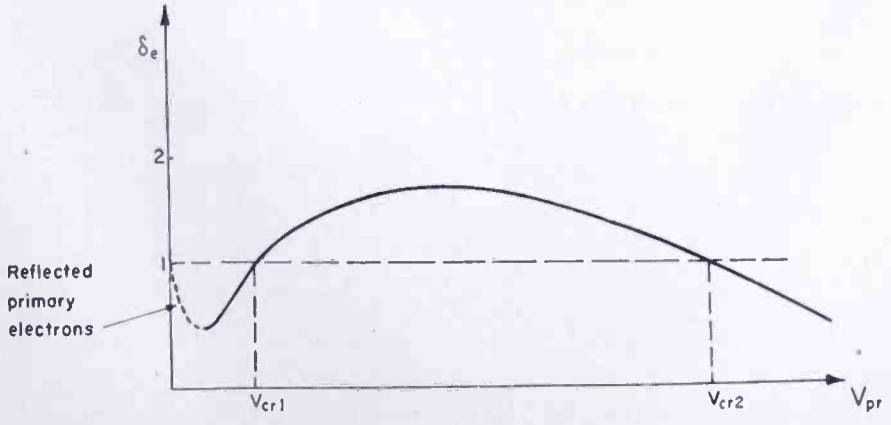

Fig. 2—Typical secondary emission curve: secondary emission ratio, δ_e, as a function of bombarding primary electron energy, V_{pr}, at the target.

and therefore are absorbed to a greater degree with increasing V_{pr}. At very low energies, a large fraction of the primary electrons is reflected by collision with the target atoms. If these reflected electrons are collected together with the secondary electrons, the apparent secondary emission ratio (shown by the dotted portion of the curve) approaches unity as V_{pr} approaches zero.

If the conductivity of the target is sufficiently high, such as for metals, the secondary emission curve of Figure 2 can be obtained by direct-current measurements. For an insulating target film, the portion of the curve corresponding to higher primary electron velocities may also be obtained by direct-current measurements using the effect of bombardment-induced conductivity of a penetrating beam (see Part 1 —I and Bibliography (17), (32)); otherwise, the curve must be obtained by pulse techniques (Bibliography (9), (24), (40)). In obtaining this curve it is assumed that the accelerating field between the collector and target is sufficient to remove all secondary electrons emitted from the surface of the target.

In operation of storage tubes, such an accelerating field does not always exist and some of the emitted secondary electrons return to the target. To differentiate clearly between the secondary-electron current, i_s, emitted by a certain target material under bombardment and the portion i_c of this electron current (consisting of either secondary or reflected primary electrons, or both, from the target) which lands at the collector, the following notations are used:

$$\frac{i_s}{i_{pr}} = \delta_e \text{ (secondary-emission ratio as commonly used in the literature), and}$$

$$\frac{i_c}{i_{pr}} = \delta_c \text{ (collected-current ratio).}$$

For a given material and a given primary electron velocity at the target, δ_c will always be equal to or smaller than δ_e except for very low primary energies where the collected electrons include the reflected electrons. The condition $\delta_c \leqq \delta_e$ is caused by a decelerating field between the target and collector which results when the target is positive with respect to the collector (see Section D), or from a space-charge-potential minimum near the target due to the low velocity of the emitted secondary electrons.

V_{eq}, the equilibrium potential of a target element bombarded by the primary electrons, is experimentally known to be a function of the cathode potential, V_k, with respect to the collector (Bibliography (28)).

This relationship is indicated by the curve of Figure 3. For values of V_k which correspond to values of V_{pr} *below* V_{cr1}, V_{eq} decreases linearly with increasing magnitude of V_k and usually jumps to a slightly positive value for a value of V_k *equal to* or *greater than* V_{cr1}. Under some conditions, however, the target may be caused to assume potentials along the dashed line b-c′ as V_k is increased beyond the value V_{cr1} (see section C.) For values of V_k corresponding to V_{pr} *greater than* V_{cr2}, V_{eq} again decreases linearly[3] with increasing value of V_k. A more detailed discussion of the equilibrium curve is given below.

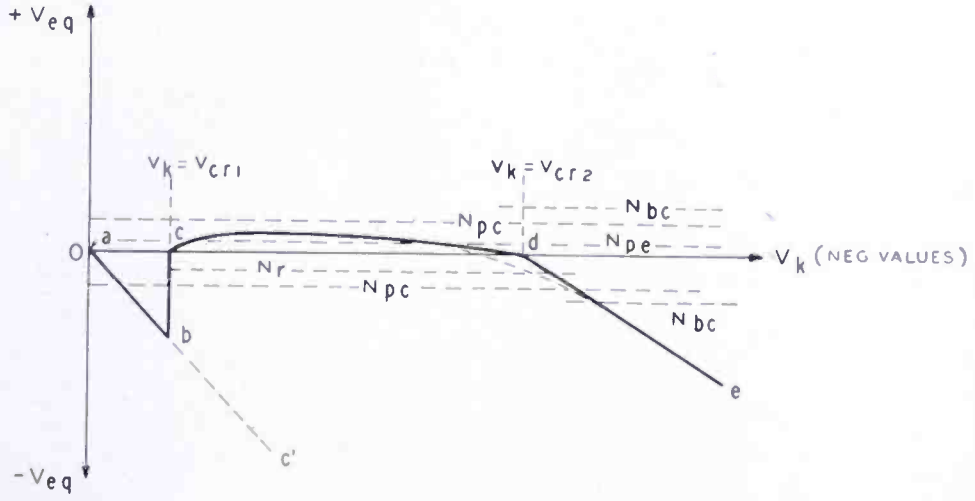

Fig. 3—Curve of secondary emission equilibrium potential, V_{eq}, as a function of cathode voltage.

N_{bc} = typical potential levels resulting from bombardment-induced conductivity,
N_{pe} = typical potential level resulting from photoemission,
N_{pc} = typical potential levels resulting from photoconductivity,
N_r = typical potential level resulting from redistribution.

B. Target Potential Shifting Diagram

The origin of the experimental equilibrium curve (Figure 3) of a "floating" insulated target element may be understood with the help of Figure 4. This figure indicates by means of arrows the direction of potential shift of an insulated target element with any initial potential V_{ft}, when bombarded with primaries from a cathode at any potential V_k with respect to the collector. Since the values of V_k (along the x axis) and V_{ft} (along the y axis) are plotted on the same scale, lines of 45-degree slope represent lines of constant potential difference,

[3] Although, as indicated in Figure 3 (and also Figure 4) the portion d-e of the equilibrium curve is a straight line intersecting the line c-d at the point d, actually, in the case of insulators the line d-e becomes curved as it joins the portion c-d. This is indicated by the dotted line near point d of Figure 3.

$V_{ft} - V_k$. (Note that while V_k is always a negative number, it is indicated along the positive x axis.) This potential difference, $V_{ft} - V_k$, is actually the potential V_{pr}, and thus these sloping lines represent values of constant electron energy V_{pr} at the target.

In Figure 4, three 45-degree lines are drawn for the particular electron energies zero, V_{cr1}, and V_{cr2}. The entire area between the lines $V_{pr} = 0$ and $V_{pr} = V_{cr1}$ (area A) includes only points where $\delta_e < 1$ and therefore also $\delta_c < 1$ since for all these points (as indicated by Figure

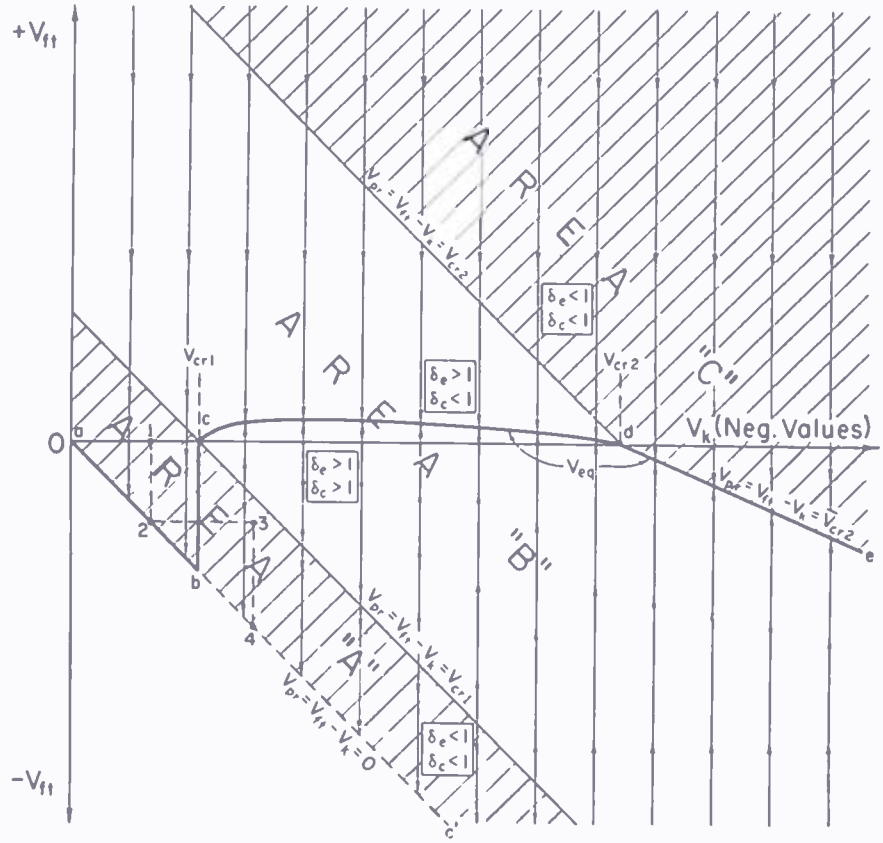

Fig. 4—Potential shift of a floating target under electron bombardment as a function of its initial potential, V_{ft} and the cathode voltage, V_k.

V_{ft} = instantaneous potential of target surface,
V_{eq} = particular value of V_{ft} at equilibrium potential of target surface,
V_k = cathode potential of bombarding primary beam.

2) the target will be bombarded with an energy less than the first crossover potential.

The area between the lines $V_{pr} = V_{cr1}$ and $V_{pr} = V_{cr2}$, in similar manner, includes only points where $\delta_e > 1$. However, since the second crossover potential does not remain constant, but increases with increasing accelerating field at the target (see Section F), the region of $\delta_e > 1$ is extended (for negative values of V_{ft}) to the line d-e which

has a slope of less than 45 degrees. This line is indicated as $V_{pr} = \overline{V}_{cr2}$ and represents the condition $\delta_c = 1$, since along the line the secondary emission ratio, δ_c, is by definition equal to unity, and all the secondaries are attracted to the collector.

The entire region of $\delta_c > 1$ of Figure 4 (area B) is divided into two portions by the slightly curved line c-d which represents the condition $\delta_c = 1$. (The reasons for the shape and position of this line are discussed in Section D.) Above the line, δ_c is less than unity since some or all of the secondary electrons are returned to the target by the decelerating field between the target and collector. Below the line, δ_c is greater than unity since there is less decelerating field or an increasing accelerating field.

To the right of the line $V_{pr} = V_{cr2}$ (above the V_k axis) and to the right of the line $V_{pr} = \overline{V}_{cr2}$ (below the V_k axis), the energy of the primary electrons at the target is greater than the second crossover potential. All points in this region (area C), therefore, correspond to $\delta_c < 1$ and thus to $\delta_c < 1$ as well.

Since a floating target element, when bombarded with primaries under the condition $\delta_c > 1$, becomes more positive and, when bombarded under the condition $\delta_c < 1$, becomes more negative, the direction of these potential shifts can be indicated by the arrows of Figure 4 in the corresponding regions. These arrows converge on the line c-d-e from above and below, thus indicating it to be a line of stable equilibrium since along it $\delta_c = 1$ and any small potential deviations from it will be compensated by such change in δ_c as will shift the target back toward the line. Since arrows end on only one side of the line a-b-c′, points on this line are quasi-stable in the sense that although the condition $\delta_c = 1$ exists, only positive potential deviations will be compensated by a change in δ_c. Negative potential deviations, however, will not be compensated since, for points below the line $V_{pr} = 0$, primary electrons will no longer have sufficient energy to reach the target. Only by removal of the charge by leakage or other means, such as positive ions or the use of an auxiliary electron beam with a more negative cathode potential, can the target charge positively toward the line a-b-c′. (Although δ_c is also equal to unity along the line $V_{pr} = V_{cr1}$ below the V_k axis, stable equilibrium cannot be achieved in this case since slight potential deviations from the line will cause the target to shift away from the line (as indicated by the arrows) instead of toward the line.)

As mentioned above, the portion d-e of the equilibrium curve corresponds to the condition $V_{pr} = \overline{V}_{cr2}$ and since $V_{pr} = V_{ft} - V_k$, the resulting relationship $V_{ft} - V_k = \overline{V}_{cr2}$ exists along this line. Because of this relationship, indicating that at equilibrium the target potential

cannot exceed the cathode potential by more than the amount $\overline{V}_{cr2}$ as the cathode potential is increased, $\overline{V}_{cr2}$ is frequently referred to as the "sticking potential."

C. Equilibrium of the Branch b-c′ of the V_{eq} Curves of Figures 3 and 4

Target elements can only be shifted to the line b-c′ if the target and cathode potentials correspond to points which fall in the area A to the right of the line b-c′. If the target element is assumed to be initially at zero potential, one means of shifting its potential to a point on the line b-c′ is as follows: The target element is first bombarded with primary electrons from a cathode whose potential, V_k, is between 0 and V_{cr1} as indicated by point 1 of Figure 4. If the cathode potential is maintained at V_k, the target element will shift its potential by secondary emission action to point 2, the time required being determined by the primary beam current and the capacity of the target element to all the other target elements and electrodes in the tube. If the cathode potential is now increased by an additional quantity less than V_{cr1}, but such that the total cathode potential, V'_k, is greater than V_{cr1}, the target will be at point 3 and again be shifted by secondary emission action to the point 4 on the line b-c′. In similar manner, other points corresponding to $V_{pr} = 0$ can be reached along the dashed equilibrium line b-c′.

D. Influence of the Velocity Distribution of the Secondary Electrons on the Shape of Branch c-d of Figures 3 and 4

The position and slightly curved shape of the line c-d of Figures 3 and 4 can be qualitatively understood from Figure 5 where the relative number of secondary electrons is plotted as a function of their emission energy, V_e, expressed in volts. Two curves, (1) and (2), are shown corresponding to the bombardment of a given target with primary electrons of energy V_{pr1} and V_{pr2} respectively.

As indicated in Figure 5, a maximum occurs in each curve at a relatively low emission energy[4] and another more narrow peak at a higher energy. The latter peak occurs at an emission energy equal to the particular energy V_{pr} of the primary electrons striking the target. In general, the majority of the secondary electrons are emitted with not more than a few volts energy and are in the vicinity of the low-

[4] For insulators, this peak in the curve occurs at about one volt of emission energy or less. For metals, the peak is somewhat higher but generally less than five volts.

voltage maximum. From the physical standpoint these electrons constitute the "true" secondaries.

Although the transition is not sharp, electrons emitted with higher energies consist of primary electrons which have given up a part of their energy to the target atoms by collision and are inelastically reflected. The sharp peak at the emission energy V_{pr} is produced by the elastic reflection of a fraction of the primary electrons which undergo no loss of energy in striking the target. In the discussions which follow, the expression "secondary electrons" will be taken to mean the total of all of the emitted electrons unless otherwise specified.

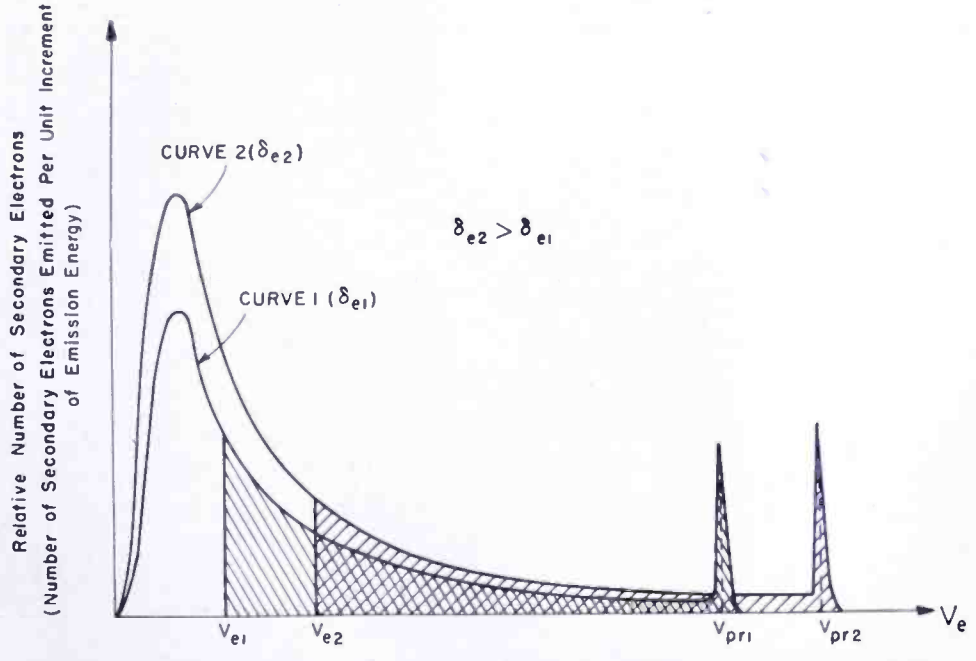

Fig. 5—Velocity distribution curves of secondary electrons showing minimum energy of secondary electrons which can reach the collector.

V_e = emission energy of secondary electrons, in volts.

If the vertical coordinate of Figure 5, indicating the relative number of secondary electrons, is assumed to be more explicitly defined as the number of secondary electrons emitted per unit interval of emission energy, the entire integrated area under each curve will represent the total number of secondary electrons. The ratio of the total number of secondaries represented by each curve to the number of primary electrons corresponds, therefore, to the secondary emission ratios δ_{e1} and δ_{e2} respectively.

Referring to curve 1 of Figure 5, if the target has a small positive potential V_{ft} equal to V_{e1} only the electrons represented by the corresponding hatched area will have sufficient energy to reach the

collector against the decelerating field.[5] For any positive target potential V_{ft}, it is therefore possible to determine the number of electrons able to reach the collector by setting the value of V_e equal to V_{ft} and measuring the area under the curve to the right of the ordinate V_e. The ratio of the number of electrons reaching the collector to the number of primary electrons is, by definition, the value of δ_c. Of special interest is V_{eq}, the particular value of V_{ft} which corresponds to the condition $\delta_c = 1$. This is determined from the particular value of V_{e1} $(= V_{ft})$ such that the hatched area represents a number of secondary electrons equal to the number of primary electrons.

Since, by definition, the total area under the velocity distribution curve will be increased with increases in δ_e, due to changes in primary electron velocity V_{pr}, the value of V_{eq} will also be increased to some extent by increases in δ_e (assuming approximately the same shape of velocity distribution curve). This is indicated in Figure 5 where curve (2), having the same shape but a higher value of δ_e than curve (1), causes the potential V_{e2} to be higher than the potential V_{e1} of curve (1) for the condition $\delta_c = 1$. Return now to Figure 4. The line c-d, which is a plot of target potential V_{eq} for the equilibrium condition $\delta_c = 1$, is therefore slightly above the horizontal axis, representing the small positive values of V_{eq}, and rises and falls in height as δ_c varies with V_{pr} as shown in Figure 2.

Assuming that the shapes of the velocity distribution curves for different materials are geometrically similar, materials having greater values of δ_e will have higher values of V_{eq} for $\delta_c = 1$. The line c-d will thus be somewhat higher for such materials but of the same general shape.

Actually, the emitted secondaries will cause a space-charge cloud to form between the bombarded target element and the collector. This space charge, if sufficiently great, will produce a potential minimum in its neighborhood, preventing additional low-velocity secondaries from reaching the collector. The resulting net increase in electrons at the target will thus cause it to assume a new equilibrium potential, somewhat less positive than the ideal value, V_{eq}, discussed above, or a few volts negative with respect to the collector. The shift to a more negative equilibrium potential enables the number of secondaries leaving to equal the primary electrons (due to the reduction in decelerating field or the creation of an accelerating field), re-establishing the condition $\delta_c = 1$. Since the current density of the secondaries leaving the target determines the amount of space charge created, the equilibrium

[5] For simplicity, it is assumed here that the secondary electrons are emitted only in the direction of the electric field between target and collector.

potential assumed by the target during bombardment will depend on the current density of the primary beam.

E. Variation of Instantaneous Collector Current as a Function of the Floating Target Potential

For values of V_k whose magnitudes lie between V_{cr1} and V_{cr2}, the typical variation of the collected-current ratio δ_c with respect to V_{ft} is indicated by the solid curve of Figure 6. In this figure, the dotted line, which is partially superimposed on the solid line, indicates the curve of secondary emission ratio δ_e as a function of V_{pr}, the primary electron energy at the target. The solid curve is drawn with the

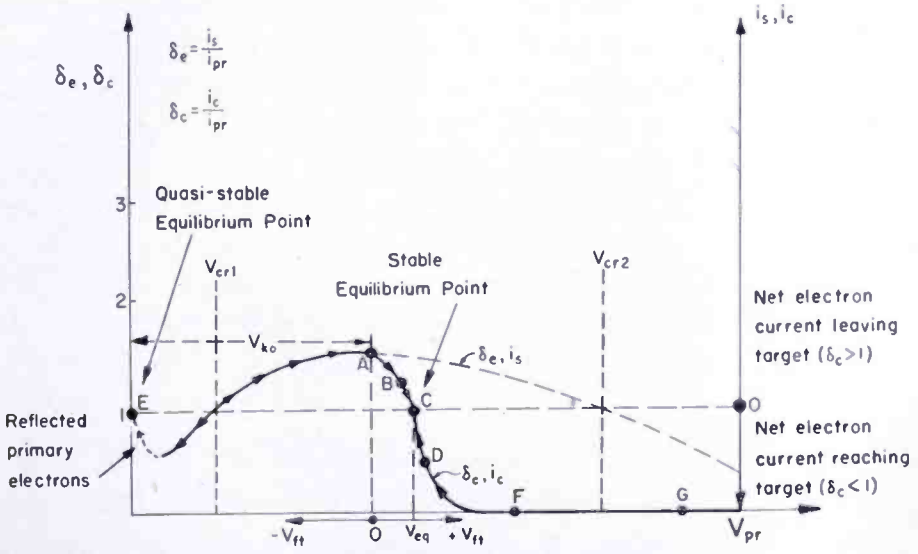

Fig. 6—Instantaneous collected current as a function of floating target potential, V_{ft}.

V_{ft} = floating target potential with respect to collector.

assumption that the cathode potential, V_k, is held at some particular value V_{ko}, and the target potential, V_{ft}, varied.

Since, by definition, V_{ft} is the target potential with respect to the collector, the abscissa $V_{ft} = 0$ corresponds to a primary energy V_{pr} at the target which is equal in magnitude to V_{ko}, the cathode potential with respect to the collector (Bibliography (51), (54)). For values of $V_{ft} < 0$ where an accelerating field exists between the target and collector, essentially all of the emitted secondary electrons will be collected and the curves of δ_e and δ_c will therefore be superimposed.

For $V_{ft} > 0$ a decelerating field will exist at the target. If V_{ft} has a small positive value, the emission energies of the secondary electrons will enable a fraction of them to reach the collector as indicated in Section D. However, as V_{ft} is increased, the number of secondaries

reaching the collector will decrease until essentially none of them will be capable of reaching the collector for large values of V_{ft}. This decrease in the collected current i_c is indicated by the solid line[6] in Figure 6 which includes points B, C, and D. The particular positive value of V_{ft} where the δ_c curve crosses the line $\delta_c = 1$ (point C) corresponds to the stable equilibrium potential V_{eq}. The exact value of δ_c for a particular positive value of V_{ft} can be obtained by determining the area under the energy distribution curve of Figure 5 to the right of the abscissa V_{ft} as discussed in Section D. Since a target with a potential V_{ft} tends to shift positively or negatively, depending on whether $\delta_c > 1$ or $\delta_c < 1$, respectively, these potentials are indicated by the arrows on the δ_c curve of Figure 6. Point C on the curve where the arrows converge from both sides is a point of stable equilibrium ($V_{ft} = V_{eq}$) and point E where the arrows arrive from one side only ($V_{pr} = 0$) is a quasi-stable point (as mentioned in Section B).

It should be noted that the point E (where $V_{pr} = 0$) corresponds to a target potential V_{ft} which is negative with respect to the cathode by a fraction of a volt, since the primary electrons are emitted from the cathode with a small amount of thermal energy. Although not indicated in Figure 6, the point $V_{ft} = 0$ thus corresponds to a primary energy $V_{pr} = V_{ko}$, plus a fraction of a volt.

F. Slope of the Branch d-e of the V_{eq} Curve of Figures 3 and 4

It is experimentally observed that the slope of the branch d-e is less than 45 degrees (Bibliography (21), (22)). This may be accounted for by assuming that as the accelerating field between the target and collector is increased, the value of δ_c becomes greater for a given material, with an accompanying increase in the value of V_{cr2}. Physically, the change in δ_c may be explained by assuming that more of the secondary electrons emitted in random directions inside the material can escape, since they are drawn toward the surface by the internal accelerating field.

Referring to Figure 4, it is assumed that near the point d, where the accelerating field is approximately zero, the value of the second crossover is V_{cr2}. It is also assumed, for the purpose of illustration, that along the line d-e the value of V_{cr2} increases by an increment which is linearly proportional to V_{ft} so that $\bar{V}_{cr2} = V_{cr2} - \alpha V_{ft}$. (Note

[6] In practice, the slope of this line will be influenced by the geometry of the target and collector system. For closer spacing of the collector to the target surface, the slope tends to increase.

that α is a positive quantity and V_{ft} is always a negative quantity along the line d-e.) Since, by definition, the relationship $V_{pr} = V_{ft} - V_k$ exists, it is possible to write for the conditions along the line d-e, where $V_{pr} = \overline{V}_{cr2}$ holds true:

$$\overline{V}_{cr2} = V_{ft} - V_k.$$

Substituting

$$V_{cr2} = \alpha V_{ft} \text{ for } \overline{V}_{cr2}$$

gives

$$V_{cr2} - \alpha V_{ft} = V_{ft} - V_k,$$

or

$$V_{ft} = \frac{V_{cr2} + V_k}{1 + \alpha} = \frac{V_k}{1 + \alpha} + \text{constant}.$$

This is the equation of a line whose slope, as indicated in Figure 4, is less than 45 degrees in magnitude.

G. Photoemission Levels Above the V_k Axis of Figure 3

In some cases the storage target may be covered with a mosaic of photoemissive elements insulated from each other. These elements can be charged by the action of incident light as well as by the action of secondary emission (Bibliography (4b), (25), (26), (94), (95), (96), (97)). Since by photoemission such target elements can only lose electrons, they always tend to charge in the positive direction. However, in charging by photoemission, the elements cannot shift more positively than the potential corresponding to the maximum energy of the emitted photoelectrons for a particular color or frequency of light. If the potential V_{ft} of a photoemissive element is shifted (by the capacitive action of a voltage applied to the backplate, for example) to a value greater than this potential, none of the emitted photoelectrons will be able to reach the collector, due to the decelerating field, and will be returned to the target surface. Since the number of photoelectrons emitted is proportional to the light energy incident on the surface, the charge lost is a linear function of the light energy, assuming sufficient accelerating field between target and collector. In Figure 3, a typical potential level established by photoemission is indicated by the dashed line N_{pe}. This potential is of the order of several volts for visible light.

H. Photoconductivity Levels Above and Below the V_k Axis of Figure 3

If a potential difference has been established between the front surface and backplate of a thin insulating target, and the target material is photoconductive, the effect of incident light at a particular element will be to reduce this potential difference by increasing the conductivity of the target material (Bibliography (4a), (4b), (18a), (20a), (77), (96)).

The initial potential difference may be established by secondary emission action. If, for example, the target surface is bombarded with primary electrons from a cathode whose potential is between V_{cr1} and V_{cr2} so that the surface is charged to approximately the collector potential, and at the same time the backplate is maintained at a different potential (either negative or positive) with respect to the collector, a corresponding potential difference will result between the target surface and backplate.

In general, the conduction current from the target surface to the backplate will decrease with time of illumination because of the reduced gradient as the surface approaches the backplate potential. Unlike the process of photoemission, the process of photoconduction does not cease at the instant of cutting off the incident light but persists, decaying rapidly at first, followed by an extended tail. The decay time varies considerably for different materials, the time required for the initial rapid drop in conductivity being in the order of a few milliseconds or less to reach 1/e of its initial value and the tail extending in some cases for as long as several minutes.

I. Bombardment-Induced Conductivity Levels Above and Below the V_k Axis of Figure 3

If a potential difference exists between the target surface and backplate (established by secondary emission, for example, as described in section H) the target surface may be caused to shift to the backplate potential by means of bombardment-induced conductivity. This effect occurs when the target is thin (one micron, for example) and the primary beam has sufficient energy to penetrate through the target material (Bibliography (1), (4), (10), (15), (17), (18)). Such induced conductivity may exceed by several orders of magnitude the conductivity of the unbombarded insulating target.

In Figure 7, typical curves (taken from Pensak, Bibliography (17)) are shown for a target of silica, .25 micron thick, indicating the ratio of bombardment-induced current to primary current as a function of primary beam energy, V_{pr}. It should be noted that these curves do not

continue to rise with increasing primary beam energy but go through a maximum. For a given target this maximum occurs at approximately the primary beam voltage at which the greatest fraction of beam energy is absorbed in the target. As also shown by the curves, the bombardment-induced conductivity depends somewhat on the polarity of the initial potential difference established between target surface and backplate, being greater for most materials when the target surface is negative with respect to the backplate. (For exceptions see Bibliography (18).)

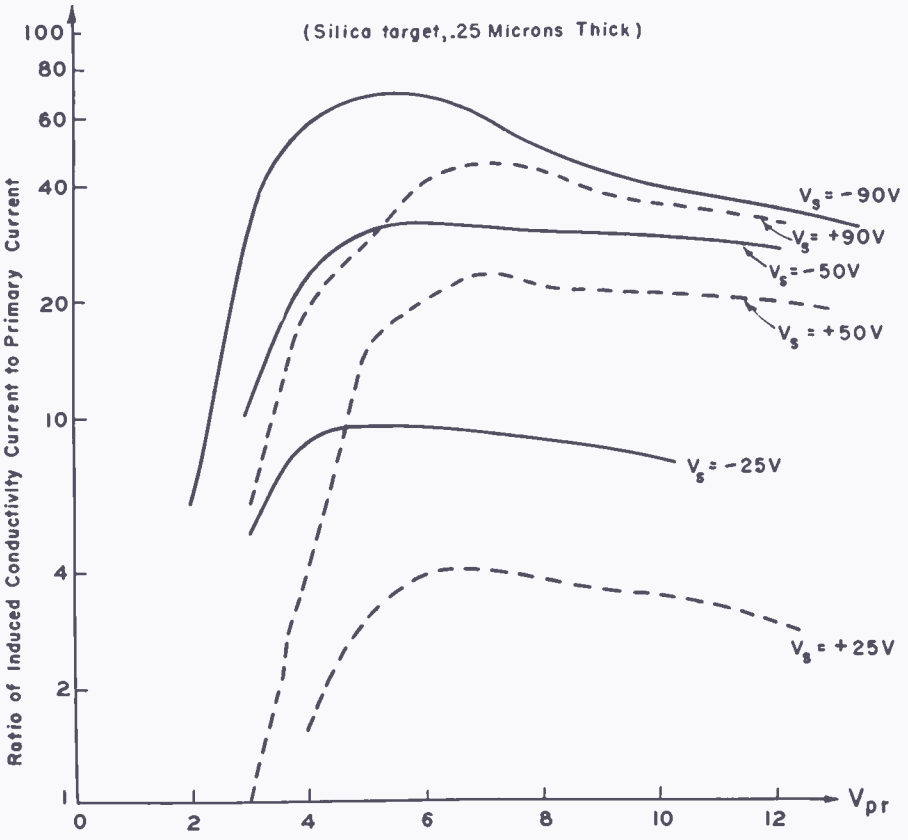

Fig. 7—Typical curves showing change in bombardment-induced conductivity with primary beam energy.

V_{pr} = primary beam energy in kilovolts,
V_s = potential of target surface with respect to backplate.

Since secondary electrons will be emitted simultaneously from the surface of the target during bombardment, the tendency of the surface to assume the backplate potential by induced conductivity will be either aided or opposed by the secondary emission action of the primary beam depending on the equilibrium potential associated with the primary beam cathode potential (see Figure 4). Neglecting secondary emission effects, the potential shift which an element of the target surface under-

goes depends on the energy of the primary beam and the potential difference initially established between the target surface and backplate as well as the time of bombardment. In Figure 3, typical potential levels established by bombardment-induced conductivity are indicated by the dashed lines N_{bc}. These lines may be either above or below the V_k axis, depending on the backplate potential, and are drawn in the region where the cathode potential, V_k, assumes relatively large values (producing high bombarding energies).

J. Redistribution Levels Below the Line c-d of the Equilibrium Curve of Figure 3

In the preceding discussion relating to the potential shifting of a floating target under electron bombardment, no account was taken of secondary electrons emitted from a particular bombarded target element returning to other target elements (case of a scanned target). This "redistribution effect" is important since a target element, after having reached the equilibrium potential V_{eq} during bombardment, will become more negative as the primary electron beam later scans other elements. Redistribution usually occurs when a weak decelerating field exists at the target such as at points along the branch c-d of the equilibrium curve of Figure 3, or when a weak accelerating field exists such as at points slightly below the V_k axis.

In Figure 8a, a bombarded target element is shown at a positive equilibrium potential, V_{eq}, of +5 volts with respect to the collector. Also indicated are the equipotential lines in the space between the target and collector. Since, as mentioned in Section D, a large fraction of the secondary electrons is emitted with energies of 5 volts or less, these electrons will be reflected back to other elements of the target surface as well as to the bombarded element by the decelerating field above the target. Included in the secondaries which are reflected is a fraction of the electrons with greater than 5 volts energy but whose energy in the direction of the decelerating field is less than 5 volts because of their emission angle. The reflected electrons thus tend to charge negatively other elements of the target surface[7] at a rate depending on their distance from the bombarded spot (Bibliography (37)).

The redistribution effect can be substantially reduced or entirely eliminated if a fine-mesh barrier grid is placed very close to the target surface as indicated in Figure 8b and the collector cylinder is maintained at a positive potential with respect to the grid. In this case, secondary electrons escaping through the holes of the mesh will be un-

[7] In general, a large fraction of the redistributed electrons will return to the target surface in the neighborhood of the bombarded spot within a distance of a spot diameter.

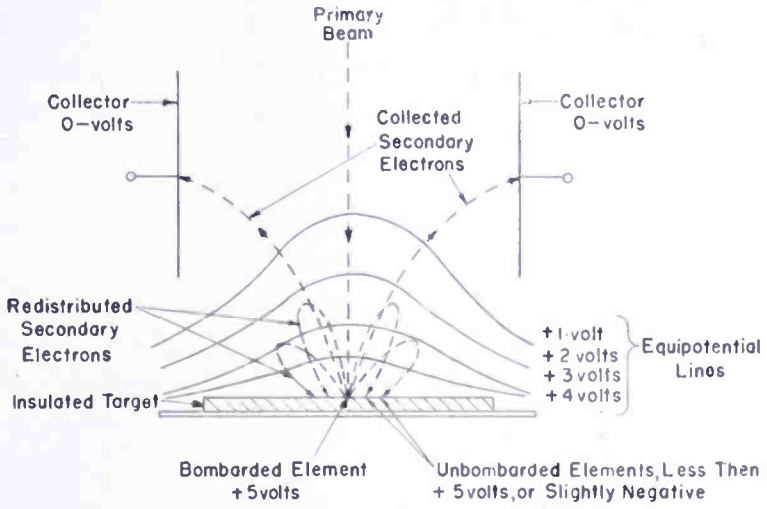

Fig. 8a—Typical target potentials due to electron redistribution.

able to return to the target surface because of the accelerating field existing between the mesh and the collector. On the other hand, secondary electrons with insufficient energy to escape through the mesh holes will return to the target surface very close to the point from which they were emitted. It is important to note that although a large fraction of the collected secondary electrons may reach the collector cylinder through the holes of the mesh, the barrier grid acts as the effective collector in determining the equilibrium potential of the target elements since it tends to prevent secondary electrons from leaving the target if the surface becomes positive with respect to the grid.

In addition to preventing redistribution, the barrier grid serves to prevent coplanar grid effects at the target surface, i.e., the tendency of a target element which has acquired a large negative charge to prevent the leaving of secondary electrons from or landing of primary electrons on adjacent elements during scanning.

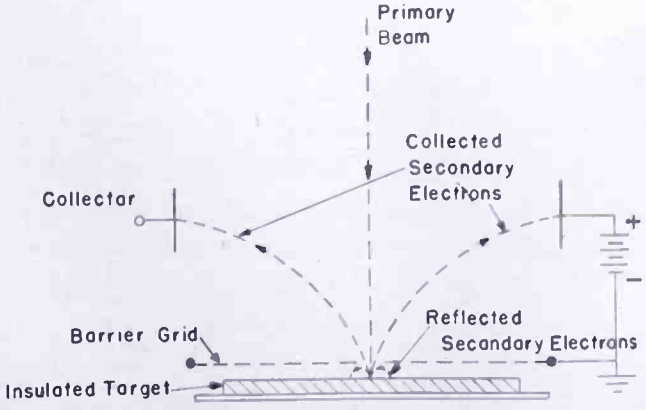

Fig. 8b—Barrier grid for reducing electron redistribution.

PART 2—DEFINITIONS

The discussion in Part 3 covering the dynamic processes in storage tubes is based on the following definitions.[8] These definitions are primarily concerned with charge-controlled storage tubes. Definitions relating to other storage processes in computers are given in the IRE Standards on Electron Computers: Definition of Terms, 1950 (*Proc. I.R.E.*, Vol. 39, pp. 271-277, March, 1951).

(1) *Storage Tube* (General): An electron tube into which information can be introduced and then extracted at a later time.

(2) *Storage Tube* (Charge-controlled): A storage tube in which information is retained by means of static electric charges. Such charges are generally retained on a homogeneous insulating surface or on an array of discrete insulated (metallic or nonmetallic) areas.

(3) *Storage Element:* The smallest portion of the target which can be distinguished in the output signal from other differently charged portions under specified writing and reading conditions.

(4) *Writing:* The action of establishing a charge pattern corresponding to the input signal. This may also be referred to as *storing*.

(5) *Maximum Writing Speed* (storage elements per second): The maximum rate at which successive storage elements can be charged to establish the desired charge pattern (determined by the output requirements).

(a) In the case where halftones are required in reading, the maximum speed will be determined by the specified level of output variations, the resolution, and the amount of signal deterioration (see definition 17a) introduced in the writing and reading processes.

(b) In the case of bistable writing, the maximum speed is defined as the maximum rate at which successive storage elements can be shifted from one equilibrium potential to another.

(c) In the case of viewing storage tubes employed for oscilloscope purposes, the maximum speed is defined analogously to nonstoring oscilloscope tubes as the maximum rate at which successive storage elements can be charged to produce a useful visual output.

---

[8] In the formulation of these definitions the suggestions of A. S. Jensen, F. H. Nicoll, J. A. Rajchman, A. Rose, P. Rudnick, R. Serrell, and especially those of L. Pensak are gratefully acknowledged.

(6) *Reading:* The generation of an electrical or visual output signal corresponding to the stored charge pattern.

(7) *Maximum Reading Duration* (seconds): The maximum uninterrupted time of signal generation under specified scanning or viewing conditions. This period may depend on such factors as the required degree of contrast, constancy of halftones, number of distinguishable halftone levels, resolution, magnitude of output signal, and output signal to noise ratio.

(8) *Erasing:* The removing of a previously stored charge pattern with the aid of a controllable process such as secondary emission, photoconductivity, etc.

(9) *Erasing Speed* (storage elements per second): The maximum rate at which storage elements charged in writing can be discharged to a specified low value.

(10) *Retention:* The retaining of a stored charge pattern for a period of time such as by means of target insulation or holding action, but without writing, reading, erasing, or external circuit regeneration.

(11) *Retention Time* (seconds): The maximum time after writing that may elapse without reading which will permit a satisfactory electrical or visual signal to be produced.

(12) *Holding:* The maintaining of the storage elements at their equilibrium potentials by electron bombardment against the action of leakage, or the loss or gain of charge due to the landing of undesired electrons or ions.

(13) *Decay:* The reduction in magnitude of a stored charge pattern without writing, reading, erasing, or holding action.

(14) *Decay Time Constant* (seconds): The decay time for the stored charge to fall to 1/e of its initial value without holding action. This time constant is usually a function of the target insulation.

(15) *Charge Factor* (per cent): The fraction of the desired potential shift which is produced at a particular target element during a single scan with a given writing-beam current.

(16) *Discharge Factor* (per cent): The fraction of potential shift of a particular target element from the potential established in writing towards equilibrium potential by a single scan during erasing.

(17) *Useful Number of Storage Elements:* The maximum number of storage elements which can be employed for storing equally spaced "black" and "white" (or on-off) input signals with a specified deterioration in the output signal.

(a) The deterioration of the output signal may manifest itself by first, the addition of thermal noise, noise caused by scattering, or from target irregularities; or second, changes in the signal shape due to the spot sizes and their density distributions, redistribution, and target leakage.

(b) In general, the useful number of elements will be dependent on the required number of distinguishable output levels of each element.

(18) *Resolvable Number of Storage Elements:* The maximum number of storage elements which can be employed for storing equally spaced "black" and "white" (or on-off) input signals which will produce a resolvable[9] visual or electrical output. This number is equal to the product of the number of resolvable scanning lines and the number of resolvable elements per line.

PART 3—METHODS OF WRITING AND READING

A. Writing Methods

The purpose of writing is to establish a desired charge pattern on the storage surface. This process usually consists of two steps: (a) charging the entire target surface, usually by secondary emission, to a uniform potential equal or close to the equilibrium potential V_{eq} (frequently accomplished in the process of erasing or as a result of continuous reading), and (b) adding or subtracting charges from the target surface in a pattern corresponding to the input signal. Since each insulated target element comprises a miniature condenser between its front surface and the backplate, the process of establishing a charge pattern can be considered as a capacity charging action.

The first step, charging the target to a uniform potential, may be accomplished either by flooding the entire target surface with primary electrons or by scanning the target elements with an unmodulated beam. The second step, the writing as such, can be accomplished in a number of ways as described below.

1. Equilibrium Writing

In one form of equilibrium writing (described below as cathode modulation) the direct-current potential of the electron-gun cathode

[9] A detailed description and evaluation of the effect of spot size on resolution in television systems is given by O. H. Schade, "Electro-Optical Characteristics of Television Systems," *RCA Review*, Vol. IX, 1948.

is set at a value below V_{cr1} or above V_{cr2} so that the target elements when bombarded assume an equilibrium potential on either the sloping portion a-b or d-e of the equilibrium curve of Figure 3. The target is then scanned by the primary beam and voltage variations are applied to the cathode which cause the corresponding target elements to assume new equilibrium potentials along one of these lines in accordance with the input signal.

In another form of equilibrium writing (backplate or collector modulation) the cathode potential of the electron gun is set at a value above V_{cr1} and voltage variations are applied to the backplate[10] or collector[11] so that the potential V_{ft} between the target surface and collector will vary as the target is scanned by the unmodulated primary beam.[12] At the moment of bombardment, the surface of each target element will then be maintained at the equilibrium potential by the charging action of the beam against the action of the instantaneous backplate or collector voltage. As a result, each element will acquire a net charge such that after scanning it will have a potential (with respect to V_{eq}) equal[13] and opposite to the instantaneous potential variations V_{ft} applied to the target surface during scanning.

In practice, when the cathode potential, V_k, is between V_{cr1} and V_{cr2}, this form of equilibrium writing requires a *barrier grid* spaced close to the target surface as indicated in Figure 8b to prevent the landing

---

[10] When the input signal is applied to the backplate, a large fraction of the voltage will usually appear at the target surface by capacitive action since the capacity between the backplate and front surface of the target is generally large compared with the capacity of the front surface to the other tube electrodes.

[11] Actually, in this type of writing a barrier grid (which is the effective collector) is usually provided near the storage surface, in addition to a collector cylinder such as electrode *G* as shown in Figure 1. The signal is then applied either to the backplate or barrier grid (see, for example, Part 3-C). Since modulation of the effective collector (barrier grid) causes corresponding shifts in the potential difference V_k between the cathode and effective collector, shifting of the equilibrium potential must be taken into account when V_k exceeds V_{cr2}.

[12] If the target surface is composed of photoemissive elements, writing may be accomplished by scanning the target with a light beam instead of an electron beam while modulating the backplate (or barrier grid collector). In this case, as discussed in Part 1-G, the target elements will tend to shift to a photoemission equilibrium level a few volts positive with respect to the collector. The target potential V_{ft} with respect to the collector may then be varied only in the negative direction by the input signal, since the photoemission process can shift the target elements only in the positive direction.

[13] In operation it may not always be possible or practical to provide sufficient beam current to shift each target element completely to the equilibrium potential. This difficulty is increased by the fact that as the target elements approach the equilibrium potential, δ_e approaches unity (see Figure 6), and the rate of potential shift of the target elements is slowed. In practice, however, the target elements can acquire potentials which are a substantial fraction of the input signals.

of redistribution electrons on the target surface (see Part 1-J). If a barrier grid is not employed, the redistribution charges acquired by the elements may completely mask the charge pattern intended to be stored (Bibliography (37)). As indicated in Part 3-B-4, the redistribution effect, although undesirable for equilibrium writing, can be employed as the basis for a different type of writing, namely redistribution writing.

2. Bistable Writing with the Aid of a Holding Beam

When the individual target elements are not required to assume more than two possible potentials (yes and no, or black and white operation) and the reading duration and retention time are required to be very long, writing may be accomplished by means of a writing beam and an auxiliary holding beam. The holding beam action is based on the fact that if the cathode of this beam is operated at a potential greater than V_{cr1} with respect to collector (see Figure 4), a target element bombarded by this beam will shift to an equilibrium potential either on the portion of the equilibrium curve c-d-e, or to a point on the dashed line b-c′. The particular potential which a target element assumes will depend on the potential it first acquires as a result of bombardment by the writing beam.

If, as a result of the writing beam action alone, the target element acquires a potential with respect to the holding beam such that it falls on a point above the line $V_{pr} = V_{cr1}$ of Figure 4, subsequent bombardment by the holding beam will shift it to the line c-d-e, whereas if the target element acquires a potential such that it falls below the line $V_{pr} = V_{cr1}$, the holding beam will shift it to the dashed line[14] b-c′. Bistable writing may also be accomplished if a particular element is simultaneously bombarded by the writing beam and the holding beam. In this case the writing-beam current must be sufficiently large compared to the holding-beam current so that the potential shift produced by the writing beam predominates.

If, as a result of the writing-beam and holding-beam action, the target elements have all been shifted to one or the other of the two equilibrium potentials, subsequent shifts in the potentials of the elements due to leakage or removal of a fraction of the charge by reading may be restored. This is accomplished by the secondary emission action of the holding beam which tends to shift the target elements to the initial equilibrium potentials existing before the leakage or reading action. The ability of the holding beam to provide indefi-

[14] In practice the holding beam may either scan the target elements sequentially, or flood them simultaneously. It may also bombard the target either during the time of scanning by the writing beam or after.

nitely long reading time under proper conditions is of considerable practical value, making this type of writing desirable in many cases despite the lack of resolution and the absence of halftones (Part 3-E).

Since the holding beam tends to maintain all the elements of the target at either of two potentials which may differ by approximately 50 volts or more, the gradient across the boundary between elements of different potential will be correspondingly high and leakage will occur through the target. In general, for such high gradients the potential boundaries will tend to shift under the action of the holding beam, especially if the target surface is homogeneous. These boundary shifts will manifest themselves by a continuous growing of the areas at holding-gun cathode potential at the expense of the areas at approximately collector potential, or vice versa.

The shifting of the potential boundaries can be reduced or prevented by employing a target whose surface is covered with a mosaic of *conducting* particles or islands which are sufficiently small so that each storage element includes a number of these particles. In this case the potentials assumed by the individual particles in writing will tend to remain unchanged by leakage to the surrounding areas since the leakage currents to the edge of a particle will be replenished by the secondary emission action of the holding beam over the *entire* area of the conducting particle. In the case of a homogeneous target without a mosaic, however, any leakage current across a potential boundary can only be compensated for by the action of the holding beam at the actual boundary itself since the target insulation prevents the flow of currents to the boundary from adjacent areas which are also under the holding beam.

3. Nonequilibrium Writing

This type of writing, accomplished by either secondary emission or photoemission action, involves two steps: (a) adjusting the electrode potentials so that the point of operation on Figure 4 is shifted off the secondary emission equilibrium curve or a photoemission equilibrium level (depending on which of these processes is employed for writing) and (b) allowing each element to shift a controlled amount by secondary emission or photoemission toward the equilibrium level in accordance with the input signal.

If *secondary emission* action is employed, step (a), shifting off the equilibrium curve is achieved by either changing V_{ft}, i.e., shifting the backplate or collector potential, or shifting the potential of the cathode, V_{kc}, making use of either of the sloping portions of the equilibrium curve. For step (b) the primary current striking each target element

is modulated by the input signal so that each element is allowed to shift toward the equilibrium potential by a controlled amount. In practice, modulation of the primary current may be accomplished in several ways. If the target is *scanned* by the writing beam, the primary current striking the individual elements may be modulated by applying signal voltage variations to the primary current control grid, assuming the scanning velocity to be constant, or the input signal may be applied to the deflection circuits so that the instantaneous rate of scanning of the target elements varies in accordance with the signal thus causing variations in the time of bombardment of the successive elements by the constant-current beam (Bibliography (50), (95)). For the *non-scanning* case, step (b) may be accomplished by allowing an extended pattern of primary currents to fall on the target surface such as from an image photosurface (e.g., as in the image orthicon, Bibilography (86)).

If *photoemission* action is employed for writing, shifting off the equilibrium level, step (a), is similarly accomplished by changing the potential V_{ft} of the target surface with respect to the collector, i.e., shifting either the backplate or collector potential. Since, as mentioned in Part 1-G, the elements can only charge positive by photoemission, the potential shift of step (a) must be in the direction such that the target surface is made negative with respect to the collector. Step (b) is then achieved by allowing a controlled amount of light to strike each target element so that its potential shifts by a corresponding amount toward the equilibrium level. The light striking the elements may be in the form of a pattern or picture focused on the surface of the target (e.g., as in the orthicon, Bibliography (84)), or it may be in the form of a modulated beam which scans the element sequentially.

Although not usual, nonequilibrium writing may also be accomplished by scanning the target with an unmodulated electron beam of low current under the condition $\delta_c > 1$ and applying the input signals to the backplate (Bibliography (46)). In this case the input signal voltages, assumed to be small, cause the potential of the target surface to assume instantaneous values along the sloping portion B-C-D of the δ_c curve of Figure 6. Because of the very low primary current, each element will not be shifted to the equilibrium potential V_{cq} when bombarded, but will acquire or lose a net amount of electrons proportional to the variations in δ_c from its equilibrium value of unity.

4. Redistribution Writing

For targets which do not have a barrier grid, redistribution generally interferes with the writing process (see Part 1-J). However, redistribution can also be usefully employed for writing. If the target

surface is approximately at collector potential, such writing can be accomplished by bombarding the target elements with primary electrons from a cathode whose potential is between V_{cr1} and V_{cr2} or illuminating them with light if the elements are photoemissive.

In the first case the bombarded elements tend to lose electrons by secondary emission, since the bombardment is under the condition $\delta_c > 1$. However, because of the lack of accelerating field between target and collector, a large fraction of the secondary electrons will return to other target elements by redistribution (see Part 1-J). If a controlled amount of primary current is allowed to strike each element (as, for example, when the writing beam consists of a pattern of currents from an extended photocathode), the net effects of the secondary emission and redistribution will be to cause the elements bombarded with the greatest amount of current to charge most positively and the elements bombarded with less current to be shifted less positive or possibly negative (see, e.g., Bibliography (72), (77)).

In the second case, where the target elements are photoemissive (Bibliography (94)), redistribution writing may be accomplished by focusing a pattern of light on the target surface. Although the illuminated elements tend to lose electrons by photoemission, a large fraction of the photoelectrons will be returned to other target elements by redistribution as in the case of secondary emission, due to the lack of an accelerating field. In similar manner the net effect of photoemission and redistribution will cause those elements receiving the most light to charge most positively and those elements receiving less light to charge less positively or possibly negative.

In general the magnitude of the potential variations established on the target surface by redistribution writing is relatively small, not exceeding a few volts. On the one hand the maximum positive potential of the elements is set by either the secondary emission equilibrium potential or the photoemission equilibrium potential, both of which are only a few volts positive with respect to the collector; on the other hand, the minimum potential is set by the redistribution level which is only a few volts negative.

Redistribution writing may also be accomplished by scanning the target elements sequentially with a modulated primary beam or light beam. In one form of such writing (Bibliography (66)), writing is performed by modulating the primary current with a dot and dash signal, thus producing a corresponding redistribution charge pattern.

5. Induced-Conductivity Writing (Electron Bombardment or Light)

Before writing by this method, it is assumed that the target surface is shifted to a common equilibrium potential (usually collector poten-

tial) while the backplate is maintained at a voltage different from the equilibrium potential. As a result, a uniform potential difference will exist between the front and back surfaces of the insulating target and each of the elementary target condensers will be equally charged.

Writing may now be accomplished by causing the conductivity of each target element to increase by a controlled amount so that the front surface of the target will shift to varying degrees toward the backplate potential. The conductivity of the target elements can be controlled by either of the two methods as follows:

a. Bombardment-Conductivity Writing—If the target is thin (approximately 0.5 micron) and a high-velocity writing beam is used (10,000 volts, for example), primary electrons will penetrate the insulating target causing bombardment conductivity at the corresponding elements (see Part 1-I). By controlling the number of primary electrons striking each element (either by scanning the target with a current-modulated primary beam, or by focusing an extended pattern of primary currents on the target from an auxiliary photoemitting surface), a pattern of charges or potential variations can be established on the target surface.

b. Photoconductivity Writing—If the target is composed of a thin layer of photoconductive material, incident light on the surface will cause the conductivity to increase at the elements which are illuminated (see Part 1-II). By controlling the amount of incident light at each element (such as by focusing an optical image on the surface), a pattern of charges or potential variations can also be established on the target surface.

6. Methods of Applying the Input Signals During Writing

In practice, writing is accomplished by modulation of the control-grid voltage, deflection voltage or current, cathode voltage, collector voltage, backplate voltage, or modulation of the light falling on the target if it is photoemissive or photoconductive. These types of modulation are illustrated in Figure 9 where a single-beam charge-controlled storage tube with its basic elements is shown.

The following types of modulation are thus possible for writing:

a. primary-current modulation
b. scanning-velocity modulation
c. cathode-voltage modulation[15]

[15] Since by definition, cathode-voltage modulation is meant to exclude simultaneous primary-current control-grid modulation, a coupling condenser, indicated in dashed lines between the cathode and control grid of Figure 9, may be employed when cathode modulation is used.

d. collector-voltage modulation
e. backplate-voltage modulation
f. light-intensity modulation.

It should be noted that whereas the modulations of (a), (b) and (f) regulate charging of the target elements by control of the number of incident primary electrons or photons, the modulations of (d) and (e) regulate charging of the target elements by control of the number of

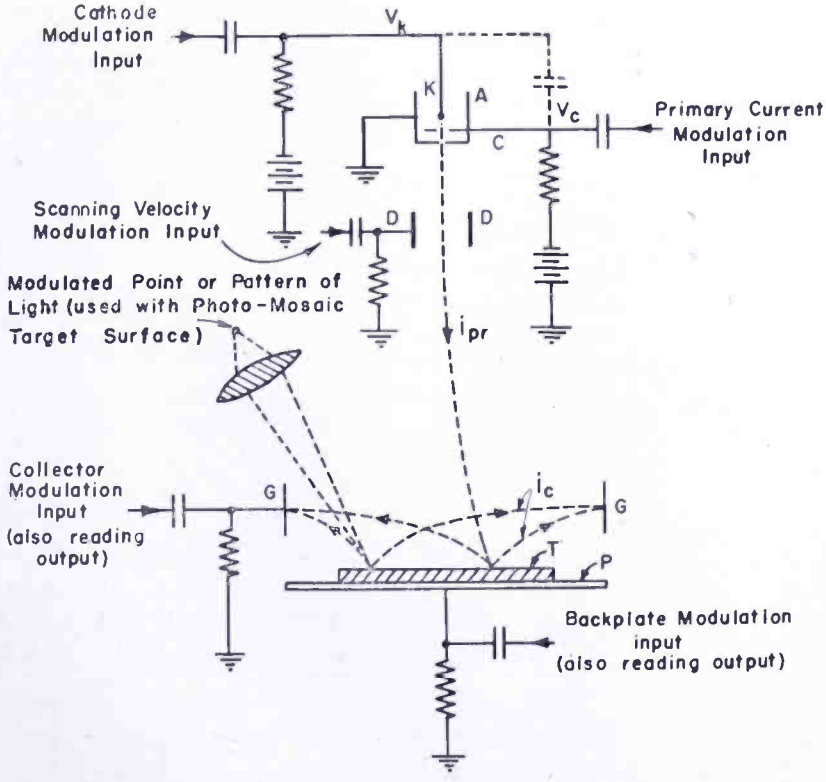

Fig. 9—Methods of applying input signals to a storage tube.

A = accelerating anode,
C = control grid,
D = deflection plates,
G = collector,
i_c = collected current,
i_{pr} = primary current,
K = cathode,
P = backplate,
T = target,
V_c = control grid bias voltage,
V_k = cathode bias voltage.

secondary electrons leaving the target as a result of controlling the field between target surface and collector. The modulation of (c) regulates charging by changing the secondary emission ratio δ_e (operation above the second crossover potential V_{cr2}), or the reflection of primary electrons (operation below the first crossover potential, V_{cr1}).

B. Reading Methods

The process of reading is basically one of obtaining output currents corresponding to the charge stored in writing on each of the target elements. In general, three methods may be employed for reading as described below.

1. Capacity-Discharge Reading

This method of reading is based on the fact that each target element, between its front and back surface, is a miniature condenser. As indicated in Figure 10, the target is shown divided by the dashed lines into its effective capacitive elements (each of which is approximately equal in area to the cross section of the primary beam).

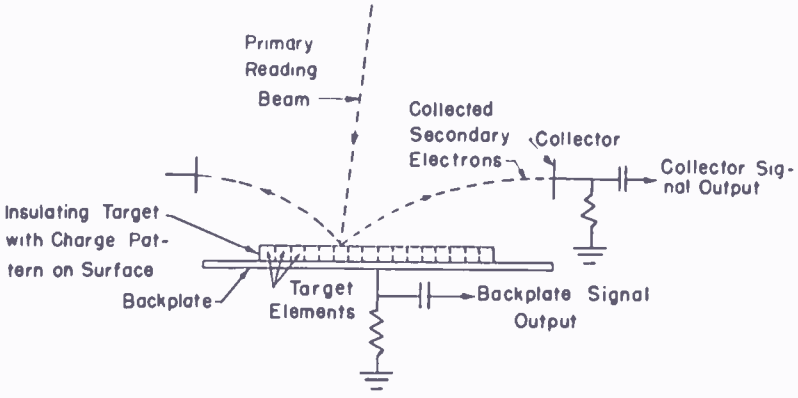

Fig. 10—Capacity discharge reading system.

If in the writing process a charge pattern was established on the front surface of the target elements, the corresponding elementary condensers will be charged to varying degrees. In reading, these elements are scanned by an unmodulated primary beam so that they tend to shift toward the equilibrium potential, V_{eq}, when bombarded. The amount of potential shift each element undergoes will depend on the beam current and the value of δ_c for each element. As a result of scanning by the reading beam, capacity discharge currents will be produced in the backplate[16] circuit corresponding to the potential shifts of the target elements. At the same time, current variations of opposite polarity will result in the collector circuit, since the instantaneous collected current, i_c, is equal to the difference between the primary current (which is unmodulated) and the instantaneous capacitive

[16] Capacity-discharge reading systems sometimes do not employ a backplate (such as indicated in Figure 9). An example of this is the image orthicon, where the writing beam establishes the charge pattern on one side of the insulating target and the reading beam capacitively "neutralizes" these charges from the opposite side. In such an arrangement the reading signal is obtained from the collector-current variations.

target current. By inserting a resistor either between the backplate or collector and ground, output voltage variations may be obtained corresponding to the initial input writing signal.

In capacity-discharge reading, the beam current may be sufficient to shift each of the target elements to the equilibrium potential in a single scan or it may be set at a smaller value so that the elements are shifted only a portion of the way toward equilibrium in one scan. In the latter case an output signal can be obtained for a number of scans (copies) before all of the elements are shifted to the equilibrium potential. (The choice of reading-beam current will also affect the generation of halftones as discussed in Part 3-E. For example, sufficient beam current to discharge the target elements in one scan will produce linear halftones, whereas lower beam currents will produce nonlinear or no halftones.)

In general, the beam current needed in reading to shift the target elements the required amount toward the equilibrium potential depends on the capacity of the individual target elements. This capacity will similarly determine the amount of beam current required in writing. For a given insulating material, the target thickness is usually in the range of 0.5 to 100 microns depending on the required target capacity. The choice of target capacity is based on a number of factors. If, for example, large output currents are required in reading, it is necessary to have a high-capacity target for storing large quantities of charge. If the charge pattern is established by equilibrium writing with backplate-voltage modulation, it is desirable that the loading of the target on the input amplifier be small, necessitating a small capacity between backplate and barrier grid, i.e., a thick target. If bombardment-induced conductivity is used for writing, the target must be sufficiently thin (approximately one micron or less) to allow penetration by the primary beam, resulting in a relatively high target capacity.

In capacity discharge reading as described above it is assumed that no redistribution effects are present (see Part 1-J).[17] If redistribution exists, it will reduce the magnitude as well as cause distortion of the output signal. Redistribution effects may be prevented by employing a barrier grid such as indicated in Figure 8b. If a barrier grid is not used, redistribution may also be prevented by applying a potential shift to the backplate or collector so that the target element potentials are all substantially negative with respect to the collector and not allowing the elements to shift positive to a point close to the collector potential

[17] Although undesirable in capacity-discharge reading, the redistribution effect plays a definite rôle in producing the output signal as described below under redistribution reading.

in reading. By such means the accelerating field at each target element can be made sufficiently strong to prevent redistribution.

2. Redistribution Reading

This type of reading is usually carried out while the input signals are applied simultaneously to the target by redistribution writing as for example in the iconoscope. The target-potential variations established in writing are small and are in the neighborhood of the collector potential. As in capacity-discharge reading, the target is scanned by the unmodulated reading beam under the condition $\delta_e > 1$ and the output signal is obtained from the backplate or collector electrode.

In order to explain the generation of the output signal, it is convenient to consider first the target during scanning by the reading beam before writing signals have been applied. During this scanning, each target element will periodically undergo a positive shift at the moment of bombardment and gradually shift negative by an equal and opposite amount as it acquires redistribution electrons between successive times of bombardment. A typical curve of the potential of a target element with time is indicated by the solid line a-b-c-d in Figure 11a. Since the reading-beam current is usually low in such writing (a fraction of a microampere, for example) the target elements will generally not be shifted sufficiently positive to reach the equilibrium potential, V_{eq}, when bombarded.

If now, during scanning by the reading beam, potential variations caused by redistribution writing (involving photoemission, for example, as in the iconoscope) are superimposed on the target potentials, the individual elements will have new potentials such as indicated by the dotted lines a′-b′-c′-d′ and a″-b″-c″-d″ of Figure 11a depending on whether they lost or gained electrons respectively in the writing process. Nevertheless, despite the loss or gain of electrons by an element in writing, its positive potential shift when bombarded will be approximately the same, i.e., the lines b-c, b′-c′, and b″-c″ are approximately equal in Figure 11a (Bibliography (37)).

During bombardment of each element by the reading beam, a large fraction of the secondary electrons will return to the target surface as a whole by redistribution. However, the number of electrons which escape to the collector will depend on the potential of the element under bombardment (Bibliography (37)). For example, if the element had acquired a slightly positive charge in writing such as indicated by the line a′-b′-c′-d′ of Figure 11a, fewer secondaries would reach the collector and more redistribution electrons return to the target as a whole when the element was bombarded. The opposite would be the case if the

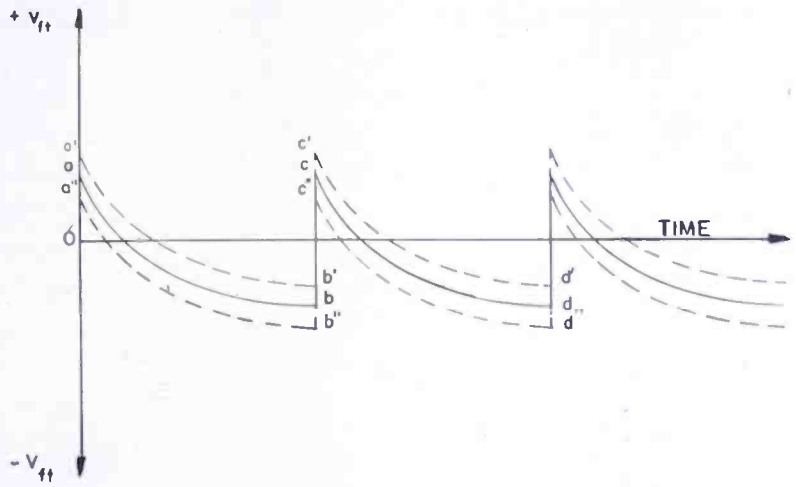

Fig. 11a—Instantaneous target-element potentials as a result of redistribution reading. (Scanning with low beam current).

element had acquired a negative charge such as indicated by the line a″-b″-c″-d″. (Since the potential variations of the target are assumed to be very small, each element can be considered to have the same value of δ_c.) As a result of scanning by the reading beam, collector current and capacitive current variations through the target will arise due to potential variations such as b-b′ (Figure 11a) on successive target elements, thus producing an output signal at either of the two electrodes.

The curves of Figure 11a assume that the writing signal (light pattern) is maintained continuously during reading and that the primary current is low. If the writing signal is not maintained, the continuous landing of redistribution electrons on all the elements will gradually reduce the potential differences. In practice, a reading signal

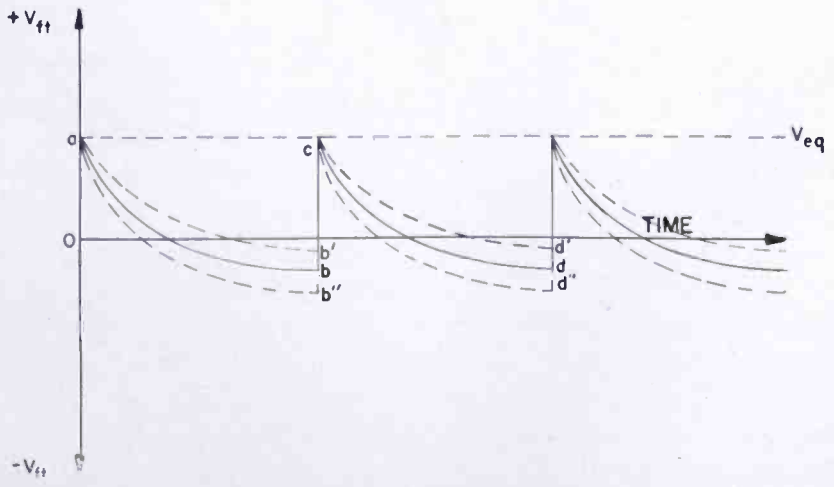

Fig. 11b—Instantaneous target-element potentials as a result of redistribution reading. (Scanning with high beam current.)

may be obtained for several scans after the writing signal has been cut off.

If higher beam currents are employed in reading, each element will be shifted to the equilibrium potential, V_{eq}, when bombarded, as in capacity-discharge reading, regardless of the potential variations acquired in writing. This condition is indicated in Figure 11b where the solid line a-b-c-d indicates the potential with respect to time of an element before writing, and the dotted lines a-b′-c-d′ and a-b″-c-d″ represent the potentials of elements which acquire positive and negative charges respectively under continuous writing action.

3. Grid-Control Reading

In this type of reading the local electrostatic fields at the target, produced by the charges established in writing, control (a) the amount of reading-beam current passing through target holes, (b) the currents emitted from the target surface, or (c) the deflection of primary electrons as they are being reflected at the target surface. In all of these cases the modulation of the reading beam is not dependent on the landing of reading electrons on the insulated target elements as in capacity discharge or redistribution reading. Although limited by target leakage and the landing of ions, grid-control reading is thus suitable for reading where output signals are required for relatively long periods of time.

Grid-control reading can be accomplished either by scanning the target with a focused beam or by flooding all of the elements with electrons or light. For the production of time-varying output signals the target elements are scanned, while for the production of a visual picture the target is either scanned or flooded with the reading beam and the resulting pattern of reading currents made visible on a phosphor surface.

The three different methods of grid-control reading are described below.

a. Transmission Modulation—In this reading method the target is constructed of a metal mesh or perforated conducting plate with insulating material surrounding the holes on either the reading gun side (Figure 12a and Bibliography (52a)) or the opposite surface (Bibliography (49)). From previous writing, a pattern of charges is assumed to have been established on the insulating elements, producing corresponding electrostatic fields in the neighborhood of the target holes. In the reading operation, the potential of the reading-gun cathode is adjusted so that the reading-beam electrons have low velocity as they approach the target surface. The electrostatic fields produced by the stored charges are thus able to control, by coplanar grid action,

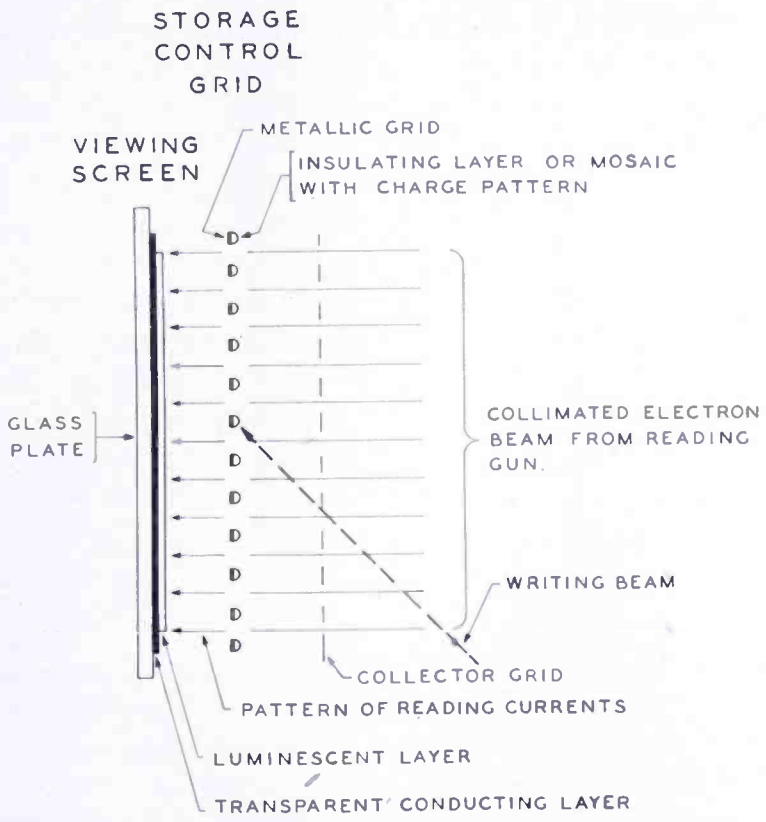

Fig. 12a—Transmission modulation (visual output).

the number of electrons penetrating each target hole and the corresponding number reflected. The resulting variations in the reading-beam currents which emerge from the target holes constitute the output signal. This form of reading is generally accomplished with the insulating elements sufficiently negative so that none of the reading-beam electrons are able to land on them.

b. Emission Modulation—In this method (Bibliography (42), (52), (57)), the reading-beam currents originate at conducting elements on the target surface as a result of photoemission (see Figure 12b), thermal emission, or secondary emission. Between the conducting elements on the target surface are insulated elements assumed to be charged from previous writing. As in transmission modulation, the stored charges produce local electrostatic fields at the target surface which, in this case, control the number of electrons leaving the individual conducting elements of the target. The insulated elements here also are charged to potentials negative with respect to the conducting area of the target so that none of the emitted electrons are able to land on them.

c. Reflection Modulation—In one form of such reading (see Figure 12c) a thin insulating target is provided with a close-spaced

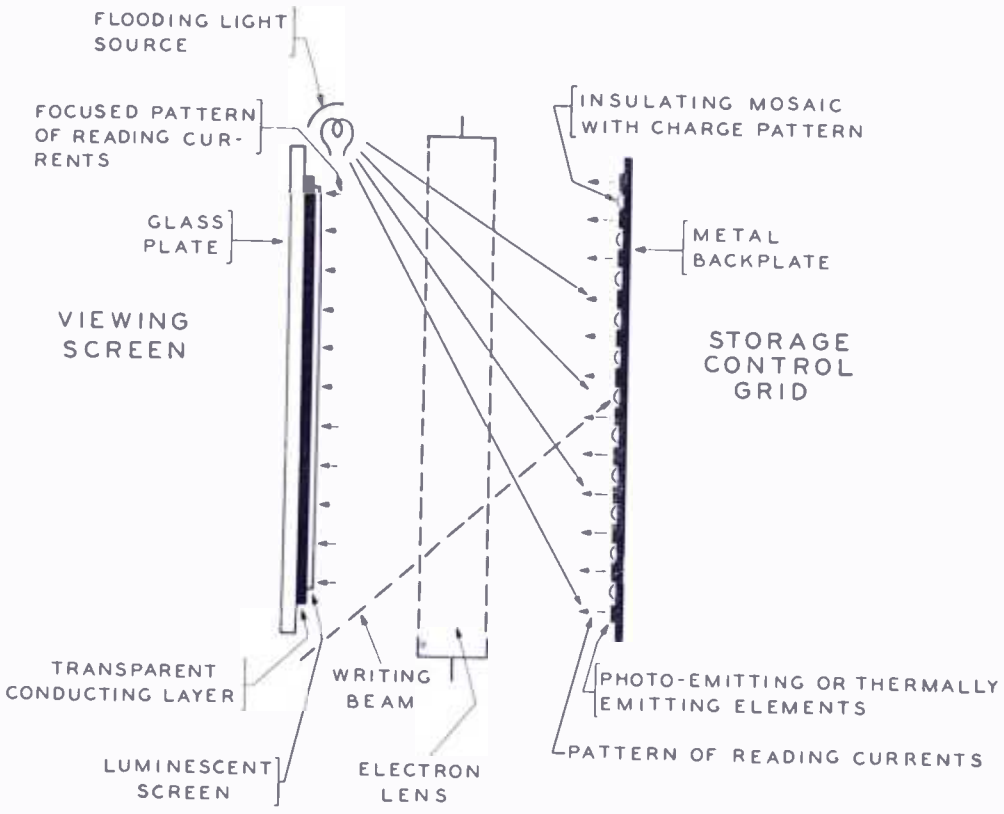

Fig. 12b—Emission modulation (visual output).

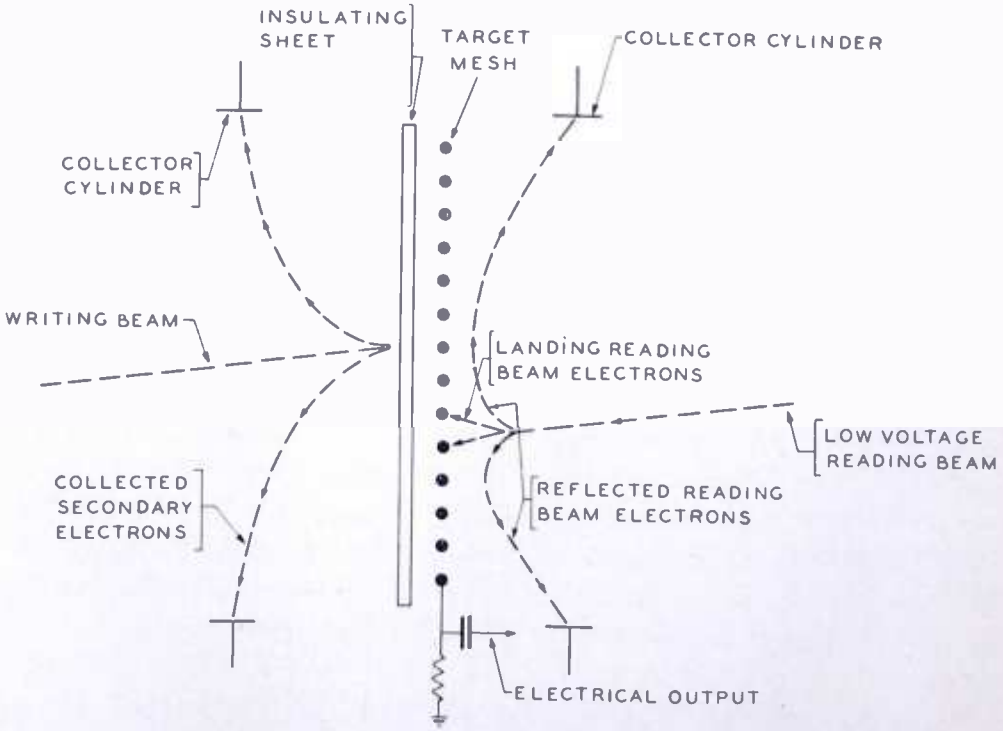

Fig. 12c—Reflection modulation (electrical output).

metallic mesh on one side, and a charge pattern is established by the writing gun on the opposite side. The cathode potential of the reading gun is adjusted so that primary electrons approach a given element on the mesh side of the target with very low velocity. The insulating elements are sufficiently negative, with respect to the target mesh, that the reading-beam electrons are unable to land on them. The reading electrons are thus either deflected to the target mesh, or partially or wholly reflected back to the collector, depending on the amount of negative charge stored on the back side of the corresponding target element. By scanning the target with the reading beam, time-varying output currents to the target mesh are produced (and also opposite polarity current variations to the collector mesh) in accordance with the stored charge pattern (Bibliography (90)).

In another form of reflection modulation, without a target mesh (Bibliography (89)), all the reading-beam electrons are reflected at the target surface and directed back to the reading gun where a special collector is provided. Due to the variations in the deflection of the reading beam at the target as it undergoes reflection, the trajectories of the returning electrons are correspondingly modulated. These variations in the trajectories in turn cause variations in the number of electrons landing on the special collector as successive target elements are scanned.

C. Erasing and Decay

The removal of a stored charge pattern may be accomplished in two ways, either allowing the charges to decay as a result of leakage of the insulated target elements, or erasing them such as by secondary emission action. When capacity-discharge reading systems are employed, erasing by secondary emission action is always involved during reading since the output signals are obtained from the discharge of the target elements themselves. At the same time, decay of the stored charges may also be a factor assisting in the charge removal.

When grid-control reading systems are employed, the reading process, as such, generally does not erase the stored charges by secondary emission action. In this case, the decay of the charges by leakage and gas ions are the only erasing actions during the reading process. If the decay in this case is not sufficiently rapid or uniform, it is necessary to resort to secondary emission action to assist in removing the charges. It is also frequently possible to erase a charge pattern by *writing* over it if equilibrium writing is employed, since in such writing the target elements will shift to the new potentials regardless of their previous

charge.[18] It is understood, of course, that all of the previously charged elements must be rescanned if erasure of the entire pattern is to be accomplished.

The *decay time* is determined in general by the leakage of the target material and the number of gas ions in the tube. Except insofar as these two conditions can be varied by factors such as the temperature of the insulating target or the residual pressure of the storage tube respectively, the decay time is fixed. The *erasing time*, however, may be varied within limits, by adjusting the current of the erasing beam or its cathode voltage. In a capacity discharge reading system where reading and erasing are carried on simultaneously, such current adjustment will control the reading time as well (since the reading time is approximately equal to the erasing time) and also the magnitude of the output signal.

D. Halftones

In general, if the output signal or reading current corresponding to a particular element is *continuously variable* as a function of the input voltage or writing signal over a substantial range, it is possible to employ a storage tube for halftone signals. Whether or not the halftones in the output are *linear* with respect to those in the input will depend on (a) the linearity with respect to the input signal of the charge stored during writing on each element, and (b) the linearity of the output current from a particular element with respect to the charge stored on that element. These two factors will be discussed below as "Halftone Writing" and "Halftone Reading" for the various writing and reading methods.

1. Halftone Writing

a. Equilibrium Writing—In this type of writing, the target element potentials can be varied over a continuous range by potentials applied either to the cathode, backplate, or collector, thus resulting in a halftone charge pattern. When the input signals are applied to the *backplate* or *collector* the target elements will acquire potentials approximately equal in magnitude to the input signals so that the halftones will be linear. When the input signals are applied to the *cathode*,

[18] This is generally true except for the case of equilibrium writing by cathode modulation where the direct-current potential of the writing beam cathode is less than V_{c_1}. In this case, since the target elements assume potentials equal to the writing-beam cathode, rewriting can only be accomplished if an element is to be shifted to a new potential which is more negative. If the instantaneous potential of the writing-beam cathode is made more positive than the existing potential on an element, primary electrons will be unable to land on that element.

the target elements will be shifted along either the sloping portion a-b or d-e of the equilibrium curve of Figure 3. Since the line a-b is straight, as is the line d-e with the exception of the curved part near d (see Footnote 3, page 707), the target elements, will, in this case, generally acquire linear halftones.

Equilibrium writing is in some respects to be preferred for the production of linear halftones in that it is to a considerable degree independent of parameters which in other types of writing must be more carefully controlled, such as the linearity of beam current as a function of input voltage or the uniformity of scanning speed when nonequilibrium writing is employed.

b. Bistable Writing—This type of writing, by its mechanism, is intended to give the individual target elements one of two equilibrium potentials. However, methods for retaining halftone information by means of bistable writing have, until the present, not been published.

c. Nonequilibrium Writing—Since in this type of writing the degree of potential shift of a target element is controlled over a continuous range by the magnitude of the input signal, a halftone charge pattern can be established. The degree of halftone linearity, however, will depend (assuming that the number of primary electrons or light quanta striking each target element is proportional to the input signal voltage) on whether the charging of the target element is proportional to the number of primary electrons or light quanta.

In particular, if writing is accomplished with a modulated electron beam, the production of linear halftones requires that the collected-current ratio δ_c from each element remain relatively unchanged during the charging of each element in writing. This can be accomplished if first, the target surface has a potential before writing which falls on a flat portion of the δ_c curve such as to the left of point A or on part F-G, and second, the potential shifts of the elements do not carry them to sloping portions of the curve such as near points B and D where δ_c varies rapidly with target potential. For producing linear halftones when V_{ft} is positive, it is assumed that redistribution is avoided by the use of a barrier grid at the target surface.

If modulated light is employed for writing, linearity of halftones requires that the storage elements always be maintained sufficiently negative with respect to the collector so that all of the emitted photoelectrons reach the collector.

If the writing is accomplished by backplate modulation, a linear halftone charge pattern can be established provided first, a very low beam current is used so that none of the elements are shifted to the equilibrium potential, V_{eq}, when bombarded and second, the input sig-

nals are maintained sufficiently small so that the target surface potential variations occur on the relatively linear portion of the δ_o curve of Figure 6 near point C.

d. Redistribution Writing—This type of writing is capable of producing halftones, but because of the relatively small potential variations possible in such writing (see Part 3-A-4), the halftone range is correspondingly small. In practice, if small writing signals are applied, halftone picture signals can be produced which are relatively linear.

e. Induced-Conductivity Writing—Since the degree of induced conductivity can be controlled by the amount of primary current or incident light, a halftone charge pattern can be established in this type of writing. Although the induced conductivity is a more or less linear function of primary current or light, assuming small values, the discharge of the target elements is an exponential function, $e^{-k\sigma}$, of the induced conductivity σ (the bombarding time and capacity of all elements being equal). The degree of halftone linearity will therefore depend on how small a portion of the exponential curve is used, i.e., the variations in the induced conductivity σ should be small, restricting the writing to small signals.

2. Reading Halftones

a. Capacity-Discharge Reading—This type of reading may be accomplished either with the reading-beam current sufficiently large that all of the stored potential variations are removed in a single scan, or the reading-beam current small so that output signals are obtained for a number of successive scans.

If reading is accomplished under the first condition, the current variations in the collector or backplate circuits will be *linearly* related to the magnitude of the stored charge since variations in the rate of removal of the charges constitute the output-current variations.

If reading is accomplished under the second condition, the production of halftones will depend on which portion of the δ_o curve of Figure 6 the target potentials fall. If the target elements are charged to potentials which fall near the upper portion of the curve such as near point A, the collected current, i_c, will be essentially constant over a considerable range of variations of V_{ft} and, as a result, the output will be largely a black-and-white signal with relatively small amounts of halftones. Similarly, potential variations which fall on the curve near point F, where δ_c is also relatively constant, will produce almost entirely black-and-white output signals.

If, on the other hand, the target potential variations fall on the sloping portion B-C-D of the δ_o curve, variations in the target-element

potentials will cause corresponding variations in the output current so that halftones will appear in reading. For potential variations close to point C, where the values of V_{ft} are small, an essentially linear halftone output can be obtained, since the δ_c curve is most linear at this point.

For example, in the Graphechon (Bibliography (54)), halftones can be produced if the potential V_{ft} is less than 10 volts with respect to V_{eq}. For more negative potentials of V_{ft}, black-and-white output signals are produced.

Because of the gradually changing slope of the curve as it approaches the point $V_{ft} = 0$, target elements initially on the flat portions (to the left of point A and to the right of point D) will, after partial discharge in reading with a low beam current, shift to the more sloping portion B-C-D, thus producing halftones during later scans toward the end of their discharge.

b. Redistribution Reading—This type of reading is capable of producing halftone output signals which are linear. If very low beam currents are used so that the elements when bombarded do not reach the equilibrium potential V_{eq}, the output will be linear since the amount of current, i_c, escaping to the collector from a particular element is essentially linear as a function of the target potential (Bibliography (37)). If higher beam currents are employed, so that each target element is shifted to the equilibrium potential V_{eq} in a single scan, the output will also be linear since it will be proportional to the amount of charge gained or lost by each element.

c. Grid-Control Reading—This type of reading, depending on a negative-grid control by means of the charged elements, is generally capable of providing halftones, since the output-signal current is continuously variable as a function of the potential of the control elements. The actual shape of the curve of output current versus potential on the storage elements will be a function of the geometry of the target and collector system so that the degree of linearity of halftones in reading and the range of target element potentials for such operation will be determined by these factors.

d. Combination of Writing and Reading Methods—Summarizing the above discussion of halftones, under proper operating conditions any one of the writing methods, with the exception of bistable writing, may be employed for establishing a halftone charge pattern. Similarly, any one of the reading methods, with the exception of the capacity-discharge method, may be employed for obtaining a halftone output signal when the target element potentials fall on the flat portions of the δ_c curve and each element is not completely discharged in a single scan.

If long reading time with halftones is required, a grid-control reading method must be employed.

ACKNOWLEDGMENT

The authors wish to express their appreciation for the support of John E. Gorham of the Evans Signal Laboratory and in addition wish to acknowledge the many stimulating discussions with L. Pensak and other members of RCA Laboratories Division. The authors are also indebted to Miss Ruth Pearl for her assistance in preparing the manuscript.

PART 4 — BIBLIOGRAPHY

A. SECONDARY EMISSION, PHOTOEMISSION, PHOTOCONDUCTIVITY AND BOMBARDMENT CONDUCTIVITY OF INSULATORS

1. F. Ansbacher and W. Ehrenberg, "Electron Bombardment Conductivity," *Nature*, Vol. 164, p. 144, 1949. (Experiments made with dielectric films sandwiched between conducting layers one of which is evaporated onto the surface.)

1a. F. Ansbacher and W. Ehrenberg, "Electron Bombardment Conductivity of Dielectric Films," *Proc. Phys. Soc.* (London), Series A, Vol. 36, p. 362, 1951.

2. H. Bruining, *Die Sekundärelektronen-Emission fester Körper* (The secondary emission of solids), Julius Springer, Berlin, 1942. (Relatively complete text on subject.)

3. H. Daene and G. Schmerwitz, "Prüfung der theoretischen Erklärungen der Sekundärelektronen-Emission von Isolatoren" (Proof of theories of secondary emission of insulators), *Zeit. für Phys.*, Vol. 53, p. 404, 1929.

4. M. F. Distad, "Equilibrium Currents Induced in Zincblende by Electron Bombardment of Negative Electrode," *Phys. Rev.*, Vol. 80, pp. 879-886, 1950.

4a. W. Ehrenberg, Chi-Shi Lang and R. West, "The Electron Voltaic Effect," *Proc. Phys. Soc.* (London), Series A, Vol. 36, p. 424, 1951.

4b. S. V. Forgue, R. R. Goodrich, and A. D. Cope, "Properties of Some Photoconductors, Principally Antimony Trisulfide," *RCA Review*, Vol. XII, pp. 335-349, September, 1951.

4c. A. L. Hughes and L. A. DuBridge, *Photoelectric Phenomena*, McGraw-Hill Book Co., New York, N. Y., 1932. (Extensive survey of experimental and theoretical aspects of photoemission and photoconductivity.)

5. G. Kalckhoff, "Über die Geschwindigkeitsverteilung der an Isolatoren ausgelösten Sekundärelektronen" (Velocity distribution of sec-

ondary electrons from insulating materials), *Zeit. für Phys.*, Vol. 80, pp. 305-323, 1933.

6. M. Knoll and B. Kuehnreich, "Sekundäre Elektronenemission von Kristallphosphoren und MgO bei hohen Elektronengeschwindigkeiten" (Secondary electron emission of phosphors and MgO at high electron energies), *Reichsberichte für Physik*, pp. 108-110, 1944.

7. E. Krautz, "Zur Aufladung u. Aufladungserniedrigung elektronenbestrahlter Leuchtstoffe und Halbleiter" (Charging and discharging of electron bombarded luminescent materials and semiconductors), *Zeit. für Phys.*, Vol. 114, pp. 459-464, 1939. (Decelerating field at a luminescent screen bombarded with fast electrons ($\delta_c < 1$) decreased by additional bombardment with slower ($\delta_c > 1$) electrons.)

8. H. B. Law, "Formation of Insulating Layers by the Thermal Decomposition of Ethyl Silicate," *Rev. Sci. Instr.*, Vol. 20, p. 958, 1949.

9. K. G. McKay, "Secondary Electron Emission," *Advances in Electronics*, Vol. I, Academic Press, New York, 1948, pp. 65-130, (Exhaustive survey, insulators).

10. K. G. McKay, "Electron Bombardment Conductivity in Diamond," *Phys. Rev.*, Vol. 74, pp. 1606-1621, 1948, and Vol. 77, pp. 816-825, 1950.

11. K. G. McKay, "A Pulse Method of Determining the Energy Distribution of Secondary Electrons from Insulators," *Jour. Appl. Phys.*, Vol. 22, pp. 89-94, 1951.

12. H. Mahl, "Feldemission aus geschichteten Kathoden bei Elektronenbestrahlung" (Field emission from striated cathodes under electron bombardment), *Zeit. Tech. Phys.*, Vol. 18, pp. 559-563, 1937. ("Malter effect" on 0.2-micron cesiated Al_2O_3 target, observed in electron microscope. Positive potential on the surface determined as 10-40 volts; measurement of velocity distribution of "field electrons".)

13. S. T. Martin and L. B. Headrick, "Light Output and Secondary Emission Characteristics of Luminescent Materials," *Jour. Appl. Phys.*, Vol. 10, pp. 116-127, 1939.

14. C. W. Mueller, "The Secondary Emission of Pyrex Glass," *Jour. Appl. Phys.*, Vol. 16, pp. 453-458, 1945. (50 to 10,000 volts; sharp max. at 400 volts ($\delta_c = 2.4$); upper crossover at ~2300 volts.)

15. R. R. Newton, "Space-Charge Effects in Bombardment Induced Conductivity through Diamond," *Phys. Rev.*, Vol. 75, pp. 234-246, 1949.

16. W. B. Nottingham, "Electrical and Luminescent Properties of Willemite under Electron Bombardment," *Jour. Appl. Phys.*, Vol. 8, pp. 762-778, 1937, and Vol. 10, pp. 73-83, 1939. (Floating target potential as a function of final anode potential.)

17. L. Pensak, "Conductivity Induced by Electron Bombardment in

Thin Insulating Films," *Phys. Rev.*, Vol. 75, pp. 472-478, 1949. (Two beam scanning technique, steady state currents observed.)

18. L. Pensak, "Electron Bombardment Induced Conductivity in Selenium," *Phys. Rev.*, Vol. 79, pp. 171-172, 1950.

18a. A. Rose, "An Outline of Some Photoconductive Processes," *RCA Review*, Vol. XII, pp. 362-414, September, 1951.

19. H. Salow, "Über die Winkelabhängigkeit der S. E. von Isolatoren" (Secondary emission of insulators as a function of angle of incidence), *Phys. Zeit.*, Vol. 41, pp. 434-442, 1940. (Pulse method as described in *Zeit. Tech. Phys.*, Vol. 21, p. 8, 1940; δ_e varies for glass at 3500 volts from 1.2 to 3, at 500 volts from 3.2 to 4 between 0 and 70°; similar for mica; slope is smaller for ZnS; discussion of former measurements.)

20. P. K. Weimer, "Measurement of Secondary Emission of Insulators at Low Primary Energies," *Phys. Rev.*, Vol. 74, p. 1219, 1948.

20a. P. K. Weimer and A. D. Cope, "Photoconductivity in Amorphous Selenium," *RCA Review*, Vol. XII, pp. 314-334, September, 1951. (Study of photoconductivity by television scanning techniques.)

B. Charging Processes of an Electron-Bombarded Insulating Surface and Their Measurement

21. H. Bey, "Aufladepotentiale elektronenbestrahlter Leuchtmassen" (Potentials of electron bombarded luminescent materials), *Phys. Zeit.*, Vol. 39, pp. 605-611, 1938. (Influence of charge potentials on brightness of luminescence and electron spot size; slope of equilibrium curve above second crossover for glass and luminescent materials $<45°$ which is explained by a loss of charge of the screen due to the electric field in its volume. Under bombardment with 2×10^{-6}A/cm^2 and 8 kilovolts, second crossover shifts for Willemite from 6.5 to 4 kilovolts in 50 minutes, similar in $CaWO_4$, $CdWO_4$ and CdS:Cu.)

22. C. Hagen, "Aufladepotentiale, Sekundäremission u. Ermüdungserscheinungen elektronenbestrahlter Metalle u. Leuchtsubstanzen" (Equilibrium potentials, secondary emission and fatigue of electron bombarded metals and luminescent materials), *Phys. Zeit.*, Vol. 40, pp. 621-640, 1939. (Slope of equilibrium potential versus collector potential above second crossover, which is 45 degrees for floating metals, decreases for zinc silicate from 34 to 27 degrees if field strength at the target is increased from 1500 to 3000 volts per centimeter. Reason: Increase of secondary emission factor by the electric field in the interior of the insulator. Smooth glass surface shows second crossover at 2.3 kilovolts and 39-degree slope, powder surface from the same glass shows second crossover at 3.7 kilovolts and 26-degree slope. Reason for higher

crossover is a greater angle of incidence, reason for smaller slope is higher field strength at the top of glass particles. Measurement of target potential with electrometer between target and collector.)

23. C. Hagen and H. Bey, "Aufladepotentiale elektronenbestrahlter Isolatoren" (Charge potentials of electron bombarded insulators), *Zeit. für Phys.*, Vol. 104, pp. 681-684, 1937. (Measurement of screen potential by electrometer filament within the collector-target field; second crossover of S.E. curve 1900 volts for glass, 4300 volts for willemite, 3100 volts for zinc silicate, 6000 volts for $CaWO_4$.)

24. W. Heimann and K. Geyer, "Ein Verfahren zur direkten Messung der Sekundärelektronen-Ausbeute an Isolatoren" (A method for direct measurement of the secondary emission of insulators), *El. Nachr. Technik*, Vol. 17, pp. 1-5, 1940. (Pulse method employing oscilloscope; secondary emission characteristics of mica, alkali-glass, and electrolytically prepared Al_2O_3 between 100 and 2500 volts; second crossover for mica and Al_2O_3 1700 volts; for glass, 450 volts.)

25. W. Heimann and K. Wemheuer, "Über die Ursache des Störsignals bei Bildfängerröhren" (On the cause of the shading signal in picture pickup tubes), *Zeit. für Tech. Phys.*, Vol. 19, pp. 451-454, 1938. (Plastic model of mosaic potential during scanning; oscillograms from an insulated element within the mosaic plate.)

26. W. Heimann and K. Wemheuer, "Beitrag zur Wirkungsweise des Elektronenstrahl-Bildabtasters" (Mechanism of the iconoscope), *El. Nachr. Technik.*, Vol. 15, pp. 1-9, 1938. (Measuring of mosaic surface potential by coplanar probe observed by television picture and oscillogram.)

27. H. Hintenberger, "Uber Sekundärelektronen-Emission u. Aufladungserscheinungen an Isolatoren" (Secondary electron emission and charge effects on insulators), *Zeit. für Phys.*, Vol. 114, pp. 98-109, 1939. (Mica, NaCl, Al_2O_3 in 4-micron layer; for bombarding energies above first crossover of secondary emission curve; negative space charge below the surface of insulator is produced which draws an electron current from the interior to the surface. δ_e may suddenly change from $\delta_e > 1$ to $\delta_e < 1$ after the development of this space charge.)

28. M. Knoll, "Aufladepotential und Sekundäremission elektronenbestrahlter Körper" (Equilibrium potential and secondary emission of electron-bombarded bodies), *Zeit. für Techn. Phys.*, Vol. 16, pp. 467-475, 1935. (Equilibrium potential curve of floating targets, monoscope; scanning microscope.)

29. M. Knoll, "Änderung der sekundären Elektronenemission von Isolatoren und Halbleitern durch Elektronenbestrahlung" (Change of secondary emission of insulators and semiconductors by electron

bombardment), *Naturwissenschaften*, Vol. 24, p. 345, 1936. (Image iconoscope effect with writing-beam spot; positive or negative picture as a function of backplate-voltage; storage time on Al_2O_3, several minutes.)

30. M. Knoll, "Die Bedeutung des 'Streuelektronen-Effekts' für die Wirkungsweise der Bildabtaströhren" (The significance of the "redistribution-effect" for the operation of television pickup-tubes), *Zeit. für Techn. Phys.*, Vol. 19, pp. 307-313, 1938. (Redistributed secondary electrons produce negative equilibrium potential on the insulating surface of pickup-tubes. Discussion of signal-production in the iconoscope (including shading and "return line effect") and in the image-iconoscope.)

31. M. Knoll, "Steuerwirkung eines geladenen Teilchens im Felde einer Sekundäremissions-Kathode" (Control effect of a charged particle in the field of a secondary emission target), *Naturwissenschaften*, Vol. 29, p. 335, 1941. (Coplanar grid effect as a function of potential, height and diameter of the charged particle.)

32. M. Knoll, O. Hachenberg, and J. Randmer, "Zum Mechanismus der Sekundäremission im Inneren von Ionenkristallen," *Zeit. für Phys.*, Vol. 122, pp. 137-162, 1944. (Secondary emission characteristics of KCl from 500 to 10,000 volts; δ_e decreases with increasing temperature; radiated areas (F — centers) exhibit smaller secondary emission which may be restored by heating. Transient suppression of secondary electrons by photoelectrons or secondary electrons from writing beam; image of secondary electron distribution in a KCl layer 1 micron below the surface.)

33. M. Knoll and R. Theile, "Kapazitätsgesteuerte Bildabtaströhren" (Capacitance-controlled scanning tubes), *Tel. Funk- und Fernsehtechnik*, Vol. 27, pp. 538-540, 1938. (The capacity distribution between backplate and surface of an insulated target can be observed if the elementary capacities are charged by redistributed or additional low velocity electrons and then discharged periodically by a reading beam.)

34. M. Knoll and R. Theile, "Elektronenabtaster zur Strukturabbildung von Oberflächen u. dünnen Schichten" (Imaging the structure of surfaces and thin layers by electron scanning), *Zeit. für Phys.*, Vol. 113, pp. 260-280, 1939. (Secondary emission picture of the surface of insulators and metals on which may be superimposed a picture of the resistance and capacity distribution of the target.)

35. H. B. Law, "A Technique for the Making and Mounting of Fine Mesh Screens," *Rev. Sci. Instr.*, Vol. 19, pp. 879-881, 1948. (200 to 1500 meshes per inch, up to 50 per cent transmission.)

36. I. G. Maloff, "Electron Bombardment in Television Tubes,"

Electronics, Vol. 17, pp. 108-111 and 327-331, January, 1944. (Discussion of redistribution effect of secondaries on the target of iconoscopes.)

37. R. A. McConnell, "Video Storage by Secondary Emission from Simple Mosaics," *Proc. I.R.E.*, Vol. 35, pp. 1258-1264, 1947. (Discussion of the secondary electron redistribution process in the case of homogeneous insulating targets, such as employed in the iconoscope, and on the storage of signals by modulation of the writing-beam current (grid modulation).)

38. H. Nelson, "Method of Measuring Luminescent-Screen Potential," *Jour. Appl. Phys.*, Vol. 9, pp. 592-599, 1938. (Target potential of a kinescope is measured by heating a graphite-covered spot of the glass bulb from outside with hot air and connecting it to an electrostatic tube voltmeter.)

39. C. V. Parker, "Charge Storage in Cathode-Ray Tubes," *Proc. I.R.E.*, Vol. 39, pp. 900-907, 1951. (Analysis of charging and surface potentials, including effects of redistribution, in a conventional cathode-ray tube.)

40. H. Salow, Über den Sekundäremissionsfaktor elektronenbestrahlter Isolatoren" (Secondary emission factor of insulators), *Zeit. für Tech. Phys.*, Vol. 21, pp. 8-15, 1940. (Pulse method with alternating current of 50,000 cycles; secondary electron characteristics of mica, silica and glasses between 100 and 4,000 volts; change of secondary electron curves with time for mica.)

41. H. Strübig, "Das Potential eines im Hochvakuum isolierten Auffangschirmes bei Beschiessung mit Elektronen" (Potential in a high vacuum of an insulated electron-bombarded target), *Phys. Zeit.*, Vol. 37, pp. 402-409, 1936. (Second crossover of secondary emission curve for Aquadag, 900 volts.)

C. Signal Converter and Viewing Storage Tubes

(Retention Time $\cong$ Reading Time $\cong$ 1 second to several hours)

42. J. F. Adams, "The Krawinkel Image-Storing CR Tube." Fiat final report 1027, PB-78273, April, 1947. (Recording kinescope with coplanar grid-controlled photocathode. Cathode consists of quartz plate upon which a metallic line grid (60 lines per cm) is evaporated which contacts photomosaic elements (3600/cm^2). Photoemission is controlled by coplanar grid action of free quartz surface, charged by the writing beam.)

43. P. R. Bell, G. D. Forbes and E. F. MacNichol, Jr., "Storage Tubes," Chapter 21, *Wave Forms*, Radiation Laboratory Series, No. 19, McGraw-Hill Book Company, New York, N. Y., p. 707. (Storage

by means of a conventional cathode-ray tube with capacitively coupled signal plate.)

43a. A. H. Benner and L. M. Seeberger, "Graphechon Writing Characteristics," *RCA Review*, Vol. XII, pp. 230-250, June, 1951.

44. J. S. Donal, "Cathode-Ray Control of Television Light Valves," *Proc. I.R.E.*, Vol. 31, pp. 195-208, 1943. (Mica tube face (0.25-0.5 mm) is charged by high-velocity electron beam ($\delta_e < 1$) and controls a suspension light valve mounted on it. Charges are removed by rescanning (erasing) with the same beam at reduced velocity ($\delta_e > 1$).)

45. J. S. Donal and D. B. Langmuir, "A Type of Light Valve for Television Reproduction," *Proc. I.R.E.*, Vol. 31, pp. 208-213, 1943.

45a. L. E. Flory, J. E. Dilley, W. S. Pike and R. W. Smith, "A Storage Oscilloscope," *RCA Review*, Vol. XII, pp. 220-229, June, 1951.

46. J. V. Harrington and T. F. Rogers, "Signal-to-Noise Improvement Through Integration in a Storage Tube," *Proc. I.R.E.*, Vol. 38, pp. 1197-1203, 1950.

47. J. V. Harrington, "Storage of Small Signals on a Dielectric Surface," *Jour. Appl. Phys.*, Vol. 21, pp. 1048-1053, 1950. (Analysis of charge storage in a barrier-grid type of storage tube.)

48. A. V. Haeff, "A Memory Tube," *Electronics*, Vol. 20, pp. 80-83, September, 1947. (Recording kinescope and signal converter tube; uses in addition to writing and reading beam a "holding" beam which bombards or is reflected respectively from the "white" or "black" areas of a floating luminescent screen.)

49. R. C. Hergenrother and B. C. Gardner, "The Reading Storage Tube," *Proc. I.R.E.*, Vol. 38, pp. 740-747, 1950. (Storage of charges by reflection on the back side of a storage grid; reading by electrical output or by means of an internal fluorescent screen.)

50. M. A. Honnell and M. D. Prince, "Television Image Reproduction by Use of Velocity Modulation Principles," *Proc. I.R.E.*, Vol. 39, pp. 265-268, 1951. (Intensity modulation of nonstoring cathode-ray tube produced by modulation of scanning velocity.)

51. A. S. Jensen, J. P. Smith, M. H. Mesner and L. E. Flory, "Barrier Grid Storage Tube and its Operation," *RCA Review*, Vol. IX, pp. 112-135, March, 1948. (One unmodulated electron beam scans insulating target. Writing is accomplished by backplate-voltage modulation; the local charges thereby produced on the target surface cause variations in collector current during reading.)

52. M. Knoll and J. Randmer, "Ladungs-Bildspeicherröhren mit Speichergitter" (Control grid reading type of storage tubes), *Archiv für El. Übertragung*, Vol. 4, p. 238, 1950.

52a. M. Knoll, "Electron Lens Raster Systems," Report of the

National Bureau of Standards Symposium on Electron Physics, November 5-7, 1951.

52b. M. Knoll and P. Rudnick, "Electron Lens Raster Viewing Storage Tube," Report of the National Bureau of Standards Symposium on Electron Physics, November 5-7, 1951.

53. G. Krawinkel, W. Kronjäger and H. Salow, "Zur Frage der el. Bildspeicherung" (Electrical Picture Storage), *Tel. und Fernsprechtechnik*, Vol. 27, pp. 527-533, 1938. (Properties of a one-beam, homogeneous (slightly conducting) glass target signal converter storage tube; writing and reading voltage $\cong$ 700 volts.)

54. L. Pensak, "The Graphechon — A Picture Storage Tube," *RCA Review*, Vol. X, pp. 59-73, March, 1949. (Potential control of the surface of a thin insulating film, penetrated by the writing beam and locally charged by a negative backplate. Reading is accomplished by scanning the film surface with an unmodulated beam.)

55. L. Pensak, "Picture Storage Tube," *Electronics*, Vol. 22, pp. 84-88, July, 1949.

56. J. Randmer, "Über eine gitterartige Steuerung der Sekundäremission für Bildübertragungszwecke" (Grid-like control of secondary emission for picture transmission purposes), Diss. Techn. Hochschule München, 1948.

57. F. Schroeter, "Bildspeicherung im Fernsehempfang" (Image storage in Television reception), *Optik*, Vol. 1, pp. 406-409, 1946. (Two-sided photocathode target in storage kinescope for reducing the frame number to 16 per second. Advantage: narrow frequency band and brighter picture.)

58. F. Schroeter, "Image Storage Problems," *Bull. Schweiz. Elektrot. Verein*, Vol. 40, pp. 564-566, 1949.

59. M. Von Ardenne, "Methoden u. Anordnungen zur Speicherung beim Fernsehempfang" (Methods and devices for storing in television reception), *Tel. Funk- und Fernsehtechnik*, Vol. 27, pp. 518-524, 1938. (Charge-controlled light valve screen for storage kinescopes; discussion of equilibrium potential curves; writing- and erasing-beam operation and different light valve principles.)

D. Computer Storage Tubes

60. S. H. Dodd, H. Klemperer and P. Youtz. "Electrostatic Storage Tube," *Elec. Eng.*, Vol. 69, pp. 990-995, 1950. (Storage of 400 binary digits on a mica sheet on which is evaporated a beryllium mosaic. By means of a writing beam electrostatically positioned; each element is shifted to one of two stable potentials and maintained at equilibrium by a holding gun.)

61. J. P. Eckert, Jr., H. Lukoff and G. Smoliar, "A Dynamically Regenerated Memory Tube," *Proc. I.R.E.*, Vol. 38, pp. 498-510, 1950. (Uses standard cathode-ray tube; signal obtained from redistribution effect; dot and circle pattern.)

62. J. W. Forrester, "High-Speed Electrostatic Storage," Symposium of Large Scale Calculating Machinery, Harvard University Press, Cambridge, 1948, pp. 125-129. (One gun, insulating target storage cathode-ray tube for computers; 32 × 32 storage locations on the target; writing with positive or negative collector grid, reading with neutral grid, output from backplate.)

63. J. A. Rajchman, "The Selectron," Symposium of Large Scale Calculating Machinery, Harvard University Press, Cambridge, 1948, pp. 133-145. (Figure 3: Storage mechanism. A great number of storage elements are pulsed separately by a common backplate into a negative or positive equilibrium position. Reading by luminescence (if insulated storage elements are covered with luminescent material) or by checking the displacement current to the backplate.)

64. J. A. Rajchman, "The Selectron, A Tube for Selective Electrostatic Storage," *Mathematical Tables and Other Aids to Computation*, Vol. II, No. 20, pp. 359-561, October, 1947 (Brief discussion of the basic storage principles.)

65. J. A. Rajchman, "The Selective Electrostatic Storage Tube," *RCA Review*, Vol. XII, pp. 53-97, March, 1951.

66. F. C. Williams and T. Kilburn, "A Storage System for Use with Binary-Digital Computing Machines," *Proc. Inst. Elec. Eng.* (London), Vol. 96, Part II, pp. 183-202, and Part III, pp. 77-100, 1949, and Vol. 97, Part IV, pp. 453-454, 1950. (Uses normal cathode-ray tube with external pickup plate at the screen. Writing and reading by redistribution effect of secondary electrons; spot raster with 32 × 32 elements; mechanism corresponds to "return-line effect" in iconoscope.)

E. Television Camera Storage Tubes

(Reading Time (in general) ≅ Writing Time ≅ 0.01 — 0.1 second)

67. M. Berthillier, "L'Eriscope," *Le Vide*, Vol. 2, pp. 355-359, November, 1947. (Image iconoscope with homogeneous insulator target.)

68. D. G. Fink, "The Orthicon," *Electronics*, Vol. 12, pp. 11-14, 58-59, July, 1939. (Mechanism is explained, partly in pictures.)

69. S. V. Forgue, "The Storage Orthicon and its Application to Teleran," *RCA Review*, Vol. VIII, pp. 633-650, December, 1947. (High-capacity target (an order of magnitude thinner than in the usual orthicon) with higher resistivity than that of the image orthicon; low

reading current; storage and continuous reproduction of the signal for several hundred scanning frames.)

70. W. Heiman, "Über die Wirkungsweise u. Steigerung der Empfindlichkeit von Bilfängerröhren" (Mechanism and improvement of sensitivity of picture pickup tubes), *Tel. und Fernsprechtechnik*, Vol. 27, pp. 541-544, 1938. (Discussion of double-sided targets, slightly conducting target layers and image iconoscope.)

71. H. Iams and A. Rose, "Television Pickup Tubes with Cathode-Ray-Beam Scanning," *Proc. I.R.E.*, Vol. 25, pp. 1048-1070, 1937. (Use of Cu-, Al- and Zr-oxide, activated with Cs, Se; Ge was used as a target sensitive to heat radiation; image iconoscopes with one-sided and two-sided targets.)

72. H. Iams, G. A. Morton and V. K. Zworykin, "The Image Iconoscope," *Proc. I.R.E.*, Vol. 27, pp. 541-547, 1939. (Discussion of three different targets: (a) Cesiated silver mosaic on mica sheet, 40 microns thick; (b) homogeneous mica sheet, glowed in O_2 and cesiated; (c) metallic signal plate covered by finely divided insulating powder (China clay).)

73. R. B. Janes and W. H. Hickok, "Recent Improvements in the Design and Characteristics of the Iconoscope," *Proc. I.R.E.*, Vol. 27, pp. 543-540, 1939. (Spectral response adapted to the eye; diminishing of "spurious signals"; cylindrical envelope; sandblasting of mosaic; measuring methods.)

74. R. B. Janes, R. E. Johnson and R. R. Handel, "A New Image Orthicon," *RCA Review*, Vol. X, pp. 586-592, December, 1949. (Panchromatic photosurface.)

75. R. B. Janes, R. E. Johnson and R. S. Moore, "Development and Performance of Television Camera Tubes," *RCA Review*, Vol. X, pp. 191-223, June, 1949.

76. R. B. Janes and A. A. Rotow, "Light-Transfer Characteristics of Image Orthicons," *RCA Review*, Vol. XI, pp. 364-376, September, 1950. (Discussion of redistribution effects on the target at high lights and possible changes in tube design for minimizing effects.)

77. M. Knoll and F. Schroeter, "Elektronische Bild u. Zeichenübertragung mit Isolator — bezw. Halbleiterschichten" (Picture transmission by insulating or semi-conducting layers), *Phys. Zeitschrift*, Vol. 38, pp. 330-333, 1937. (Mechanism for obtaining an electrical signal from a photoconductive homogeneous insulating target, and image iconoscope.)

78. G. Krawinkel, W. Kronjäger and H. Salow, "Über einen speichernden Bildfanger mit halbleitendem Dielektrikum" (Storage television pickup tube with semiconducting dielectric), *Zeitschr. techn. Physik*,

Vol. 19, pp. 63-73, 1938. (Possible improvement of efficiency of iconoscopes by replacement of the nonconducting target layer (mica) by a semiconducting one (e.g., slightly conducting glass). Higher field strength at the target surface will increase charges of photomosaic and reduce redistribution of electrons at the surface.)

79. J. D. McGee and H. G. Lubszynski, "EMI Cathode Ray Television Transmission Tubes," *Jour. Inst. Elec. Eng.*, Vol. 84, pp. 468-482, 1939. (Description of an iconoscope and an image iconoscope with mosaic targets; mosaic potential diagram; discussion of operation of writing or reading beam above second crossover of secondary emission curve.)

80. J. D. McGee, "Distant Electric Vision," *Proc. I.R.E.*, Vol. 38, pp. 596-608, June, 1950. (Survey and description of the various types of television camera tubes.)

81. M. Nagashima, K. Shinozaki, Y. Udagawa and K. Kizuka, "The Tecoscope Cathode-Ray Television Transmitter," *Rep. Rad. Res.* (Japan), Vol. 7, pp. 12-13, June, 1937. (Image iconoscope. No difference between cesiated and clean silver mosaic target observed.)

82. A. Rose, "The Relative Sensitivity of Television Pickup Tubes, Photographic Film and the Human Eye," *Proc. I.R.E.*, Vol. 30, pp. 293-300, 1942. (Influence of storage on sensitivity of pickup tubes.)

83. A. Rose, "Television Pickup Tubes and the Problem of Vision," *Advances in Electronics*, Vol. 1, pp. 131-166, 1948.

84. A. Rose and H. Iams, "The Orthicon, a Television Pickup Tube," *RCA Review*, Vol. IV, pp. 186-199, October, 1939. (Uses low-velocity scanning with target at cathode potential.)

85. A. Rose and H. Iams, "Television Pickup Tubes using Low-Velocity Beam Scanning," *Proc. I.R.E.*, Vol. 27, pp. 547-555, 1939. (Advantages: low level of spurious signals; high maximum signal output; high efficiency of conversion of light into signal; discussion of the mechanism compared with high velocity ($\delta_e > 1$) scanning.)

86. A. Rose, P. K. Weimer and H. B. Law, "The Image Orthicon, a Sensitive Television Pickup Tube," *Proc. I.R.E.*, Vol. 34, pp. 424-432, 1946. (Low-velocity scanning, two-sided target, image converter; target consists of a thin (several microns thick) sheet of low-resistivity glass which neutralizes charges on opposite sides during a frame time = 1/30 second; mesh screen collector on the image side of the glass target has 500-1,000 meshes per linear inch and an open area of 50-75 per cent.)

87. P. Schagen, "On the Mechanism of High-Velocity Target Stabilization and the Mode of Operation of Television Camera Tubes of the Image-Iconoscope Type," *Philips Res. Rep.*, Vol. 6, pp. 135-153, 1951.

88. R. Urtel, "Die Wirkungsweise der Kathodenstrahlbildzerleger mit Speicherwirkung", *Hochfrequenstechnik und Elektroakustik*, Vol. 48, p. 150, 1936. (Mechanism of storage camera tubes.)

89. P. K. Weimer, "The Image Isocon," *RCA Review*, Vol. X, pp. 366-386, September, 1949. (Reduction of beam noise in an image orthicon device by separation of scattered electrons from reflected electrons and obtaining the output signal from the scattered electrons only.)

90. P. K. Weimer, U. S. Patent No. 2,537,250, January 9, 1951 (Discussion of a method of grid-control reading.)

91. P. K. Weimer, H. B. Law and S. V. Forgue, "Mimo—Miniature Image Orthicon," *RCA Review*, Vol. VII, pp. 358-366, September, 1946. (Same mechanism employed as in standard image orthicon.)

92. P. K. Weimer, S. V. Forgue and R. R. Goodrich, "The Vidicon—Photoconductive Camera Tube," *Electronics*, Vol. 23, pp. 70-73, May, 1950; also *RCA Review*, Vol. XII, pp. 306-313, September, 1951. (Use of a photoconducting target for establishing a charge pattern instead of photocathode as in the orthicon.)

93. V. K. Zworykin, "Industrial Television and the Vidicon," *Elec. Eng.*, Vol. 69, pp. 624-627, 1950.

94. V. K. Zworykin, G. A. Morton and L. E. Flory, "Theory and Performance of the Iconoscope," *Proc. I.R.E.*, Vol. 25, pp. 1071-1092, 1937. (Discussion of limits and improvements of sensitivity; range of operation: 2.5 to 6 millilumens/cm^2 on the target; curve of instantaneous potential at the mosaic surface.)

95. V. K. Zworykin and G. A. Morton, *Television*, John Wiley and Sons, Inc., New York, N. Y., 1940. (Includes material on theory and construction of iconoscope and image iconoscope.)

96. V. K. Zworykin and E. G. Ramberg, *Photoelectricity and Its Applications*, John Wiley and Sons, Inc., New York, N. Y., 1949. (Basic processes and their application to television camera tubes.)

97. V. K. Zworykin, "The Iconoscope — A Modern Version of the Electric Eye," *Proc. I.R.E.*, Vol. 22, pp. 16-32, 1934. (Description of the iconoscope, its construction and operating principles.)

SURVEY OF RADIO-FREQUENCY RESISTORS WITH KILOWATT RATINGS*

By

D. R. Crosby

Engineering Products Department, RCA Victor Division, Camden, N.J.

Summary—The design and operating characteristics of several types of high-dissipation radio-frequency resistors are discussed. The study is mainly in the region from 300 kilocycles to 30 megacycles which includes long-range communication frequencies and high-power industrial heating.

Introduction

RADIO-FREQUENCY resistors with kilowatt ratings are widely used in the development, testing and installation of radio-frequency power generating equipment. As the result of a need for improved resistors, a survey was made. Information obtained in this survey has been used as the basis for the design of several resistors, described below, which are greatly superior to previous designs. The study was mainly in the region from 300 kilocycles to 30 megacycles, covering the long-range communication frequencies, and the region of high-power industrial heating. The power of interest was from 5 to 100 kilowatts.

The disposal of such powers at radio frequencies is conveniently done by a direct conversion to heat, thus requiring a resistor to operate at the radio frequency. Some work has been done on rectifying the radio frequency current so that the conversion occurs at direct current.[1, 2] Since it is difficult to construct a rectifier circuit with a broad frequency band, or one which is linear over a wide range of power, this approach will not be discussed further.

Resistors to be used with transmitters are usually of the order of 600 ohms. Resistors to be used with induction heating equipment are a few tenths of an ohm or less, while resistors for dielectric heating may be of the order of 10 to 100 ohms. Manufacturers of transmitting tubes give new tubes an operating test in a test oscillator. To test 100 kilowatt tubes, one or more 500-ohm resistors are found convenient.

---

* Decimal Classification: R383.1.

[1] G. F. Lampkin, "R-F Power Measurements," *Electronics*, Vol. 9, p. 30, February, 1936.

[2] P. M. Honnell, "R-F Power Measurements," *Electronics*, Vol. 13, p. 21, January, 1940.

Basic Types

Each of the three types, metal, carbon, and liquid resistors are useful for high-power applications.

The early metal resistors used at radio frequencies and high powers were in the form of two-wire outdoor transmission lines.[3] Such resistors are now standard for the termination of a rhombic antenna. High-loss, coaxial, metallic, transmission lines are now used as components of an assembled resistor usable at several hundred watts.[4] For powers of several kilowatts or more, wire-wound resistors immersed in water have long been used. For testing induction heating equipment, resistors made of steel tubing have been found useful.

High-power carbon resistors usually have the carbon as a film on a ceramic cylinder. This film is easily liquid-cooled and has excellent impedance characteristics.[5] Where the variation of impedance with frequency and power is of secondary importance, carborundum tubes or rods can be used. They are simple and rugged.

Resistors of the liquid type generally use water as the dissipating element. Tap water is generally satisfactory in performance and more convenient than distilled water. The water is used as the dielectric either in a condenser or in a transmission line.[6]

Dissipation Data

General

Most of the resistors studied were cylindrical in form and enclosed in a cylindrical glass jacket. The cooling was done by a thin film of water flowing over the resistor.

Water velocities up to 40 feet per second were found useful. The clearance between the cylindrical resistor and the enclosing glass jacket varied from .010 to .050 inch, depending on the jacket. The pressure drop in a typical jacket for one of the smaller resistors is

$$\text{pounds per square inch drop} = (\text{gallons per minute})^2 \times 1.4.$$

Usually, the power was measured using the temperature rise in the water as noted by two thermometers, and the water flow as given by a flow meter.

---

[3] E. J. Sterba and C. B. Feldman, "Transmission Lines for Short-Wave Radio Systems," *Proc. I.R.E.*, Vol. 20, p. 1163, July, 1932.

[4] "Microwave Wattmeter," *Electronics*, Vol. 19, p. 164, November, 1946.

[5] G. H. Brown and J. W. Conklin, "Water-Cooled Resistors for Ultra-High Frequencies," *Electronics*. Vol. 14, p. 24, April, 1941.

[6] "Dummy Aerials," *The Wireless World*, Vol. XLV, p. 4, July 6, 1939.

kilowatts of power = (gallons per minute) × (Δ° C) × 0.264.

As a correlated project, voltmeters were developed that would measure up to 25,000 volts at radio frequencies. At the lower frequencies, it was convenient to measure high currents by measuring the voltage induced in a small coil. This was done by using a standard vacuum tube voltmeter and a loop of one or two turns approximately an inch in diameter (See Figure 1).

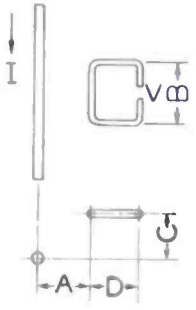

A,B,C,D IN INCHES

V = R.M.S. VOLTS

I = R.M.S. AMPERES

F = MEGACYCLES, FREQUENCY OF I

$$V = \frac{I \times F \times B}{27.2}\left[\text{LOG}_{10}\frac{(A+D)^2+C^2}{A^2+C^2}\right]$$

Fig. 1—Calculation of voltage induced in a wire loop.

Metallic Resistors

Almost any style of metallic resistor can be operated under water with power ratings of several hundred times that in free air. This is particularly true where the construction is such that all the resistance wire comes in direct contact with the water. Insulated resistors, resistors using ceramic insulated wire, or woven flexible resistors using asbestos binding also have this property to a remarkable extent. Two convenient design figures were determined experimentally for the failure power of resistors using bare wire, .008 inch in diameter:

(1) In still water, a single strand of wire fails at about 120 watts per linear inch.

(2) A winding on a cylindrical form, using 50 turns per inch and with the cooling water flowing at a velocity of 28 feet per second, fails at about 6,000 watts per square inch of coil-form surface.

The tests were made using a standard nickel-chromium alloy having a direct-current resistance of 10.3 ohms per foot.

As the power increases in the cylindrical winding, bubbles form and a hissing sound is noticed. At powers well below failure, many small bubbles are formed in the glass water jacket. This hiss and bubble formation is also characteristic of film resistors and of water-

cooled transmitting tubes.[7] To realize the maximum rating, care must be taken that there are no surges of pressure in the cooling water supply so that it is often advisable to have a surge tank installed to stabilize the pressure. In usual application the winding is conservatively operated, and the surge tank is not necessary. A strainer in the water line is desirable since a foreign particle entering the narrow space between the winding and the glass jacket is likely to cause resistor failure.

For short periods of operation a bakelite form for these resistors was found to be satisfactory, but eventually warping caused trouble. A distortion of a few thousandths of an inch may seriously interfere with the water flow. A grooved form of ceramic, glass or glass-bonded mica was found most satisfactory.

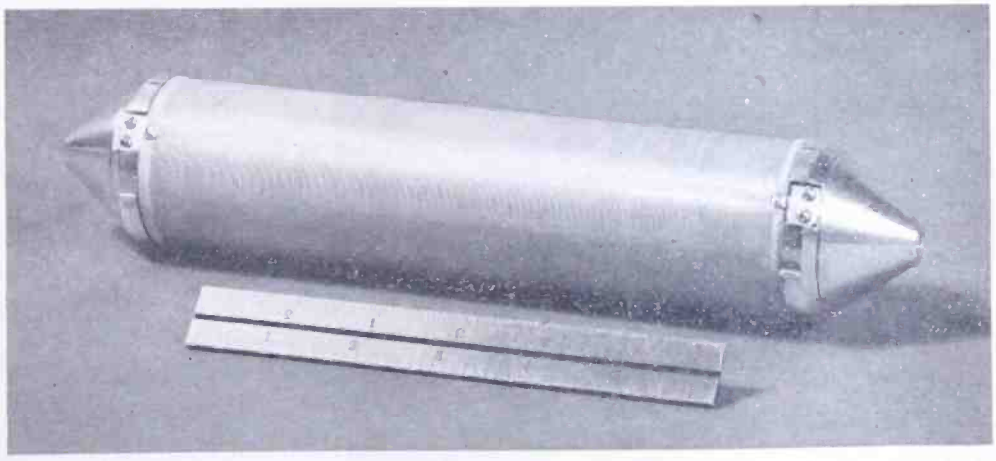

Fig. 2—Wire-wound resistor using bare wire double helix construction.

Carbon Film Resistors

Carbon film resistors of the low-temperature baked-on type and of the high-temperature deposited type were tested.[8-10] Most of these were obtained from companies who specialize in resistor manufacture. The thickness of the baked films ranged from .0015 to .006 inch, while the deposited films were of the order of .0001 inch thick, or less. Computations showed that the temperature rise in a typical baked film would be sufficient to limit its dissipation to about 1400 watts per square inch, no matter how much water velocity was available.

[7] I. E. Mouromtseff, "Water and Forced-Air Cooling of Vacuum Tubes," *Proc. I.R.E.*, Vol. 30, p. 190, April, 1942.

[8] G. V. Planer and F. E. Planer, "High Stability Carbon Resistors," *Electronic Engineering*, Vol. XVIII, p. 66, March, 1946.

[9] A. C. Pfister, "Precision Carbon Resistors," *Bell Lab. Rec.*, Vol. XXVI, p. 401, October, 1948.

[10] W. Van Roosbroeck, "High-Frequency Deposited Carbon Resistors," *Bell Lab. Rec.*, Vol. XXVI, p. 407, October, 1948.

This computation assumed that the film would fail at about 100 degrees Centigrade due to softening of the bakelite binder. Experiment verified this computation. A study was also made of film temperatures using thermocouples inside the resistor tubes.

Failure powers up to 3000 watts per square inch were obtained with the deposited films. It was not determined whether this is characteristic of the resistors, or whether it is characteristic of the cooling system.

The film resistors are easily affected by surges in the cooling system or in the testing voltage, due to the low thermal storage of the film. For the same average power, a film resistor subject to an amplitude modulated wave has a failure power lower than one subject to an unmodulated wave, because of this low thermal storage.

Impedance versus Frequency Characteristic

A theoretical study of the impedance characteristics of some film-type resistors was made and published.[11] A principal conclusion is that for such resistors to have good, broad-band frequency characteristics, they must be either quite long or quite short. If the resistors are to be short, the approximate relation for their maximum allowable length is,

$$\text{inches of length} = \frac{600}{\text{megacycles operating frequency}}.$$

Some experimental data was taken with a standard "Q" meter on a water-filled transmission line (See Figure 3). The data is presented for five different line lengths, and the five corresponding frequency regions where the line length is near one-quarter wave length.

Impedance measurements were made on many types of wire-wound resistors. A typical characteristic is shown in Figure 4. When these resistors were immersed in water, radical changes in their impedance characteristics resulted. There was evidence to indicate that these impedance characteristics may vary considerably with the impurities in the water.

It was noticed that wire-wound resistors using alloys that were nonmagnetic had superior impedance characteristics to those using magnetic alloys.

Much of the experimental impedance data taken between 5 and 30 megacycles was obtained by measuring the standing-wave pattern on a two-wire transmission line.[3] This line stretched for about 75 feet

[11] D. R. Crosby and C. H. Pennypacker, "Radio-Frequency Resistors as Uniform Transmission Lines," *Proc. I.R.E.*, Vol. 34, p. 62P, February, 1946.

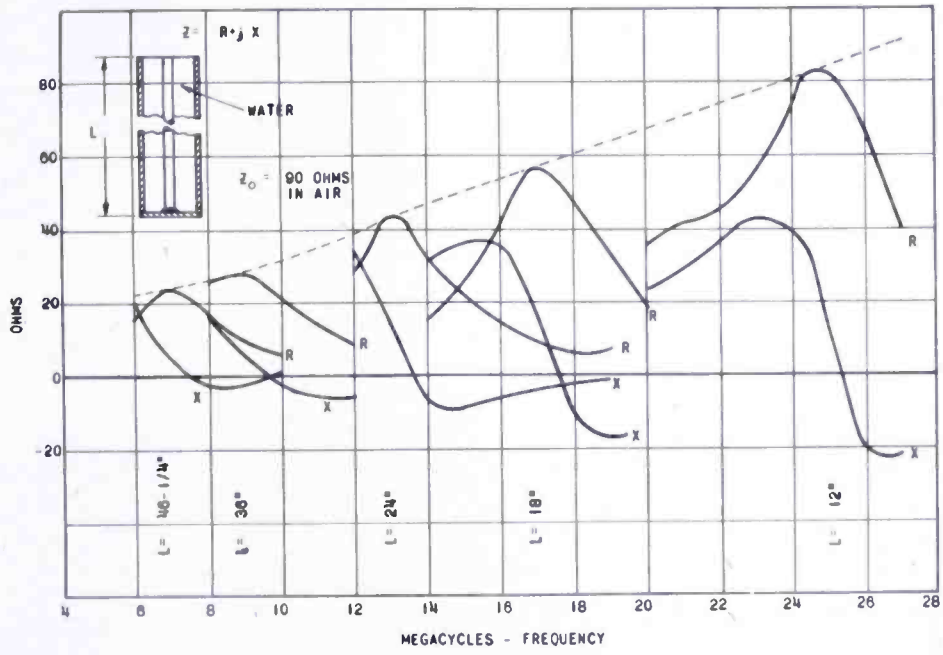

Fig. 3—Impedance measurements of water-filled transmission line for five line lengths and corresponding frequency regions where the line is near ¼ wave length.

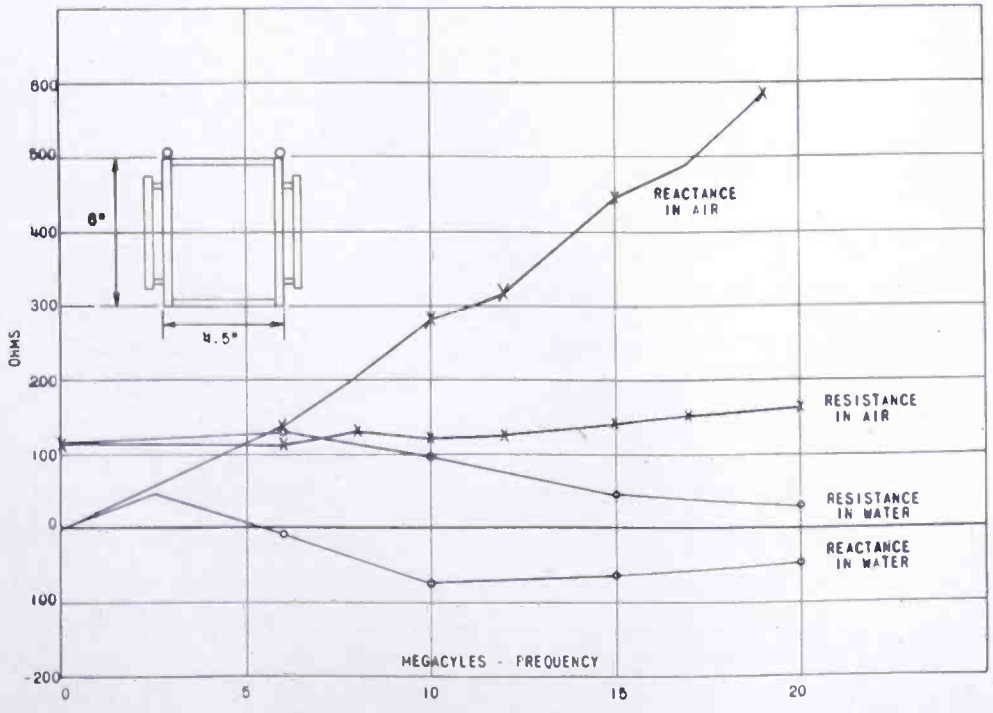

Fig. 4—Typical impedance characteristics of a card-type resistor indicating radical changes due to immersion in water.

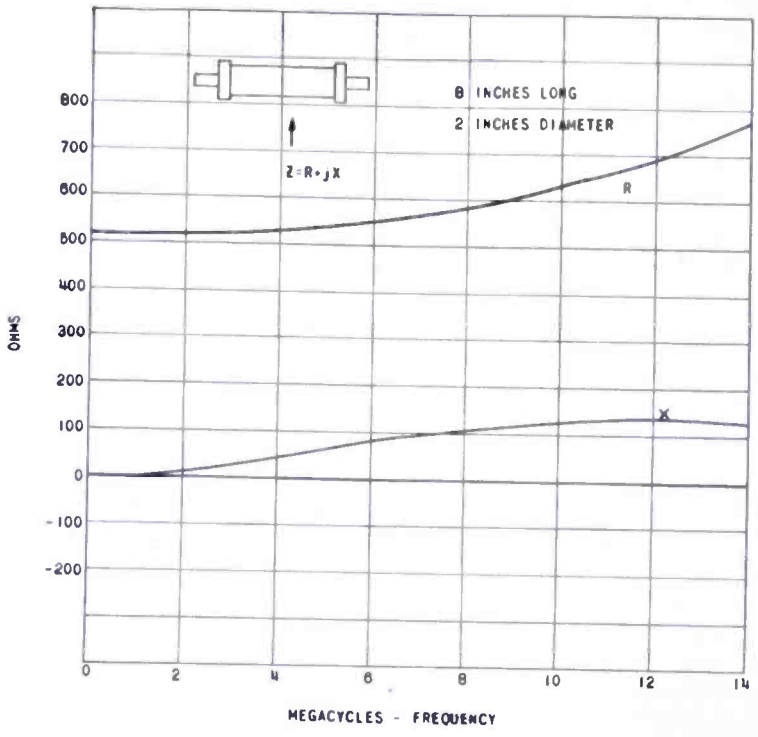

Fig. 5—Impedance characteristics of a wire-wound resistor in air.

along a corridor. The measuring trolley was pulled along the line by a string. The trolley was composed of the bakelite carriage, a shielded loop, a resonating condenser, a rectifier, and a milliammeter.

The transmission line method is particularly useful when the desired impedance equals the line-surge impedance, as then the current-standing-wave ratio along the line is a measure of the suitability of the unknown impedance.

Designs

At frequencies below 30 megacycles, wire-wound resistors can be

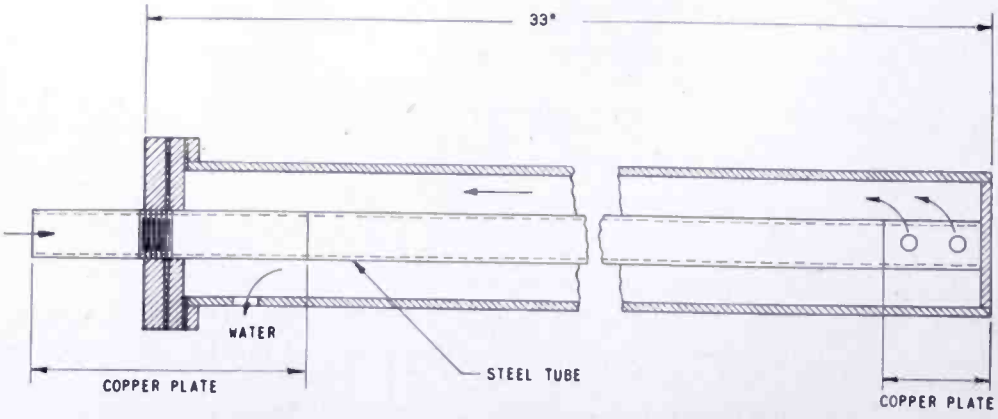

Fig. 6—Water-cooled steel tube resistor in copper jacket.

made to have tolerable frequency characteristics. Their ruggedness makes them preferable to film resistors. Of the various types of so-called noninductive windings, the arrangement using two opposing helices seems the best. A bifilar winding does not have enough insulation between turns while a card winding is not easily adapted to cooling by a water film. The problem arises of how to put two opposing helical windings on the same cylinder, using bare wire. When the windings have an advance per turn of only a few wire diameters, the cross-over points of the two helices occupy a sizable fraction of a turn, resulting in an unstable winding both mechanically and electrically.

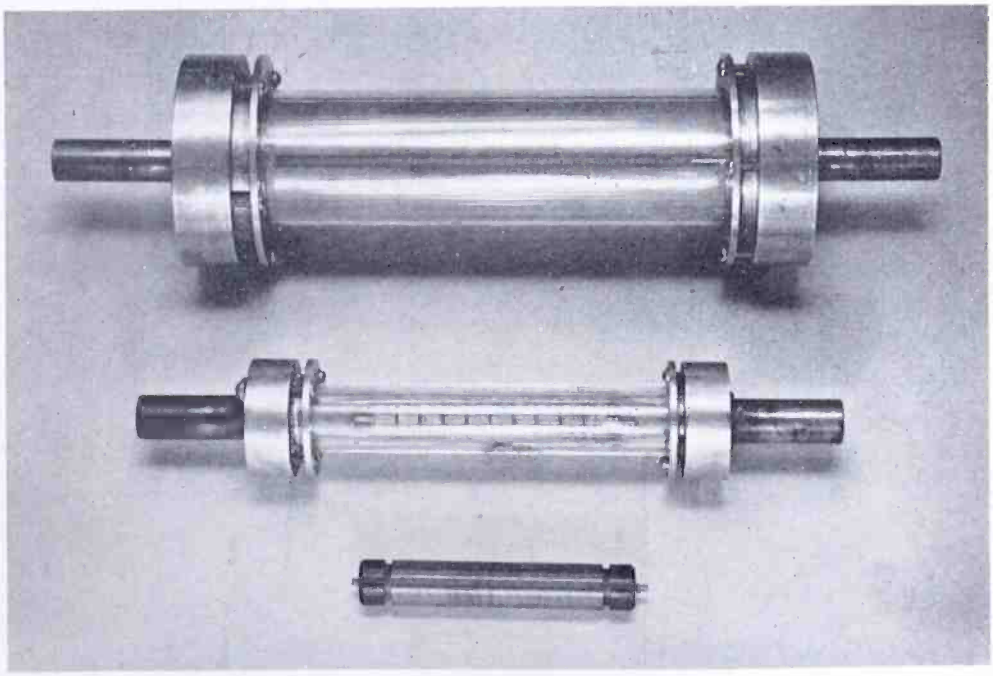

Fig. 7—Three types of wire-wound resistors.

The problem was solved by cutting a series of independent circular grooves on the core instead of the usual double helix. Two longitudinal slots spaced 180 degrees apart are cut the full length of the core.

One of the windings occupies half the circular grooves, while the winding in the opposite direction occupies the other half. The windings advance by taking a diagonal direction in crossing the longitudinal slots. The two windings may touch in the slot, but as they touch at equal voltage points no change in characteristics result. The construction is clearly shown in Figure 2.[12]

Because the grooves that hold the wires are segments of circles, they cannot be cut with the aid of the usual lathe lead screw. The

[12] D. R. Crosby, U.S. Patent 2,381,724, August 7, 1945.

coil form is a relatively expensive item as it must be fabricated with precision and made of ceramic, glass, or glass-bonded mica. The resistor shown in Figure 2 has the impedance characteristic shown in Figure 5. When mounted in a precision glass tube, such as in the top of Figure 7 and cooled by a water film of .032 inch, the impedance characteristic is substantially unchanged. With cooling water at the rate of about 14 gallons per minute, such a unit has been used at 120 kilowatts.

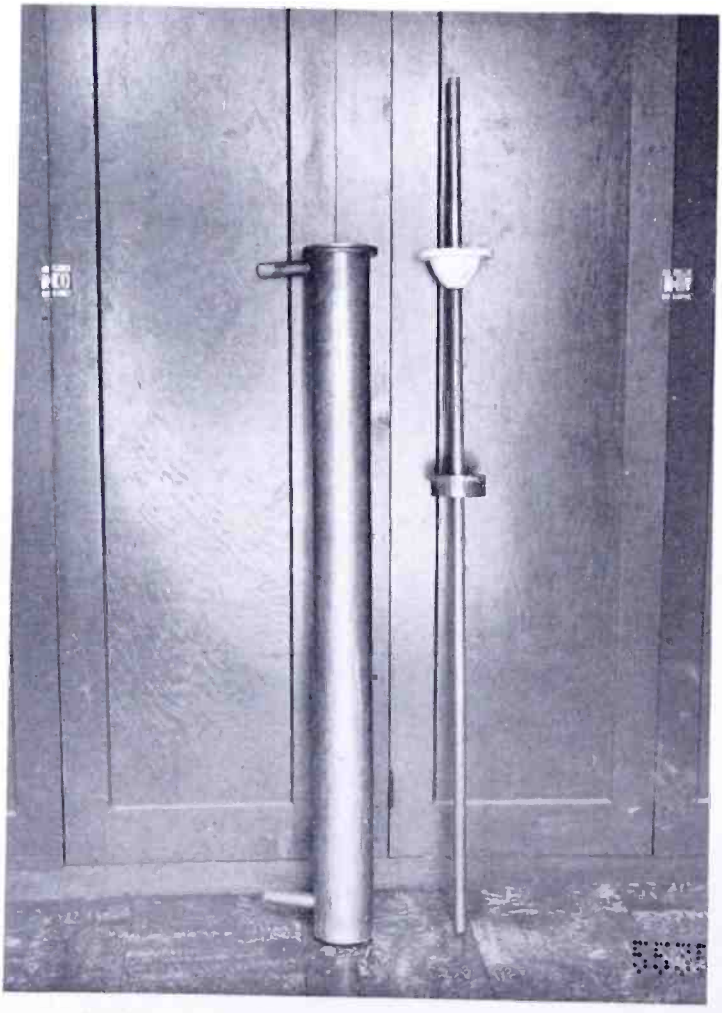

Fig. 8—Disassembled water-column resistor showing movable shorting plug.

The assembly using this resistor as the basic unit is supplied with a mounting frame, a water-flow meter and thermometer wells in the inlet and outlet water streams. This unit is recommended to users of 50 kilowatt transmitters.

The middle unit of Figure 7 is a low-resistance unit using a

slightly different type winding.[13] The lower unit of Figure 7 is ¾ inch in diameter and 4½ inches long. This unit is easily able to handle the output from a 10-kilowatt transmitter. The construction of a useful steel-tubing resistor is shown in Figure 6. When used in pairs, these resistors form a balanced load that has been used up to 110 kilowatts. This load impedance at the test frequency of 0.33 megacycle was 0.94 + j.27 ohms. The current of 1080 amperes can cause excessive heating wherever the cooling is not plentiful. It is found advisable to copper plate the steel tube heavily in the regions where the water velocity may be low. The end seal is held by means of a thread on the steel tube, avoiding the use of bolts through the sealing gasket. The bolts were found to heat excessively due to induced currents.

A water-column resistor is shown disassembled in Figure 8. The impedance data for this unit when using Camden, New Jersey, tap water is shown in Figure 3. The movable shorting plug is usually located so that the line is near resonance as indicated by the data of Figure 3. This unit has been used at 100 kilowatts.

---

[13] D. R. Crosby and W. C. Kimmich, U.S. Patent 2,397,408, March 26, 1946.

RCA TECHNICAL PAPERS†

Third Quarter, 1951

Any request for copies of papers listed herein should be addressed to the publication to which credited.

"AFC Color Synchronization Circuits," E. O. Keizer, *RCA Licensee Bulletin LB-843* (September) 1951
"Amplitude and Phase Measurements on Loudspeaker Cones," M. S. Corrington and M. C. Kidd, *Proc. I.R.E.* (September) 1951
"Audible Hum and Buzz," J. R. Meagher, *TV Servicing*, RCA Victor Division, Harrison, N. J. (September) 1951
"Broadcast Tape Speed Control," D. R. Andrews, *Electronics* (July) 1951
"A Calibrated Continuously-Variable Sampling-Wave Phase Shifter," E. A. Goldberg and N. D. Larkey, *RCA Licensee Bulletin LB-840* (August 24) 1951
"Characteristics of AM Detectors," W. E. Babcock, *Audio Eng.* (July) 1951
"Checking Quality of Aluminized Screens," H. J. Evans, *Electronics* (July) 1951
"A Color Synchronization Circuit for RCA Color System Television Receivers," M. Kronenberg, *RCA Licensee Bulletin LB-838* (July 27) 1951
"Compound Direct Radiator Loudspeaker," E. G. May, J. Preston and H. F. Olson, *RCA Licensee Bulletin LB-845* (September 28) 1951
"Controlling Engineering Design Changes," A. T. Wilson, *Product Engineering* (September) 1951
"Deflection and Convergence in Color Kinescopes," A. W. Friend, *Proc. I.R.E.* (October) 1951
RCA Review (September) 1951
"The Design of Tranmission Line Tuning Elements for Minimum Dissipation," R. W. Klopfenstein, *Proc. I.R.E.* (September) 1951
"Development and Operation of a Line-Screen Color Kinescope," D. S. Bond, F. H. Nicoll and D. G. Moore, *Proc. I.R.E.* (October) 1951
RCA Review (September) 1951
"Effects of Screen Tolerances on Operating Characteristics of Aperture-Mask Tri-Color Kinescopes," D. D. Van Ormer and D. C. Ballard, *Proc. I.R.E.* (October) 1951
RCA Review (September) 1951
"Gaseous Discharge Super-High-Frequency Noise Sources," H. Johnson and K. R. Deremer, *Proc. I.R.E.* (August) 1951
"A Grid-Controlled Color Kinescope," S. V. Forgue, *Proc. I.R.E.* (October) 1951
RCA Review (September) 1951
"Luminescence of Three Forms of Live Orthophosphate: Mn," A. L. Smith, *Jour. Electrochem. Soc.* (September) 1951
"Mechanical Design of Aperture-Mask Tri-Color Kinescopes," B. E. Barnes and R. D. Faulkner, *Proc. I.R.E.* (October) 1951
RCA Review (September) 1951
"Methods Suitable for Television Color Kinescopes," E. W. Herold, *Proc. I.R.E.* (October) 1951
RCA Review (September) 1951

† Report all corrections or additions to RCA Review, Radio Corporation of America, RCA Laboratories Division, Princeton, N. J.

"Model for the Dynamic Properties of Paper," R. E. Hurley, *Journal of the Trade Association of the Paper and Pulp Industry* (September) 1951
"New AM-FM-TV Studio Consolette," P. W. Wildow and G. A. Singer, *Audio Eng.* (September) 1951
"A One-Gun Shadow-Mask Color Kinescope," R. R. Law, *Proc. I.R.E.* (October) 1951
RCA Review (September) 1951
"An Outline of Some Photoconductive Processes," A. Rose, *RCA Review* (September) 1951
"Phosphor-Screen Application in Color Kinescopes," N. S. Freedman and K. M. McLaughlin, *Proc. I.R.E.* (October) 1951
RCA Review (September) 1951
"Photoconductivity in Amorphous Selenium," P. K. Weimer and A. D. Cope, *RCA Review* (September) 1951
"Photoconductivity in Insulators," A. Rose, *RCA Review* (September) 1951
"The Plasmatron, A Continuously-Controllable Gas-Discharge Developmental Tube," E. O. Johnson, W. M. Webster and L. Malter, *RCA Licensee Bulletin LB-844* (September) 1951
"Problems in Mobile TV," E. B. Pores, *Electronics* (September) 1951
"Properties of Some Photoconductors, Principally Antimony Trisulfide," S. V. Forgue, R. R. Goodrich and A. D. Cope, *RCA Review* (September) 1951
"RCA Electronic Multiplex and Automatic Correction Equipment," S. Sparks, *Teleg. and Teleph. Age* (July) 1951
"Residual Magnetism in Low-Noise Tubes," R. A. Wissolik and D. P. Heacock, *Tele-Tech.* (July) (Letter to the editor) 1951
"Some Antenna Systems for UHF Reception," E. O. Johnson and O. M. Woodward, Jr., *RCA Licensee Bulletin LB-842* (September) 1951
"Some Aspects of the Photoconductivity of Cadmium Sulfide," R. W. Smith, *RCA Review* (September) 1951
"Step Multiplier in Guided Missile Computer," E. A. Goldberg, *Electronics* (August) 1951
"Studies of Externally Heated Hot Cathode Arcs, Part I—Modes of the Discharge," L. Malter, E. O. Johnson and W. M. Webster, *RCA Review* (September) 1951
"Television Receiver Signal Circuit and AGC Considerations for Impulse Noise Immunity," E. I. Anderson, *RCA Licensee Bulletin LB-836* (July 9) 1951
"Television Service, Part XIII — Microphonic Troubles," J. R. Meagher, *RCA Rad. Serv. News* (September-October) 1951
"Television Studio Acoustics," M. Rettinger, *Broadcast News* (July-August) 1951
"Television-Tuner Alignment," A. Liebscher, *TV Servicing*, RCA Victor Division, Harrison, N. J. (September) 1951
"Tests of Means for Reducing Visibility of Line Structure on Television Receivers," E. O. Keizer and M. G. Kroger, *RCA Licensee Bulletin LB-837* (July 12) 1951
"Three-Beam Guns for Color Kinescopes," H. C. Moodey and D. D. Van Ormer, *Proc. I.R.E.* (October) 1951
RCA Review (September) 1951
"A Three-Gun Shadow-Mask Color Kinescope," H. B. Law, *Proc. I.R.E.* (October) 1951
RCA Review (September) 1951
"Transistor Frequency Modulator Circuit," L. L. Koros and R. F. Schwartz, *Electronics* (July) 1951
"Transmitted Signal Should be Standardized," E. W. Engstrom, *Tele-Tech.* (August) (Letter to the editor) 1951
"Transmitter Diversity Applied to Machine Telegraph Radio Circuits," G. E. Hansell, *Teleg. and Teleph. Age* (August) 1951
"Utilization of Printed Components in a Television Tuner," D. Mackey and E. Sass, *RCA Review* (September) 1951

"Video Levels in TV Broadcasting," J. H. Roe, *Tele-Tech* (August) .. 1951
"The Vidicon—Photoconductive Camera Tube," P. K. Weimer, S. V. Forgue and R. R. Goodrich, *RCA Review* (September) 1951
"A 45-Degree Reflection-Type Color Kinescope," P. K. Weimer and N. Rynn, *Proc. I.R.E.* (October) 1951
RCA Review (September) 1951

NOTE — Omissions or errors in these listings will be corrected in the yearly index.

AUTHORS

D. ROGERS CROSBY received the E.E. degree from Rensselaer Polytechnic Institute in 1934 and the M.S. degree from Harvard University in 1935. From 1935 to 1941 he was employed by the Federal Telephone & Telegraph Co. at Newark, N. J., engaged on very-high-frequency circuits for remote control of communication transmitters. Since 1941 he has been with the RCA Victor Division at Camden, N. J. For several years he was engaged in development on problems pertaining to high power transmitters. Since 1946 he has been in microwave relay development. Mr. Crosby is a Member of the American Institute of Electrical Engineers, a Senior Member of the Institute of Radio Engineers, and a member of the Executive Board of the Association of Professional Engineering Personnel.

BENJAMIN KAZAN received the B.S. degree in Physics from the California Institute of Technology in 1938 and the M.A. degree in Physics from Columbia University in 1940. In 1940 he joined the Signal Corps Engineering Laboratories and was engaged in early experimental work with radar equipment. From 1944 to 1950 he was Chief of the Special Purpose Tube Section at the Evans Signal Laboratory, responsible for the development work and application engineering in traveling-wave tubes, klystrons, cathode-ray and storage tubes, crystal rectifiers, and transistor devices. During the past year he has been associated with the RCA Laboratories Division, Princeton, N. J., being presently engaged in development work on cathode-ray tubes. Mr. Kazan is a Member of the American Physical Society and Tau Beta Pi, and an Associate Member of the Institute of Radio Engineers.

M. KNOLL received the M.S. and Ph.D. degrees in Electrical Engineering in 1922 and 1924 respectively from the Institute of Technology in Munich, Germany. From 1927 to 1945 he was in turn Assistant Professor, Associate and Full Professor for Vacuum Tube design at the Institute of Technology, Berlin-Charlottenburg, Germany, and from 1932 director of its Vacuum Tube Laboratory. After the war this Vacuum Tube Laboratory was affiliated with the University of Munich, where he taught, as a Full Professor, Electron Optics and Vacuum Tube Design until 1947. From 1932 to 1947 he was in charge of the Electron Research Laboratory of the Telefunken Corporation, and was mainly concerned with the development of the television camera, viewing and storage tubes. In December 1948, after serving one year as a consultant to the Evans Signal Laboratories, Belmar, N. J., he joined RCA Laboratories at Princeton, N. J., where he is now engaged in research in electronics. A part of his time is devoted to teaching Electron Optics and Vacuum Tube design at Princeton University as a visiting lecturer with the rank of Full Professor in the Department of Electrical Engineering. Dr. Knoll is a Senior Member of the Institute of Radio Engineers, and a Member of Sigma Xi.

T. MURAKAMI received the B.S. degree in E.E. from Swarthmore College in 1944, and the M.S. degree from the Moore School of Electrical Engineering, University of Pennsylvania in 1947. From 1944 to 1946 he was an assistant and research associate in the Department of Electrical Engineering at Swarthmore College. Since 1946 he has been with the Advanced Development Section of the Home Instrument Department, RCA Victor Division, Camden, N. J., working on radio frequency circuit development. Mr. Murakami is an Associate Member of the Institute of Radio Engineers and Sigma Xi.

WEN YUAN PAN received the E.E. Degree from Stanford University in 1939, and the Ph.D. Degree in Electrical Engineering in 1940. He served in an advisory capacity to the China Defense and Supplies in 1941 and to the Chinese Delegation to the International Civil Aviation Conference in 1944. He was engaged as a research scientist at the Radio Research Laboratory at Cambridge, Massachusetts, during the war years and was invited to be a member of the Advisory Committee of the United Nations Telecommunications in 1946. Since 1945, he has been with the RCA Victor Division at Camden, New Jersey. Dr. Pan is an honorary member of the Veterans' Wireless Operators Association, a member of Sigma XI and Senior Member of the Institute of Radio Engineers.

BERNARD N. SLADE received the B.S. degree in Electrical Engineering from the University of Wisconsin in 1948. He joined the RCA Victor Division immediately after graduation. Mr. Slade is associated with the Advanced Development Group at Harrison where he is working on the development of crystal triodes. He is taking part-time graduate work in electrical engineering at Stevens Institute of Technology. Mr. Slade is a Member of the Institute of Radio Engineers.

RCA REVIEW

a technical journal

RADIO AND ELECTRONICS
RESEARCH · ENGINEERING

INDEX

VOLUME XII — 1951

TABLE OF CONTENTS

March

	PAGE
Use of New Low-Noise Twin Triode in Television Tuners. R. M. COHEN	3
Shortwave Radio Propagation Correlation with Planetary Positions. J. H. NELSON	26
An Automatic Nonlinear Distortion Analyzer. H. F. OLSON AND D. F. PENNIE	35
Open-Field Test Facilities for Measurement of Incidental Receiver Radiation. C. G. SERIGHT	45
The Selective Electrostatic Storage Tube. J. RAJCHMAN	53
Investigation of Ultra-High-Frequency Television Transmission and Reception in the Bridgeport, Connecticut Area. R. F. GUY	98
Low-Reflection Films Produced on Glass in a Liquid Fluosilicic Acid Bath. S. M. THOMSEN	143

June

Practical Considerations in the Use of Television Super Turnstile and Super-Gain Antennas. H. E. GIHRING	159
A Diversity Receiving System for Radio Frequency Carrier Shift Radiophoto Signals. J. B. ATWOOD	177
Rapid Determination of Gas Discharge Constants from Probe Data. L. MALTER AND W. M. WEBSTER	191
A New Television Studio Audio Console. R. W. BYLOFF	211
A Storage Oscilloscope. L. E. FLORY, J. E. DILLEY, W. S. PIKE AND R. W. SMITH	220
Graphechon Writing Characteristics. A. H. BENNER AND L. M. SEEBERGER	230
Methods to Extend the Frequency Range of Untuned Diode Noise Generators. H. JOHNSON	251
High-Speed Ten-Volt Effect. R. M. MATHESON AND L. S. NERGAARD	258
Direct-Reading Noise-Factor Measuring Systems. R. W. PETER	269

September

PART I

PAGE

Utilization of Printed Components in a Television Tuner 293
D. MACKEY and E. SASS

Photoconductivity in Insulators 303
ALBERT ROSE

The Vidicon — Photoconductive Camera Tube 306
P. K. WEIMER, S. V. FORGUE AND R. R. GOODRICH

Photoconductivity in Amorphous Selenium 314
P. K. WEIMER AND A. D. COPE

Properties of Some Photoconductors, Principally Antimony Trisulfide. 335
S. V. FORGUE, R. R. GOODRICH AND A. D. COPE

Some Aspects of the Photoconductivity of Cadmium Sulfide 350
R. W. SMITH

An Outline of Some Photoconductive Processes 362
ALBERT ROSE

Studies of Externally Heated Hot Cathode Arcs, Part I — Modes of the Discharge 415
L. MALTER, E. O. JOHNSON AND W. M. WEBSTER

PART II

Methods Suitable for Television Color Kinescopes 445
E. W. HEROLD

A Three-Gun Shadow-Mask Color Kinescope 466
H. B. LAW

A One-Gun Shadow-Mask Color Kinescope 487
R. R. LAW

A 45-Degree Reflection-Type Color Kinescope 503
P. K. WEIMER AND N. RYNN

A Grid-Controlled Color Kinescope 527
S. V. FORGUE

Development and Operation of a Line-Screen Color Kinescope 542
D. S. BOND, F. H. NICOLL AND D. G. MOORE

Phosphor-Screen Application in Color Kinescopes 568
N. S. FREEDMAN AND K. M. MCLAUGHLIN

Three-Beam Guns for Color Kinescopes 583
H. C. MOODEY AND D. D. VAN ORMER

Mechanical Design of Aperture-Mask Tri-Color Kinescopes 593
B. E. BARNES AND R. D. FAULKNER

Effects of Screen Tolerances on Operating Characteristics of Aperture-Mask Tri-Color Kinescopes 603
D. D. VAN ORMER AND D. C. BALLARD

Deflection and Convergence in Color Kinescopes 612
A. W. FRIEND

December

A Method of Improving the Electrical and Mechanical Stability of Point-Contact Transistors 651
B. N. SLADE

Relative Magnitudes of Undesired Responses in Ultra-High-Frequency Receivers 660
W. Y. PAN

A Study of Grounded-Grid, Ultra-High-Frequency Amplifiers 682
T. MURAKAMI

Fundamental Processes in Charge-Controlled Storage Tubes 702
B. KAZAN AND M. KNOLL

Survey of Radio Frequency Resistors with Kilowatt Ratings 754
D. R. CROSBY

INDEX, VOLUME XII

	ISSUE	PAGE
"An Automatic Nonlinear Distortion Analyzer," H. F. Olson and D. F. Pennie	Mar.	35
"Deflection and Convergence in Color Kinescopes," A. W. Friend	Sept.	612
"Development and Operation of a Line-Screen Color Kinescope," D. S. Bond, F. H. Nicoll and D. G. Moore	Sept.	542
"Direct-Reading Noise-Factor Measuring Systems," R. W. Peter	June	269
"A Diversity Receiving System for Radio Frequency Carrier Shift Radiophoto Signals," J. B. Atwood	June	177
"Effects of Screen Tolerances on Operating Characteristics of Aperture-Mask Tri-Color Kinescopes," D. D. Van Ormer and D. C. Ballard	Sept.	603
"Fundamental Processes in Charge-Controlled Storage Tubes," B. Kazan and M. Knoll	Dec.	702
"Graphechon Writing Characteristics," A. H. Benner and L. M. Seeberger	June	230
"A Grid-Controlled Color Kinescope," S. V. Forgue	Sept.	527
"High-Speed Ten-Volt Effect," R. M. Matheson and L. S. Nergaard	June	258
"Investigation of Ultra-High-Frequency Television Transmission and Reception in the Bridgeport, Connecticut Area," R. F. Guy	Mar.	98
"Low-Reflection Films Produced on Glass in a Liquid Fluosilicic Acid Bath," S. M. Thomsen	Mar.	143
"Mechanical Design of Aperture-Mask Tri-Color Kinescopes," B. E. Barnes and R. D. Faulkner	Sept.	593
"A Method of Improving the Electrical and Mechanical Stability of Point-Contact Transistors," B. N. Slade	Dec.	651
"Methods Suitable for Television Color Kinescopes," E. W. Herold	Sept.	445
"Methods to Extend the Frequency Range of Untuned Diode Noise Generators," H. Johnson	June	251
"A New Television Studio Audio Console," R. W. Byloff	June	211
"A One-Gun Shadow-Mask Color Kinescope," R. R. Law	Sept.	487
"Open-Field Test Facilities for Measurement of Incidental Receiver Radiation," C. G. Seright	Mar.	45
"An Outline of Some Photoconductive Processes," Albert Rose	Sept.	362
"Phosphor-Screen Application in Color Kinescopes," N. S. Freedman and K. M. McLaughlin	Sept.	568
"Photoconductivity in Amorphous Selenium," P. K. Weimer and A. D. Cope	Sept.	314
"Photoconductivity in Insulators," Albert Rose	Sept.	303
"Practical Considerations in the Use of Television Super Turnstile and Super-Gain Antennas," H. E. Gihring	June	159
"Properties of Some Photoconductors, Principally Antimony Trisulfide," S. V. Forgue, R. R. Goodrich and A. D. Cope	Sept.	335
"Rapid Determination of Gas Discharge Constants from Probe Data," L. Malter and W. M. Webster	June	191
"Relative Magnitudes of Undesired Responses in Ultra-High-Frequency Receivers," W. Y. Pan	Dec.	660
"The Selective Electrostatic Storage Tube," J. Rajchman	Mar.	53
"Shortwave Radio Propagation Correlation with Planetary Positions," J. H. Nelson	Mar.	26
"Some Aspects of the Photoconductivity of Cadmium Sulfide," R. W. Smith	Sept.	350
"A Storage Oscilloscope," L. E. Flory, J. E. Dilley, W. S. Pike and R. W. Smith	June	220
"Studies of Externally Heated Hot Cathode Arcs, Part I — Modes of the Discharge," L. Malter, E. O. Johnson and W. M. Webster	Sept.	415

	ISSUE	PAGE
"A Study of Grounded-Grid Ultra-High-Frequency Amplifiers," T. Murakami	Dec.	682
"Survey of Radio Frequency Resistors with Kilowatt Ratings, D. R. Crosby	Dec.	754
"Three-Beam Guns for Color Kinescopes," H. C. Moodey and D. D. Van Ormer	Sept.	583
"A Three-Gun Shadow-Mask Color Kinescope," H. B. Law	Sept.	466
"Use of New Low-Noise Twin Triode in Television Tuners," R. M. Cohen	Mar.	3
"Utilization of Printed Components in a Television Tuner," D. Mackey and E. Sass	Sept.	293
"The Vidicon — Photoconductive Camera Tube," P. K. Weimer, S. V. Forgue and R. R. Goodrich	Sept.	306
"A 45-Degree Reflection-Type Color Kinescope," P. K. Weimer and N. Rynn	Sept.	503

AUTHORS, VOLUME XII

Atwood, J. B.—"A Diversity Receiving System for Radio Frequency Carrier Shift Radiophoto Signals"	June	177
Ballard, D. C. (Coauthor)—"Effects of Screen Tolerances on Operating Characteristics of Aperture-Mask Tri-Color Kinescopes"	Sept.	603
Barnes, B. E. (Coauthor)—"Mechanical Design of Aperture Mask Tri-Color Kinescopes"	Sept.	593
Benner, A. H. (Coauthor)—"Graphechon Writing Characteristics"	June	230
Bond, D. S. (Coauthor)—"Development and Operation of a Line-Screen Color Kinescope"	Sept.	542
Byloff, R. W.—"A New Television Studio Audio Console"	June	211
Cohen, R. M.—"Use of New Low-Noise Twin Triode in Television Tuners"	Mar.	3
Cope, A. D. (Coauthor)—"Photoconductivity in Amorphous Selenium"	Sept.	314
(Coauthor)—"Properties of Some Photoconductors, Principally Antimony Trisulfide"	Sept.	335
Crosby, D. R.—"Survey of Radio Frequency Resistors with Kilowatt Ratings"	Dec.	754
Dilley, J. E. (Coauthor)—"A Storage Oscilloscope"	June	220
Faulkner, R. D. (Coauthor)—"Mechanical Design of Aperture-Mask Tri-Color Kinescopes"	Sept.	593
Flory, L. E. (Coauthor)—"A Storage Oscilloscope"	June	220
Forgue, S. V.—"A Grid-Controlled Color Kinescope"	Sept.	527
(Coauthor)—"Properties of Some Photoconductors, Principally Antimony Trisulfide"	Sept.	335
(Coauthor)—"The Vidicon—Photoconductive Camera Tube"	Sept.	306
Freedman, N. S. (Coauthor)—"Phosphor-Screen Application in Color Kinescopes"	Sept.	568
Friend, A. W.—"Deflection and Convergence in Color Kinescopes"	Sept.	612
Gihring, H. E.—"Practical Considerations in the Use of Television Super Turnstile and Super-Gain Antennas"	June	159
Goodrich, R. R. (Coauthor)—"Properties of Some Photoconductors, Principally Antimony Trisulfide"	Sept.	335
(Coauthor)—"The Vidicon—Photoconductive Camera Tube"	Sept.	306
Guy, R. F.—"Investigation of Ultra-High-Frequency Television Transmission and Reception in the Bridgeport, Connecticut Area"	Mar.	98
Herold, E. W.—"Methods Suitable for Television Color Kinescopes"	Sept.	445

	ISSUE	PAGE
Johnson, H.—"Methods to Extend the Frequency Range of Untuned Diode Noise Generators"	June	251
Johnson, E. O. (Coauthor)—"Studies of Externally Heated Hot Cathode Arcs, Part I—Modes of the Discharge"	Sept.	415
Kazan, B. (Coauthor)—"Fundamental Processes in Charge-Controlled Storage Tubes"	Dec.	702
Knoll, M. (Coauthor)—"Fundamental Processes in Charge-Controlled Storage Tubes"	Dec.	702
Law, H. B.—"A Three-Gun Shadow-Mask Color Kinescope"	Sept.	466
Law, R. R.—"A One-Gun Shadow-Mask Color Kinescope"	Sept.	487
Mackey, D. (Coauthor)—"Utilization of Printed Components in a Television Tuner"	Sept.	293
Malter, L. (Coauthor)—"Rapid Determination of Gas Discharge Constants from Probe Data"	June	191
(Coauthor)—"Studies of Externally Heated Hot Cathode Arcs, Part I—Modes of the Discharge"	Sept.	415
Matheson, R. M. (Coauthor)—"High-Speed Ten-Volt Effect"	June	258
McLaughlin, K. M. (Coauthor)—"Phosphor-Screen Application in Color Kinescopes"	Sept.	568
Moodey, H. C. (Coauthor)—"Three-Beam Guns for Color Kinescopes"	Sept.	583
Moore, D. G. (Coauthor)—"Development and Operation of a Line-Screen Color Kinescope"	Sept.	542
Murakami, T.—"A Study of Grounded-Grid, Ultra-High-Frequency Amplifiers"	Dec.	682
Nelson, J. H.—"Shortwave Radio Propagation Correlation with Planetary Positions"	Mar.	26
Nergaard, L. S. (Coauthor)—"High-Speed Ten-Volt Effect"	June	258
Nicoll, F. H. (Coauthor)—"Development and Operation of a Line-Screen Color Kinescope"	Sept.	542
Olson, H. F. (Coauthor)—"An Automatic Nonlinear Distortion Analyzer"	Mar.	35
Pan, W. Y.—"Relative Magnitudes of Undesired Responses in Ultra-High-Frequency Receivers"	Dec.	660
Pennie, D. F. (Coauthor)—"An Automatic Nonlinear Distortion Analyzer"	Mar.	35
Peter, R. W.—"Direct-Reading Noise-Factor Measuring Systems"	June	269
Pike, W. S. (Coauthor)—"A Storage Oscilloscope"	June	220
Rajchman, J.—"The Selective Electrostatic Storage Tube"	Mar.	53
Rose, Albert—"An Outline of Some Photoconductive Processes"	Sept.	362
"Photoconductivity in Insulators"	Sept.	303
Rynn, N. (Coauthor)—"A 45-Degree Reflection-Type Color Kinescope"	Sept.	503
Sass, E. (Coauthor)—"Utilization of Printed Components in a Television Tuner"	Sept.	293
Seeburger, L. M. (Coauthor)—"Graphechon Writing Characteristics"	June	230
Seright, C. G.—"Open-Field Test Facilities for Measurement of Incidental Receiver Radiation"	Mar.	45
Slade, B. N.—"A Method of Improving the Electrical and Mechanical Stability of Point-Contact Transistors"	Dec.	651
Smith, R. W.—"Some Aspects of the Photoconductivity of Cadmium Sulfide"	Sept.	350
(Coauthor)—"A Storage Oscilloscope"	June	220
Thomsen, S. M.—"Low-Reflection Films Produced on Glass in a Liquid Fluosilicic Acid Bath"	Mar.	143
Van Ormer, D. D. (Coauthor)—"Effects of Screen Tolerances on Operating Characteristics of Aperture-Mask Tri-Color Kinescopes"	Sept.	603
(Coauthor)—"Three-Beam Guns for Color Kinescopes"	Sept.	583

	ISSUE	PAGE
Webster, W. M. (Coauthor)—"Rapid Determination of Gas Discharge Constants from Probe Data"	June	191
(Coauthor)—"Studies of Externally Heated Hot Cathode Arcs, Part I—Modes of the Discharge"	Sept.	415
Weimer, P. K. (Coauthor)—"Photoconductivity in Amorphous Selenium"	Sept.	314
(Coauthor)—The Vidicon—Photoconductive Camera Tube"	Sept.	306
(Coauthor)—"A 45-Degree Reflection-Type Color Kinescope"	Sept.	503